TRANSPORTATION RESEARCH RECORD 897

Earthwork Compaction

TRANSPORTATION RESEARCH BOARD
NATIONAL RESEARCH COUNCIL

NATIONAL ACADEMY OF SCIENCES
WASHINGTON, D.C. 1982

Transportation Research Record 897
Price $10.80
Edited for TRB by Susan Singer-Bart

modes
1 highway transportation
2 public transit
3 rail transportation
4 air transportation

subject areas
33 construction
62 soil foundations

Library of Congress Cataloging in Publication Data
National Research Council. Transportation Research Board.
Earthwork compaction.

(Transportation research record; 897)
1. Soil stabilization—Addresses, essays, lectures. 2. Earthwork—Addresses, essays, lectures. I. National Research Council (U.S.). Transportation Research Board. II. Series
TE7.H5 no. 897 [TE210.4] 380.5s [624.1'5] 83-8106
ISBN 0-309-03509-0 ISSN 0361-1981

Sponsorship of the Papers in This Transportation Research Record

GROUP 2—DESIGN AND CONSTRUCTION OF TRANSPORTATION FACILITIES
R.V. LeClerc, consultant, Olympia, Washington, chairman

Construction Section
David S. Gedney, DeLeuw Cather and Company, chairman

Committee on Earthwork Construction
Charles M. Higgins, Louisiana Department of Transportation and Development, chairman
Mehmet C. Anday, Marvin L. Byington, Joseph D'Angelo, Robert C. Deen, Albert Dibernardo, William Bryan Greene, Wilbur M. Haas, Wm P. Hofmann, J.M. Hoover, Eugene Y. Huang, Robert W. Israel, James E. Kelly, Clyde N. Laughter, W. Scott Lovelace, C. William Lovell, Willard G. Puffer, John R. Sallberg, James Chris Schwarzhoff, Walter C. Waidelich

William G. Gunderman, Transportation Research Board staff

The organizational units, officers, and members are as of December 31, 1981.

Contents

Authors of the Papers in This Record

Boncompain, Bernard, Geology and Soil Mechanics Services, James Bay Energy Corporation, 800 de Maisonneuve Boulevard East, Montreal, Quebec, Canada H2L 4M8
Dascal, Oscar, Hydro-Quebec, 855 Sainte-Catherine Street East, Montreal, Quebec, Canada H2L 4P5
Fattah, Ezzat A., Geotechnical Research Centre, McGill University, 817 Sherbrooke Street West, Montreal, Quebec, Canada H3A 2K6
Gemme, Raymond L., Soil Mechanics Bureau, New York State Department of Transportation, 1220 Washington Avenue, State Campus, Albany, NY 12232
Guyot, Christian, Menard, Inc., 211 Jonnet Building, Monroeville, PA 15145
Hannon, Joseph B., Department of Transportation, 5900 Folsom Boulevard, P. O. Box 19128, Sacramento, CA 95819
Highter, William H., Department of Civil Engineering, University of Tennessee, 111 Perkins Hall, Knoxville, TN 37916
Konrad, Jean-Marie, Geology and Soil Mechanics Services, James Bay Energy Corporation, 800 de Maisonneuve Boulevard East, Montreal, Quebec, Canada H2L 4M8
Lin, P. S., School of Civil Engineering, Purdue University, West Lafayette, IN 47907
Lovell, C. W., School of Civil Engineering, Purdue University, West Lafayette, IN 47907
Ofer, Zvi, University of the Witwatersrant, 1 Jan Smuts Avenue, Johannesburg 2001, South Africa
Pare, J.-Jacques, Geology and Soil Mechanics Services, James Bay Energy Corporation, 800 de Maisonneuve Boulevard East, Montreal, Quebec, Canada H2L 4M8
Selig, Ernest T., Department of Civil Engineering, University of Massachusetts, Amherst, MA 01003
Vallee, Robert P., McPhail Associates, 1430 Massachusetts Avenue, Cambridge, MA 02138
Verma, Narenda S., Geology and Soil Mechanics Services, James Bay Energy Corporation, 800 de Maisonneuve Boulevard East, Montreal, Quebe, Canada H2L 4M8
Walsh, Thomas J., Department of Transportation, 5900 Folsom Boulevard, P. O. Box 19128, Sacramento, CA 95819
Walter, John E., D'Appolonia Consulting Engineers, Inc., 10 Duff Road, Pittsburgh, PA 15235
Yong, Raymond N., Geotechnical Research Centre, McGill University, 817 Sherbrooke Street West, Montreal, Quebec, Canada H3A 2K6
Yoo, Tai-Sung, Daewoo Engineering Company, 286 Yang-Dong (Daewoo Building), Seoul, Korea

Compaction Procedures, Specifications, and Control Considerations

ERNEST T. SELIG

This paper provides a review of soil compaction principles and practice. The nonlinear relation of compaction energy to resulting density is shown. The need to consider the effect of change in moisture from the as-compacted state is pointed out. Factors that influence the reference test for specifying compaction are discussed to show the uncertainty in the resulting maximum dry density and optimum moisture content. Factors that influence field compaction are also described, and the possibility of a large variation in compaction results with field conditions is demonstrated. The need for more awareness of the effects of methods of preparation and uniformity of procedures is indicated. Limitations of density as a method of specifying compaction are pointed out. The type and magnitude of compaction measurement errors are defined and implications for compaction control are discussed. Finally, because knowledge of compactor performance in combination with observation of field procedures is a meaningful basis on which to judge compaction, some basic principles of compactor performance evaluation are described.

The purpose of this paper is to review and evaluate methods of specifying, achieving, and controlling field compaction. Although compaction is an important part of all earthwork projects, it is often treated casually. Present practice does not reflect the knowledge gained from the extensive past studies of compaction. Many basic principles are either not understood or not applied. Furthermore, discrepancies often exist between compaction expectations and reality.

BASIC CONCEPTS

Compaction is the process of soil densification by mechanical manipulation (1). Densification is achieved by reduction in volume of the air voids. Thus, during compaction the moisture content remains unchanged, in the absence of wetting and drying caused by weather conditions, and the percentage of saturation increases. Consolidation, in contrast, is the process of volume reduction in saturated soils that takes place gradually as pore water is expelled (1). Unfortunately, the terms compaction and consolidation are often interchanged erroneously in practice.

The obtaining of a greater unit weight of soil is not a direct objective of compaction. Instead, the reason for compacting is to improve soil properties such as increasing strength, decreasing compressibility, decreasing permeability, and reducing swelling and shrinking. However, density is the most commonly used parameter for specifying the desired amount of compaction and for determining the state of compaction. This is primarily a consequence of historical tradition and convenience. An increase in density implies an improvement in the other parameters. However, a given density, or even a given percentage of compaction, does not produce the same magnitude of strength and compressibility properties for all soils. The use of density specifications causes this fact to be deemphasized.

If we exclude certain soils, such as relatively clean sands and gravels, the most common density reference tests for compaction specifications are AASHTO T99 (ASTM D698) and AASHTO T180 (ASTM D1557). In these tests, soil is compacted by the impact of a dropped weight. The compactive effort per unit volume E for this type of test is computed as follows:

$$E = WhNn/V_m \quad (1)$$

where

W = impact hammer weight,
h = hammer drop height,
N = number of drops per layer,
n = number of layers, and
V_m = mold volume.

Thus, for the AASHTO T99 test, E = 12 300 ft-lb/ft^3, and for the AASHTO T180 test, E = 56 100 ft-lb/ft^3.

As indicated in Figure 1, the density achieved is neither proportional to the compactive effort nor linearly related to it. Thus, an increase in the amount of compaction from 95 percent AASHTO T180 to 100 percent AASHTO T180 might require a 500 percent increase in effort. This is an important fact to consider when attempting to achieve additional compaction in the field.

The general relations of dry density and strength to moisture content produced by the reference compaction tests are shown in Figure 2. These trends have been well established and are representative of most soils. The individual curves in Figure 2 are obtained by applying a constant compactive effort to samples of soil prepared with different moisture contents. The maximum dry density (MDD) occurs at a particular moisture content known as the optimum moisture content (OMC). When soil is compacted at both higher and lower moisture contents than optimum by using the same effort, the dry density achieved is less than the maximum. As the effort is increased, MDD increases and OMC decreases. The maximum as-compacted strength occurs at a compaction moisture content lower than optimum. At moisture contents well above optimum, the as-compacted strength is low, and an increase in compactive effort may actually produce a lower strength.

An important consideration, not always remembered, is that the relation in Figure 2 represents behavior of soil when the moisture content remains at the value during compaction. The equilibrium moisture content that develops in the field after compaction as a result of environmental factors may be very different from the moisture content chosen for compaction and may vary with time. Any such changes will alter the strength and density by an amount that depends not only on the magnitude of moisture change but also on the relation of the as-compacted moisture content to optimum. Consideration of this factor is an essential part of proper earthwork design.

Factors That Influence Reference Test Results

Many factors influence the values of MDD obtained with the AASHTO T99 and T180 reference tests. These have been described in detail by Johnson and Sallberg (2). In summary, these factors are as follows:

1. Size and shape of mold--Test standards fix values for these so that their influence on MDD should be consistent.
2. Mold support--Variations in this can cause up

Figure 1. Relation of density achieved at optimum moisture content to compactive effort for several soil types.

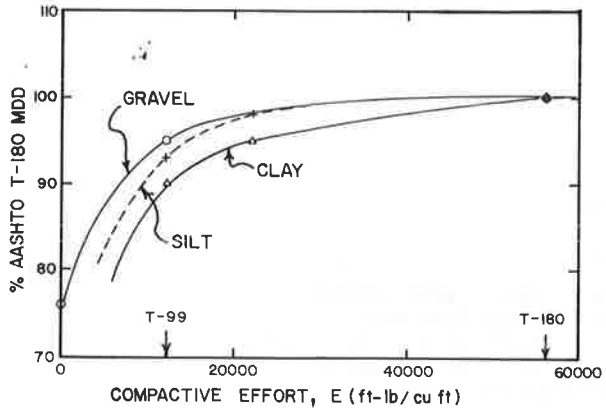

Figure 2. Moisture-density-strength relation for cohesive soils.

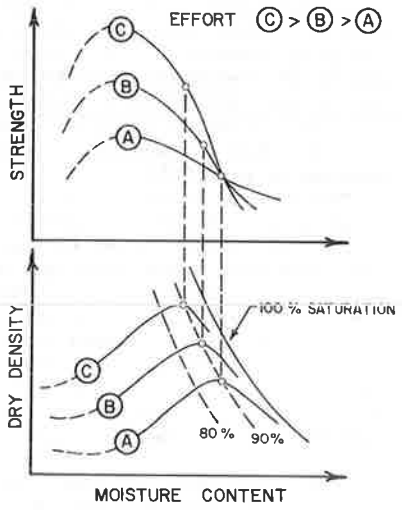

to 2 lb/ft³ change in MDD. Not only is a solid base needed, but the mold bottom and base surface must be flat to ensure solid contact.

3. Sample preparation--This includes (a) whether or not soil is reused for the different compaction moisture contents, (b) whether the soil is oven-dried before mixing with water, (c) length of absorption time after adding and mixing water, and (d) how the water is dispersed into the soil during mixing. These factors can cause a change in MDD of up to about 5 lb/ft³.

4. Type, magnitude, and distribution of compaction effort--These are fixed by the test standards. A major limitation is that the impact type of compaction from the falling weight is not representative of any common field method. Thus, the magnitude of compactive effort per unit volume of soil, the moisture-density relations, and the efficiency of compaction are not likely to be the same in the field as in the reference tests.

5. Temperature--Temperature decrease, even when the soil remains unfrozen, can cause a reduction in MDD. The effect can be as much as 1/4 lb/ft³ decrease per °F temperature decrease in clayey soils (2,3).

6. Layer thickness--This is fixed nominally in the reference tests by defining the height of the compaction mold and the number of layers. However, even with the same soil, control of layer thickness, particularly maintenance of constant layer thickness for different moisture contents and compaction efforts, is not feasible with present test procedures. The value of MDD can be significantly influenced by this factor.

7. Degradation of particles--Gravel particles in soil can be broken by the impact of the compaction hammer. Thus, the compaction characteristics can be altered. This fact must be considered in interpreting the reference density test results for field use.

The above indicate that MDD from the reference test may vary significantly, even within the constraints of the standard test specifications. Furthermore, the reference test may not be representative of field compaction conditions. The main advantages of the AASHTO T99 and T180 reference tests appear to be that (a) they are relatively simple and inexpensive to conduct; (b) they can be performed with low cost, portable apparatus; and (c) they have been so widely used that they form the basis for most of the past empirical correlations between compaction specifications and performance experience. Although these are important advantages, they do not emphasize the fundamental technical objectives.

Factors That Influence Field Compaction Results

Many factors affect the amount of compaction achieved in the field. Although most of these have been documented in the past, for example by Johnson and Sallberg (4), their influence has not always been taken into account in earthwork construction.

That MDD and OMC vary with soil type is well known; however, less well appreciated is that soil type affects field results in a manner different from the reference test because of its influence on effect of methods of soil preparation and efficiency of types of rollers. The large effect of changing compaction water content on the resulting dry density is also well known. Chemical additives such as lime or cement, which are used to stabilize the soil by modifying its properties, will also change the compaction characteristics.

The remaining factors that influence field compaction are given in the following sections.

Method of Preparation

The method of soil preparation prior to compaction is an important factor whose influence is not adequately appreciated. This factor includes a means of excavating, transporting, and spreading the soil. It also includes a means of adding water or, conversely, of drying the soil. The blending of soil to get homogeneous composition and moisture content within a placed layer is especially important. This task is generally done poorly because it is expensive and difficult to achieve, particularly in cohesive soils. As shown in Figure 3, if the moisture is not evenly dispersed, even though the compactive effort and average moisture are correct, the density results will not be satisfactory.

Blending of the soil can be started during excavation. If water must be added, doing this at the borrow area is better than waiting until the soil is spread at the compaction site. Some mixing will occur during excavation, and additional time for water absorption will be provided. Additional mixing at the fill area may also be needed. Commonly used methods are dozer, disk harrow, and pulverizing mixer. The pulverizer does the best job, but it is expensive, and hence primarily reserved for adding stabilizing chemicals. The disk is ineffective for mixing water into cohesive soils. Thus, the contractor can only sprinkle the surface and hope that the water will seep into the soil.

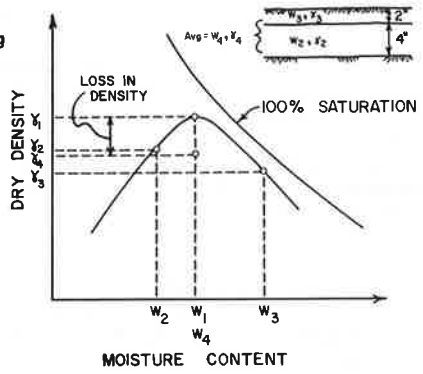

Figure 3. Illustration of effect of poor mixing on compaction.

Uniformity of Procedures

Nonuniformity in construction procedures is probably the biggest cause of density variation in the field. Soil is never homogeneous in its natural state, and it is unfeasible to blend it so that large zones in an embankment are uniform in composition. However, the manner of excavation and spreading can affect the homogeneity significantly in the horizontal direction within any layer without substantially changing the earthwork cost. The thickness of placed soil layers varies widely (often more than by a factor of two) in typical construction because it is not carefully controlled, except perhaps for layers such as the base course beneath a pavement. The roller coverage pattern is also often widely variable. Inadequate attention is given to uniformity in construction procedures, even though these cause a large variability in the end product, which can be reduced with little increase in cost.

Environmental Influences

In cold regions moist gravel and crushed stone have, of necessity, been compacted in subfreezing temperatures. With this possible exception, compaction should never be attempted with frozen soil. Although this fact is generally appreciated, the influence of low temperature (above freezing) is not. The reference MDD is usually obtained at ambient temperatures around 70°F (21°C), but field temperatures may vary by at least ±30°F (±17°C) from this value. However, more critical environmental influences are those that cause drying or wetting of the soil during the earthwork operations. Although these influences are recognized, the magnitude of their effect may not be.

Type of Roller

A variety of soil compaction machines are available. Classification of these by distinct type is not always possible. The most common groups, excluding the small machines, used for the compacting element, are as follows:

1. Smooth steel wheel,
2. Pneumatic tire,
3. Sheepsfoot or tamping foot,
4. Segmented pad or grid, and
5. Vibratory smooth-drum.

The principles of compaction with vibratory rollers are more complex and less well understood than those associated with other types of rollers. A discussion of this subject may be found elsewhere (6-8). As indicated by Johnson and Sallberg (4), with few exceptions, no one type of roller is markedly superior in its ability to achieve a desired density in any soil. However, the efficiency and economy will vary with the combination of soil and compactor used.

Compactive Effort

For any type of roller the effort can be changed by varying the magnitude of such parameters as weight, width, tire pressure, and vibration frequency. Obviously, some of these can be changed on a particular machine and others are fixed, unless a different machine of the same type is used. The value of compactive effort applied by field equipment, in comparison with the reference test effort, is generally unknown.

The total effort per unit volume of soil applied with a roller is also a function of the number of roller coverages given to the soil surface. For most rollers, the effectiveness in achieving density is largely dissipated within the first 8 coverages (8). Although measurable changes can often continue up to 16 coverages, the efficiency is low. If compaction is not achieved within 4-8 coverages, then a different roller or compaction condition should be considered.

Underlying Layer

As in the reference test, the nature of the support under the layer being compacted has an influence on the layer compaction. In general, the stiffer the underlying conditions, the higher the density that will result, other conditions remaining constant. However, this is not always the case. For example, in compaction of an overlay of asphalt concrete on a Portland cement concrete pavement with vibratory rollers, the stiff layer may cause excess pounding of the asphalt, compared with that experienced with softer underlying conditions, unless vibratory forces are diminished.

Lift Thickness

The lift or layer thickness significantly affects the density achieved. Generally, the average density decreases as the lift thickness increases. For example, field tests (8) have shown density decreases of 6-8 lb/ft³ as layer thicknesses increase from 6 to 12 in. However, there are some exceptions to this trend. The maximum density with vibratory rollers is not always at the surface (9). Also, sheepsfoot rollers tend to leave the top part of each lift uncompacted.

As each layer is placed and compacted, some additional compaction of underlying layers may also occur. Field tests have shown (10) that when compacted layers are 6- to 12-in thick, which is typical of many projects, the placing and compacting of two to six additional layers still produces measurable compaction in the first of these layers. This additional compaction is not usually considered in compaction-control decisions.

Rate of Compaction

Soils are strain-rate-sensitive materials, especially clays. However, the rate of compaction as controlled by the roller travel speed, within the normal range of values used in construction, is important only for vibratory rollers. With vibratory rollers, unlike all other types, productivity is generally improved by decreasing the travel speed. The reason is that the number of drum oscillations and, in general, the compaction per drum oscillation, increases with decreasing travel speed.

Within the range of values of the above factors

that influence field compaction, an enormous range in the results can be achieved. The only reliable way to determine the effect of any combination of these factors is by field trial. More information on these effects can be found in many publications, (i.e., 4,8,11).

FIELD METHODS OF MEASURING COMPACTION

Density of soil is by far the most widely used method for measuring the results of field compaction. This is true even though density is only an indirect measure of the desired effects of compaction. Among the reasons why density testing is still the principal approach are probably (a) density can be measured by simple and inexpensive equipment (even though more expensive equipment may be better); (b) a lower bound specification can be used for density without defining moisture content (even though this may not be best), whereas other parameters such as strength or stiffness have their maximum values at too low a moisture content; (c) the density approach can be applied to almost all soil conditions; and (d) construction requirements have been established based on experience with density specifications and control procedures, which makes a change difficult to implement.

Other parameters that can be used to measure field compaction include seismic velocity, California bearing ratio, penetration resistance, and plate bearing modulus. Examples are given elsewhere (12-15). Each method will be seen to have particular advantages and limitations. Although density methods are likely to continue to be the most common in the future, other methods ought to be given serious consideration. New methods need to be tried so experience can be gained for their implementation.

Compaction Variability

Examples of the interpretation of relative density measurements, considering random and systematic sources of error, may be found in Selig and Ladd (16). Many references are available that provide a comprehensive discussion of measurement error theory. Thus, the subject will not be considered in detail in this paper. However, several basic concepts will be reviewed to provide the background needed for evaluating compaction specifications and control procedures.

All measurements have some error. These may be categorized as random, systematic, or mistakes. Mistakes must be avoided. This is done by careful work, adequately checked. Systematic errors are those that are consistently of the same sign and magnitude for repeated measurements. Examples are weighing scales out of adjustment or incorrect equipment calibration factors. Random errors are those that vary in magnitude and sign with repeated measurement. Examples of sources of random error in density achieved by compaction are soil inhomogeneity and variations in layer thickness, coverage pattern, and moisture distribution. Sources of random error in density measurement methods include reading precision and soil surface preparation effects. Random errors have the characteristic that the error in the measured parameter approaches zero when a sufficient number of repeated measurements are averaged. In contrast, the average of repeated measurements that all contain a systematic error will also have the same error.

Accuracy is defined by the difference between the average of a set of repeated measurements and the true value. The difference is a measure of the systematic error. Precision is defined by the repeatability of a measurement, as determined by the random sources of error. A small amount of scatter in a repeated set of measurements indicates high precision. However, the average measurement will be inaccurate if a large systematic error exists. Whereas precision can be determined by repeated measurements, accuracy cannot. Unfortunately, if the systematic errors are not known, the accuracy of the measurement is not known.

Random errors in compaction measurements often follow a normal distribution. Thus, the set of repeated measurements can be characterized by a mean, which is the estimate of the true value, and a standard deviation, which is a measure of the scatter or precision. Systematic errors shift the mean value away from the true value (i.e., cause inaccuracy without altering the scatter or precision). In compaction work, these two types of errors must be distinguished to evaluate the results properly.

Information that indicates the magnitude of the errors in the reference compaction test and in field density measurements are given in a number of references (2,4,16-19). Based on data such as these, the values in the table below were established as an indication of the magnitude of the random and systematic errors for these two situations. Knowledge of these errors is essential for writing meaningful specifications and for evaluating compaction results.

Test Measurement	Systematic	Random, 1 SD
Reference		
MDD (lb/ft³)	2-10	<1
OMC (%)	1-5	<1
Field		
Embankment dry density (lb/ft³)	2-4	5-8
Embankment moisture (%)	<2	2-3
Base course dry density (lb/ft³)	1-3	2-5
Base course moisture (%)	<1	1-2

Compaction Specification and Control

Three questions need to be answered in order to prepare compaction specifications and establish control procedures for a job:

1. How much compaction is needed?
2. How should compaction be specified? and
3. How should the results be verified in the field?

How Much

Normally, the required level of compaction is determined from past experience. For example (20), 95 percent of AASHTO T99 MDD is commonly required in embankments below a depth of 1-6 ft from the surface, and a higher level of compaction (i.e., 100 percent AASHTO T99 MDD) is required in the top zone of the embankment or the subgrade, where the traffic-induced stresses are greater. Granular bases are generally required to be compacted to at least 100 percent AASHTO T99 MDD or 95 percent AASHTO T180 MDD, the latter usually being greater. However, 100 percent T99 for granular bases produces much greater strength and stiffness than 100 percent T99 for most subgrades and embankment materials.

Specification of the amount of compaction in any terms other than a level of density relative to some standard test value is unusual. The assumption is that if the required density is achieved with materials acceptable for the situation, then performance will be satisfactory. The limitation of this approach is that performance will vary widely among the acceptable soils when compacted to the same den-

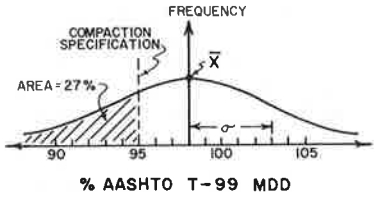

Figure 4. Variation of field density in relation to compaction specification.

sity specification. Thus, for equal performance, the compaction requirements should be a function of soil type for the same application. This refinement is not usually made. Furthermore, if density is to be used as the primary basis for specifying compaction, then the required amount should be obtained by correlation of density to desired properties such as strength or stiffness. However, this approach appears to be implemented only rarely in practice.

Another, perhaps more serious, limitation of present compaction specifications is that variability is not usually recognized or considered. Thus, when a given level of density is requested, no indication is given whether this is intended to be an average, so that 50 percent of the samples can have a lower value, or a minimum, so that 100 percent of the samples must exceed the specification, or whether some other allowable percentage below the specification is intended. Since variability is an established fact, interpretation of the specification cannot be made without resolution of this issue.

How to Specify

The two basic categories of specifications are (a) method and (b) end result. The first specifies how the compaction should be done; for example, the equipment type, maximum layer thickness, minimum number of passes, and, perhaps, the moisture content of the soil. This method is considered too restrictive to the contractor. The second specifies the required characteristics, usually a minimum dry density within a range of acceptable moisture content. This approach assumes that suitable procedures exist and will be used to check the end result.

In reality, reliance on just checking the end result has been found to be unsatisfactory. This situation derives in part from the errors in the reference test and in the field test and the variability of field densities. But, in addition, the number of reference and field measurements is generally far too few. Thus, in practice, a combination of method and end result specification is generally used. Such a specification, for example, might require approval of the compactor or specification of the acceptable compactor characteristics, then specification of a maximum layer thickness, a minimum number of passes, and a minimum required density. Restrictions would be placed on the acceptable range of moisture content relative to optimum.

Wahls and others (3) provide examples of specifications used in highway practice based on an extensive survey completed in 1968. All of the specifications are of the combination type. A distinction is made in the requirements for embankments, subgrades, backfilling of trenches, and structural backfill.

How to Control

The first step in controlling the results is to obtain a representative sample of the soil for performing the reference density test. The purpose of the reference test is to obtain a value of MDD and OMC for the soil. However, a representative sample is impossible to obtain in advance of construction. Tests are needed not only for each new soil type encountered but also for composition variations within the same soil type. Thus, samples should be taken periodically during construction to provide a continuing series of reference tests. A reference test can be justified for each field density test, although this frequency is not always essential.

The field density is measured during construction and compared with the reference value to determine whether the results comply with the specifications. To accomplish this task, the inspector must decide where to conduct the field tests and how many tests to perform. But, perhaps, more critical questions are, How appropriate is the reference value and what percentage of the compacted soil zone can be permitted to have a density below the reference value? The answers require determination of systematic errors in the reference tests relative to the field tests. Sources of these errors include the effects of soil preparation and type of compactive effort, even assuming that the samples are representative.

What happens if the results of the field test fail to meet the specified value? Remember that the purpose of the test is to check compliance. Thus, if the test does not pass, some action must be taken and a retest done until compliance is achieved. In practice, common solutions, in order of probable application, appear to be the following:

1. Rerun the field test, assuming an error in the first test. If this test passes, accept the compaction. If not, try step 2.
2. Require the contractor to do more compaction, then retest. If still unsatisfactory, try step 3.
3. Consider whether a different compactor is needed. If so, try it and then retest. If unsatisfactory, go on to step 4.
4. Rerun the reference density test. If the field test still does not pass, go on to step 5.
5. Scarify soil or remove and replace it, then recompact and retest. If the test still does not pass, go to step 6.
6. Request owner to accept a lower standard than previously specified.

The effects of compaction variability and specification interpretation on the acceptance decision can be illustrated with the following example. Assume that the specified compaction requirement is 95 percent of MDD from the AASHTO T99 reference test. Assume, too, that the variability of compaction is represented by a standard deviation of 5 percent compaction. Even though the statistical meaning of compaction specifications is unknown in general, it is reasonable to assume that at least the average density is intended to exceed the specified value. Thus, assume in this example that the average achieved is actually 98 percent.

The density distribution in relation to the specification value in this example is illustrated in Figure 4. This figure shows that 73 percent of the soil would have a density greater than the specified 95 percent MDD, and 27 percent has a lower density.

Consider three possible decision plans for compaction control.

1. Conduct a density test at a random location. Accept the compaction if the test result equals or exceeds 95 percent MDD. If the test fails, then discard it and take a second test at another random location. If this test result equals or exceeds 95 percent MDD, accept the compaction. If it fails, reject the compaction.

Plan 1 implies that the average compaction is intended to equal or exceed the specified value. If the average just equals the specified value, the probability of the first test passing is 50 percent and the probability of either the first test or the second test passing is 75 percent. Thus, the probability of plan 1 resulting in acceptance of this compaction is 75 percent (i.e., three out of four times the plan should result in the intended decision). For the example in Figure 4, the probability is even higher, specifically 93 percent, that the compaction will be accepted under Plan 1. Thus, if properly used, this simple plan can be very effective.

2. Conduct three or four compaction tests. Accept the compaction if three out of four (or 75 percent) of the tests exceed the specified value. If more than one of four tests fails, reject the compaction.

Plan 2 implies that 75 percent or more of the compacted soil is required to have a density greater than the specified value. The case illustrated in Figure 4 approximately represents this situation. For this case, plan 2 should produce the correct decision about 70 percent of the time.

3. Assume that every test must give a density that exceeds the specified value. Thus, some remedial action will be required if any test fails.

Plan 3 implies that 100 percent of the soil should exceed the specified compaction. The case in Figure 4 does not comply with this goal. If only one test is required to make a decision, then 73 percent of the time the wrong decision will be made. If two tests are required, then the wrong decision will be made 53 percent of the time. For this plan to be effective, the inspector must choose the spots that appear to be lowest in density and test at one of these. If the test passes, then the compaction should be accepted. However, this plan is unnecessarily severe because it forces the average compaction to be much higher than the specified value.

An alternative to these simple plans is a more rigorous statistical sampling plan with control charts. Examples are given elsewhere (3,19,21-23). According to Beaton (23), the reasons that such statistical control procedures have not been used generally are as follows:

1. Construction engineers and inspectors are unfamiliar with the concepts and terminology of statistical quality control,
2. Departures from the specifications are frequently needed because of changed job conditions,
3. Present specifications have not been written for use with random sampling or statistical control, or
4. Construction costs will increase unnecessarily if present quality is adequate.

All of these arguments can be circumvented by proper training and proper specifications. If compaction is generally adequate, then it is only necessary to define it unambiguously in specifications and develop an appropriate inspection plan to check it.

COMPACTOR PERFORMANCE EVALUATION

Knowledge of compactor capability is valuable for judging adequacy of compaction. Because suitable equipment specifications do not exist, this knowledge has to come primarily from field experience. To assist in interpreting field experience and in correlating the extensive range of possible conditions and rollers, a method was developed to quantify ratings of compaction equipment in terms of

1. Compaction effort per unit of soil volume,
2. Productivity in volume compacted per unit of time, and
3. Power required for compaction.

The details of the method are given elsewhere (24), and examples of application is found in Hussein and Selig (11).

In its simplest form (Figure 5), the compactor may be represented as a smooth roller of width B and weight W that requires a towing force (F) to pull it over a layer of compacted thickness (t) at a travel speed (S). The compactive effort (e) (force x distance) is given by

$$e = FLP \tag{2}$$

where L is the distance traveled per roller coverage and P is the number of roller coverages or passes. F may be related to the roller weight (W) by

$$F = fW \tag{3}$$

where f is the coefficient of compaction or rolling resistance. Thus,

$$e = fWLP \tag{4}$$

The volume compacted (V_c) is

$$V_c = LBt \tag{5}$$

The compactive effort per unit soil volume (E), analogous to the parameter used in the AASHTO T99 and T180 tests, is

$$E = e/V_c = fWP/Bt \tag{6}$$

The compaction time (T) is

$$T = PL/S \tag{7}$$

The productivity (R) thus is

$$R = V_c/T = BtS/P \tag{8}$$

Finally, the required power (H) is

$$H = C_1RE = C_2fWS \tag{9}$$

where C_1 and C_2 are constants for unit conversion.

A study of compactor performance by using this model has demonstrated that compactor weight, by itself, is an unreliable indicator of expected performance. This conclusion is illustrated by the observation that the 10-lb hammer used in the AASHTO T180 reference test can produce densities that are difficult to achieve by even the heaviest rollers available. The advantage of the heavy roller in this case is much higher productivity. Of course, heavy rollers, properly configured, can produce higher densities than lighter rollers, if other parameters such as layer thickness and coefficient of compaction are constant. However, if lighter rollers are matched in compactive effort per unit volume to heavy rollers, by appropriate selection of parameters, the heavy roller will only have a higher productivity instead.

To illustrate this point, compare two machines.

Figure 5. Simplified compactor model.

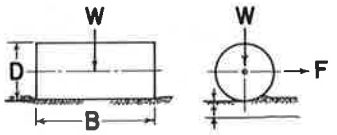

One is a self-propelled smooth steel-wheel roller that weighs 10 000 lb and has an effective rolling width of 3.5 ft. The other is a towed pneumatic tire roller that weighs 50 000 lb and has an effective rolling width of 7.1 ft. The number of coverages with both rollers is arbitrarily taken as five, but, in consideration of the weight differences, the layer thickness is designated as 4 in for the steel-wheel roller, and 10 in for the pneumatic roller. The coefficient of compaction is assumed to be the same in both cases, although, in reality, this is only approximately true.

According to Equation 6, the ratio of E for the steel-wheel roller to E for the pneumatic roller will be

$$E_{SW}/E_{PN} = (10\ 000/50\ 000)(7.1/3.5)(10/4) = 1.$$

Hence, both rollers in this case produce the same compactive effort per unit volume of soil compacted. However, according to Equation 8, and assuming that both travel at 3 mph, the corresponding ratio of productivity is

$$R_{SW}/R_{PN} = (3.5/7.1)(4/10) = 0.2.$$

Thus, the pneumatic roller has five times the productivity of the steel-wheel roller.

If, instead, the layer thicknesses were kept the same, say at 6 in for both rollers, the ratio of E would be

$$E_{SW}/E_{PN} = (10\ 000/50\ 000)(7.1/3.5) = 0.4;$$

that is, the pneumatic roller would produce greater compaction. The pneumatic roller would also achieve its higher amount of compaction with greater productivity because

$$R_{SW}/R_{PN} = (3.5/7.1) = 0.5.$$

CONCLUSIONS REGARDING PRACTICE

Observations of compaction practice over the past 20 years have led to the following conclusions.

1. Variability of density from point to point in the field is sufficiently large that compliance of 100 percent of compaction tests with a specified compaction requirement is unfeasible and unreasonable to expect.
2. Variability is significant, a typical standard deviation of density scatter is 4 to 6 lb/ft^3. This means that the range of test values could easily exceed 20 lb/ft^3 for a particular job.
3. Moisture content around optimum is generally required, but modification of moisture content during construction is rarely observed. Thus, we could logically conclude that soil naturally exists at its optimum moisture content. However, it is more reasonable to assume that the tolerance allowed in field moisture is very much wider than normally specified. In fact, modification of moisture content is rarely required unless density results are unsatisfactory. If this practice does not produce an inadequate end product then, rather than change the practice, the specifications should be modified to be consistent with it.
4. If an inspection report indicates that all or most measured field densities are in excess of the specified value, then the average of these reported values is not likely to represent the average for the compacted zone of soil. The reason is that the lower end of the density distribution must be missing for this situation to occur, assuming a normal density distribution and reasonable compaction requirements.
5. Earthwork construction productivity has greatly increased in the last several decades, but procedures for compaction inspection have changed only to the extent that nuclear instruments have been perfected for determining the field results. No really new approaches have been introduced.
6. The percentage of total compacted soil sampled in inspection is infinitesmal. Thus, most of the compacted soil must be accepted by judgment of the inspector without testing.
7. As normally practiced, testing is insufficient for reliable judging of compaction. Thus, the primary value of conducting compaction reference tests and field density measurements is either to document compliance for the record or to guide the inspector's judgment.
8. Reliable compaction evaluation requires the services of an experienced and knowledgeable inspector. However, this task is often delegated to someone in a low-level position on the staff.
9. Given the limitations of present practice and the realities of field conditions, the most reliable way to assess the adequacy of compaction is to have a knowledge of roller capabilities and then observe the construction procedures. Field density testing, as currently practiced, is no substitute for experienced observation.
10. Improvement of compaction operations in the field will require more meaningful specifications, more appropriate testing apparatus, and a better understanding by contractors and engineers of the factors that influence compaction results.
11. Alternatives to density specifications should be encouraged.

REFERENCES

1. Standard Definitions of Terms and Symbols Relating to Soil and Rock Mechanics. Annual Book of ASTM Standards, Part 19, ASTM, Philadelphia, ASTM D653, 1978.
2. A.W. Johnson and J.R. Sallberg. Factors Influencing Compaction Test Results. HRB, Bull. 319, 1962, 148 pp.
3. H.E. Wahls, C.P. Fisher, and L.J. Langfelder; North Carolina State University. The Compaction of Soil and Rock Materials for Highway Purposes. Bureau of Public Roads, Raleigh, Final Rept., Aug. 1968.
4. A.W. Johnson and J.R. Sallberg. Factors That Influence Field Compaction of Soils. HRB, Bull. 272, 1960, 206 pp.
5. E.T. Selig and T.S. Yoo. Fundamentals of Vibratory Roller Behavior. Proc., 9th International Conference on Soil Mechanics and Foundation Engineering, Vol. 2, Japan, 1977, pp. 375-380.
6. T.S. Yoo and E.T. Selig. Dynamics of Vibratory Roller Compaction. Journal of the Geotechnical Engineering Division, ASCE, Vol. 105, No. GT10, Oct. 1979, pp. 1211-1231.
7. T.S. Yoo and E.T. Selig. New Concepts for Vibratory Compaction of Soil. Proc., International Conference on Compaction, Paris, April 1980, Vol. 2, pp. 703-707.
8. E.T. Selig and W.B. Truesdale. Properties of Field Compacted Soils. HRB, Highway Research

Record 177, 1967, pp. 77-97.
9. D.J. D'Appolonia, R.V. Whitman, and E.D. D'Appolonia. Sand Compaction with Vibratory Rollers. Journal of the Soil Mechanics and Foundations Division, ASCE, Vol. 95, No. SM1, Jan. 1969, pp. 263-264.
10. E.T. Selig. Application of Soil Strain Measurements to Soil Compaction Evaluation. HRB, Highway Research Record 438, 1973, pp. 34-44.
11. J.B. Hussein and E.T. Selig. Predicting Compactor Performance. Proc., International Conference on Compaction, Paris, April 1980, Vol. 2, pp. 639-646.
12. E.T. Selig and W.B. Truesdale. Evaluation of Rapid Field Methods for Measuring Compacted Soil Properties. HRB, Highway Research Record 177, 1967, pp. 58-76.
13. E.T. Selig. The Soil Compaction Process and Methods of Measurement. Earthmoving Industry Conference, SAE, Paper No. 710513, April 1971.
14. Y. Lacroix and H.M. Horn. Direct Determination and Indirect Evaluation of Relative Density and Its Use on Earthwork Construction Projects. In Evaluation of Relative Density and Its Role in Geotechnical Projects Involving Cohesionless Soils, ASTM, ASTM STP523, July 1973, pp. 251-280.
15. D.J. Leary and R.J. Woodward. Experience with Relative Density as a Construction Control Criterion. In Evaluation of Relative Density and Its Role in Geotechnical Projects Involving Cohesionless Soils, ASTM, ASTM STP523, July 1973, pp. 381-401.
16. E.T. Selig and R.S. Ladd. Evaluation of Relative Density Measurements and Applications. In Evaluation of Relative Density and Its Role in Geotechnical Projects Involving Cohesionless Soils, ASTM, ASTM STP523, July 1973, pp. 487-504.
17. E.T. Selig. Variability of Compacted Soils. Proc., National Conference on Statistical Quality Control Methodology in Highway and Airfield Construction, Nov. 1966, pp. 181-213.
18. T.G. Williamson and E.J. Yoder. An Investigation of Compaction Variability for Selected Highway Projects in Indiana. Indiana Highway Commission, West Lafayette, Res. Rept., Dec. 1967.
19. T.G. Williamson. Embankment Compaction Variability. Indiana Highway Commission, West Lafayette, Res. Rept., Aug. 1968.
20. H.E. Wahls. Current Specifications, Field Practices, and Problems in Compaction for Highway Purposes. HRB, Highway Research Record 177, 1967, pp. 98-111.
21. J.L. Jorgenson. Development and Trial Use of Acceptance Sampling Plans for Compacted Embankments. HRB, Highway Research Record 357, 1971, pp. 24-34.
22. P.C. Kotzias and A.C. Stamatopoulos. Statistical Quality Control at Kastraki Earth Dam. Journal of the Geotechnical Engineering Division, ASCE, Vol. 101, No. GT9, Sept. 1975, pp. 837-853.
23. J.L. Beaton. Statistical Quality Control in Highway Construction. Journal of the Construction Division, ASCE, Vol. 94, No. CO1, Jan. 1968, pp. 1-15.
24. E.T. Selig. Unified System for Compactor Performance Specification. Transactions, SAE, Warrendale, PA, 1972, pp. 2454-2464.

Embankment Compaction and Quality Control at James Bay Hydroelectric Development

J.-JACQUES PARE, BERNARD BONCOMPAIN, JEAN-MARIE KONRAD, AND NARENDRA S. VERMA

Construction of 220 dams and dykes at the La Grande Complex, James Bay hydroelectric development involves several types of materials (till, sand and gravel, and rockfill) and construction procedures and equipment that must yield embankment zones of desired characteristics. Experience and design requirements, as well as the schedules, economic, and climatic restraints, have led to a general standardization of the specified material placement techniques and conditions. This paper deals with some of the practical aspects of the specifications that are developed with a suitable balance between the procedure and product specifications and reviews the relative importance placed on visual inspections and various control and verification tests. The difficulties encountered with the quality control and verification testing procedures are discussed and comments are made regarding the relative accuracy and suitability of these tests. Typical properties of the embankment materials based on extensive tests carried out on 160 Mm^3 of materials are also included.

The La Grande Complex (phase 1) of the James Bay hydroelectric development involves construction of about 220 earth and rockfill embankment dams and dykes that have a maximum height of 160 m. The complex covers a territory about 800 km long and 400 km wide and is located about 1000 km from Montreal in northern Quebec (Figure 1). Construction of these embankments at the five main project sites, namely La Grande 2 (LG2), LG3, LG4, Eastmain-Opinaca (EOL), and Caniapiscau, began in 1973 and is scheduled to be completed in 1982. The work procedures specifications and the quality control requirements and methods have been developed from the experience acquired at the Manicouagan-Outardes Project in Quebec and the Churchill Falls Project in Labrador, with almost similar geological and climatic conditions.

PROJECT DESCRIPTION

The complex lies within the Canadian Shield, a glaciated peneplain developed on a precambrian basement complex of igneous and metamorphic rocks (1). The project sites are underlain mostly by granitic rocks that range in texture from massive to gneissic. Glacial and fluvio-glacial sediments cover some 80 percent of the region. Glacial till is widespread in the form of ground moraine, locally including some drumlin deposits, and forms an excellent source of impervious material for embankment construction. Eskers and kames constitute the principal source of granular materials for filters, transitions, and

shells. Sensitive marine clay and peat deposits blanket some of the western limits of the area.

The climate is characterized by low temperatures with a mean annual temperature of -4°C. No permafrost has been encountered, although the Geological Survey of Canada maps show that the complex is located within the sporadic permafrost zone. Frost penetration of up to 3 and 9 m has been observed in till deposits and bedrock, respectively (2). Till placement under nonfreezing conditions is limited to about 150 days between May and October. Rainfall during this period, which corresponds to about 65 percent of the total annual precipitation, ranges from about 400 mm at LG2 to about 500 mm at Caniapiscau.

Typical Embankment Characteristics

The construction of the 220 dams and dykes with a total crest length of approximately 130 km involves about 30 Mm^3 of till, 60 Mm^3 of natural granular material or crushed aggregate, and 70 Mm^3 of rockfill. These materials are used in embankments with three principal types of design sections (3), namely rockfill, granular, and homogeneous. The choice of the type is dictated primarily by the material available, the height of embankment, and the foundation conditions.

As a result of well-organized construction facilities, high rates of fill placement (average of more than 1 Mm^3/week at La Grande complex) have been realized despite the difficult placement conditions (4). Typical rates of fill placement in a dam or dyke are summarized as follows:

1. Till core--30 000 m^3/week average, maximum of 120 000 m^3/week at LG2 main dam;
2. Filter and transition--15 000 m^3/week average, maximum of 40 000 m^3/week at LG4 main dam;
3. Granular shell--90 000 m^3/week average, maximum of 240 000 m^3/week at Dyke QA8 at LG4; and
4. Rockfill shell--130 000 m^3/week average, maximum of 450 000 m^3/week at LG2 main dam.

Specifications

Although the embankment construction specifications are prepared individually for each contract to take into account the specific design and construction conditions of the project involved, a general standardization has been achieved so that they vary only slightly between different projects. The specifications have been developed along the following lines:

1. Designation of borrow areas,
2. Product specifications for materials, and
3. Procedure specifications for fill placement.

Tables 1 and 2 and Figure 2 present a summary of specifications for the principal construction mate-

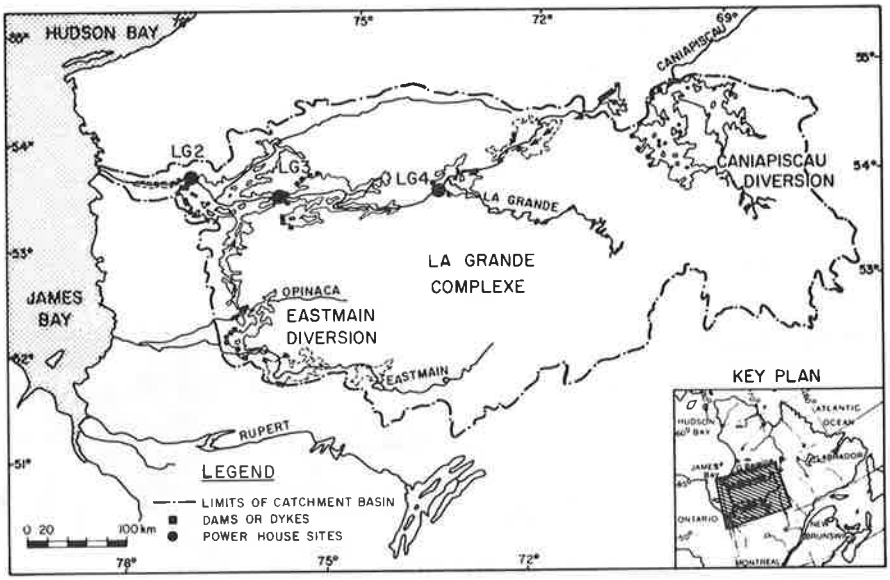

Figure 1. Location of project sites.

Table 1. Summary of material specifications.

Item	Core and Impervious Shell	Filter, Transition, and Granular Shell	Rockfill
Equipment and method	General—selected extraction according to borrow pit conditions, removal of particles > 2/3 of compaction lift thickness, and stripping of organic and weathered materials Wet material—drainage of ground and surface water, extraction on long and shallow faces, and rotary kiln drying Cold weather—use of unfrozen material and use of heated haul trucks	Stripping and drainage, selective extraction, screening, crushing, mixing, washing, and extraction along high faces	Controlled blasting and removal of particles larger than the lift thickness
Product	Within specified gradation envelopes (Figure 4); $w > (w_{opt} - 1$ percent), $w \leq w_{rut}$ or $(w_{opt} + 2$ percent), W_{rut} = water content for which 45-Mg pneumatic roller produces ruts that exceed 15-cm depth in fill surface	Within specified gradation envelopes; Figure 4 for filters and transitions, Figure 7 for pit-run material	Maximum size = lift thickness; less than 5 percent passes No. 200 sieve

rials used in the embankments.

Quality Control

Quality control includes both visual inspection and laboratory testing of materials at the borrow areas as well as on the fill. Visual inspection to control material, equipment, procedure, and product is of utmost importance because it permits a rapid and general evaluation of the quality of work, particularly of the embankment homogeneity. Survey crews and field laboratories provide the necessary technical support to the inspection units.

Three categories of tests are performed:

1. Grain-size analyses and water content determination (carried out at a rate of about 1/5000 m^3 or 1/day and 1/1000 m^3, respectively) for a quick verification of the conformity of materials to specifications;

Table 2. Summary of embankment construction specifications.

Item	Core and Impervious Shell	Filter, Transition, and Granular Shell	Rockfill
Geometry			
Lift thickness	45 cm	45 cm	90 cm for interior zone, 180 cm for exterior zone
Construction tolerance	±30 cm with respect to design lines	±30 cm	±30 cm
Equipment	Pneumatic roller—weight, 45 Mg; loading box for each wheel working independently; tire pressure, 550–650 kPa; operating speed, 5 km/h	Light vibratory roller—weight, 3600 kg, frequency, 1600 rpm; centrifugal force; 90 KN; and operating speed, 5 km/h	Heavy vibratory roller—weight, 9000 kg; frequency, 1200 rpm; centrifugal force, 150 KN; and operating speed, 5 km/h
Passes			
Number	4	4 for light roller, 3 for heavy roller	4
Overlap	25 percent	25 percent	25 percent
Required fill density, not specified	90 percent of results > 97 percent of standard Proctor maximum density; 100 percent of results > 95 percent γ_{max}	90 percent of results > 70 percent relative density or 95 percent of maximum target density; 100 percent of results > 65 percent relative density or 90 percent of maximum target density	None
Payment	By m^3 of material placed, including extraction, processing, transport, handling, and compaction; for additional compaction by hour when required density is not obtained by specified procedure; and lump sum for kiln drying and winter protection	Same as for core	Same as for core

Figure 2. Gradation specifications.

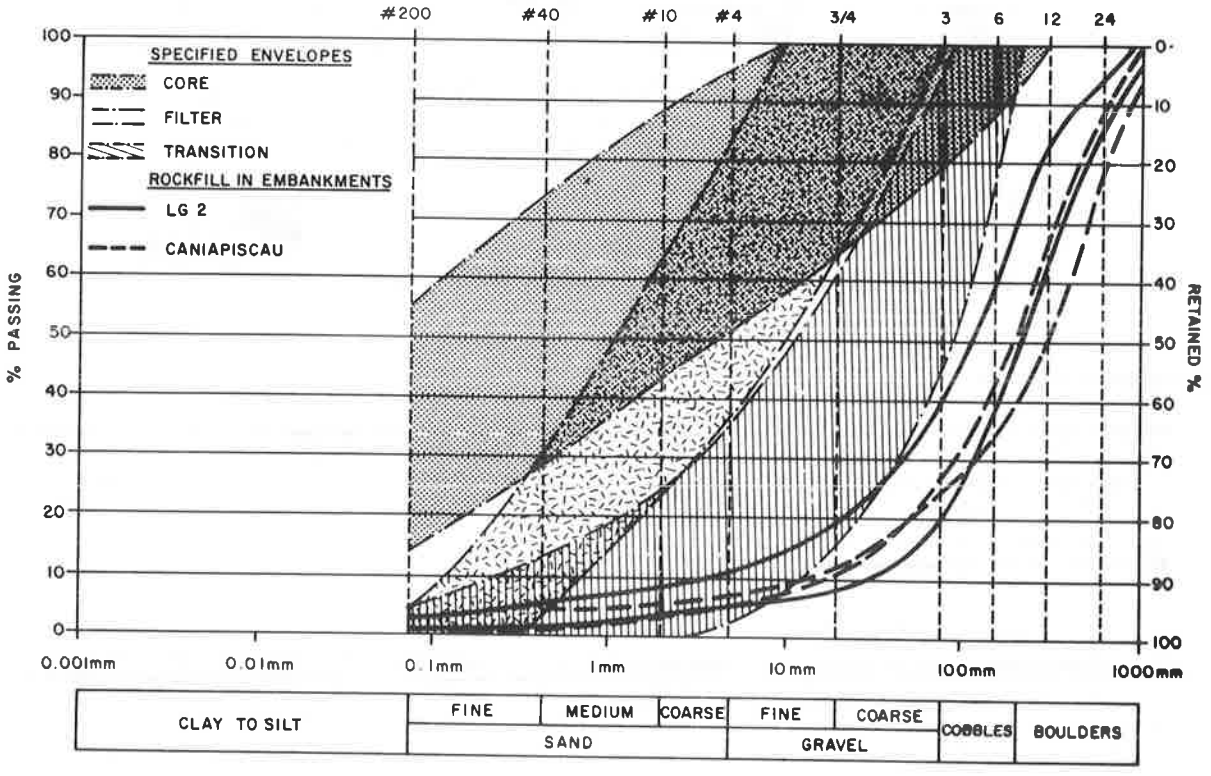

2. Measurement of field densities and reference or target densities on a regular basis with a frequency of about 1/5000 m^3 or 1/day to monitor uniformity of fill placement; and
3. Determination of permeability, compressibility, and strength characteristics of the embankment materials, carried out annually to verify the conformity of the material properties with the design assumptions.

TILL

The till encountered at the La Grande Complex and used for the impervious zones is generally a nonplastic, well-graded silty sand and gravel material with cobbles and boulders (Figures 2-4). This material is easy to compact when it is not too wet and provides a compacted fill of adequate imperviousness ($k = 10^{-5}$ to 10^{-7} cm/s). The main construction problems to be tackled during borrow pit exploitation and placement of the till are related to the presence of the oversize boulders, the natural variations in water content, and the susceptibility to frost.

Material Selection

Selective extraction, based on visual inspection, in the borrow area is the first step to obtain material of desired gradation characteristics. Oversize boulders are eliminated at the borrow areas by putting them aside in stockpiles or by means of grizzly- or kolman-type separators and on the embankment by passing a rake through the lifts. Such scalping on the embankment surfaces, although permitted in the technical specifications, is not encouraged due to the likelihood of segregation and contamination of the adjacent zones. Figure 3 shows two gradation envelopes for the same material for a given site, one as it existed in the borrow area and the other as placed in the embankment. It demonstrates the effectiveness of these control and processes.

The water content in the borrow pits is variable. The commonly encountered and maximum variations of the natural water content with respect to the standard Proctor optimum water content is about 2-3 percent and 5 percent, respectively. Water content of the wet material was adjusted at the borrow pit by suitable surface drainage, proper excavation techniques, and stockpiling to facilitate drainage and aeration. Watering on the embankment is also employed occasionally.

Kiln dryers have been used successfully when needed to meet the high production rate requirement or in the case of wet borrow areas. Use of such a plant allows fill placement during rainy or cold periods and extends the construction period by about 50 days. The rate of material processing that corresponds to a moisture content reduction of about 2-3 percent was about 450 Mg/h--the energy consumption increases with the required change in moisture content.

In view of the need to use heavy haul trucks to meet construction schedules and based on a detailed program for testing equipment performance, the 45-ton rubber-tired rollers were used with four independent loading boxes. This choice has proven to be satisfactory and has ensured better compaction for till with a relatively high percentage of boulders and cobbles and with moisture content generally above the optimum value.

Specifications permit neither the placement of frozen material in the core nor the placement of till on frozen surfaces. Protection against frost is therefore required to minimize the volume of frozen fill that must be excavated and thus allow a rapid resumption of work in the spring. Such protection has been obtained by placement of a 3-m thick layer of granular material, a 2-m thick layer of manufactured snow, or an appropriate combination. The first method is particularly suitable for dykes that have granular shoulder zones where protection material can be reused in the embankment.

Visual Inspection

The main items on which the visual inspection efforts were concentrated are as follows:

1. Material quality and presence of contaminants;
2. Material gradation and homogeneity;
3. Water content, presence of wet spots, and ruts;
4. Condition at interfaces of embankment zones;
5. Roller type, weight, speed, and tire pressure;
6. Placement, lift thickness, number of passes, and overlap between passes; and
7. Ambiant climatic conditions.

Material Control Tests

The determination of water content has been performed either by 18-h oven drying as per ASTM D2216-71 or by rapid drying (20 min) in a microwave oven or in a moisture teller apparatus. Both methods have provided identical results. The speedy moisture tester and the nucleodensitometer did not give satisfactory results compared with those of the oven-drying method and have not been employed. In order to achieve a procedural uniformity that permits a valid comparison between samples from borrow area or fill and between tests for natural and optimum values, the testing of moisture content has been carried out on a specified fraction of the material (fraction smaller than the gravel size). Analyses of grain size distribution have been performed in the laboratory by sieve and hydrometer analyses after removal of boulder and cobble sizes on the fill.

Compaction Control Tests

Evaluation of the material compactness and homogeneity has been based on a comparison of the field dry density with the maximum Proctor density corrected for the gravel content of the sample as per relationship developed by the U.S. Bureau of Reclamation (E-38) Earth Manual 1974.

In Situ Density

Two procedures, the sand cone and the nucleodensitometer, have been used to measure the field densities. At the early stages of construction at LG2 and EOL, although both procedures were employed simultaneously, confidence was placed in the results of the sand-cone test. The nucleodensitometer densities were corrected based on the results of parallel testing done by these two methods, such as shown on Figure 5. Progressively with experience, due confidence was placed on the results of the tests by nucleodensitometers that were regularly calibrated.

The collective experience gained at all project sites over the years has shown that numerous factors, in addition to those considered in the testing standards, influence the accuracy of the results of both types of tests. Thus, the results of the sand-cone test are prone to errors due to cone volume changes in a wet material and to the vibrations generated by the nearby construction operations. Similarly, the nucleodensitometer results are influenced by depth of probe penetration and by the presence of cobbles within the energy flux field and

the accuracy of the apparatus that may be sensitive to field conditions. Nevertheless, the nucleodensitometer has proven to be a quick and reliable apparatus for field-density measurements provided its calibration is checked regularly and four measurements in the crosswire positions are made with a probe penetration of 20 cm for each test.

Maximum Density and Optimum Water Content

The optimum water contents and the maximum dry den-

Figure 3. Till gradation in borrow pits and as placed in embankments.

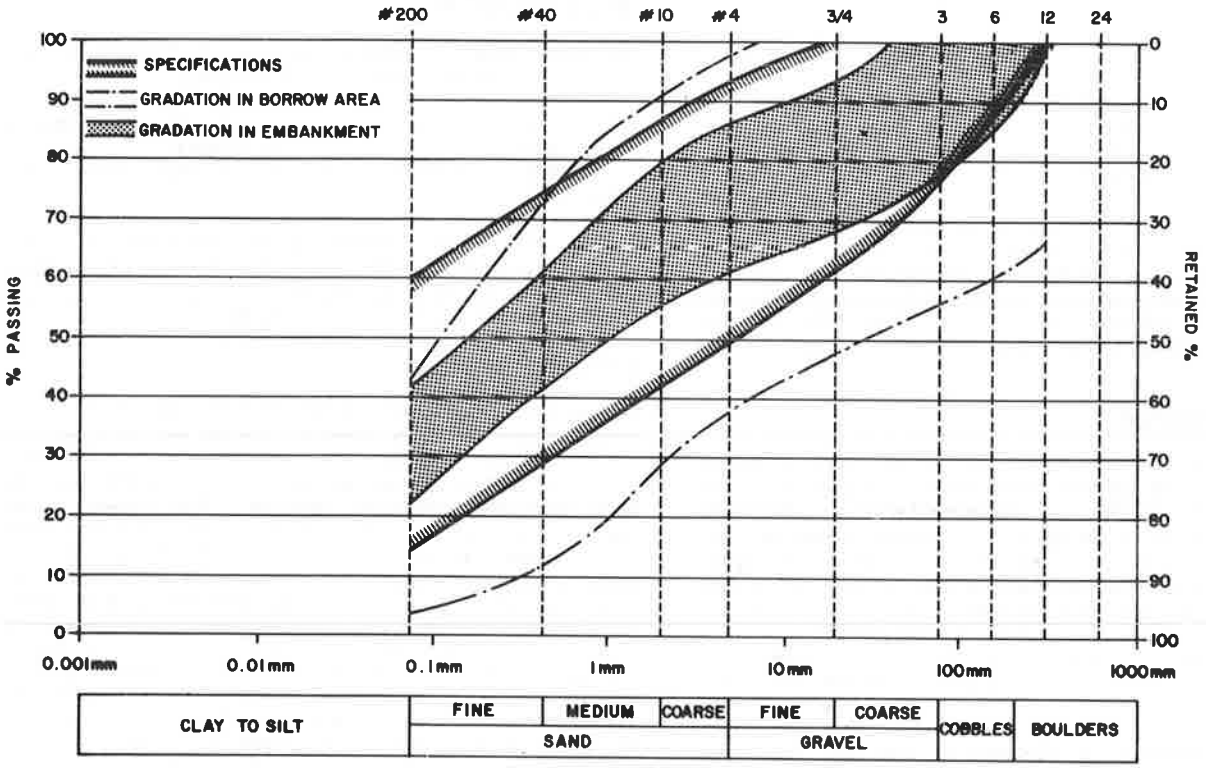

Figure 4. Mean gradation of placed till at different sites.

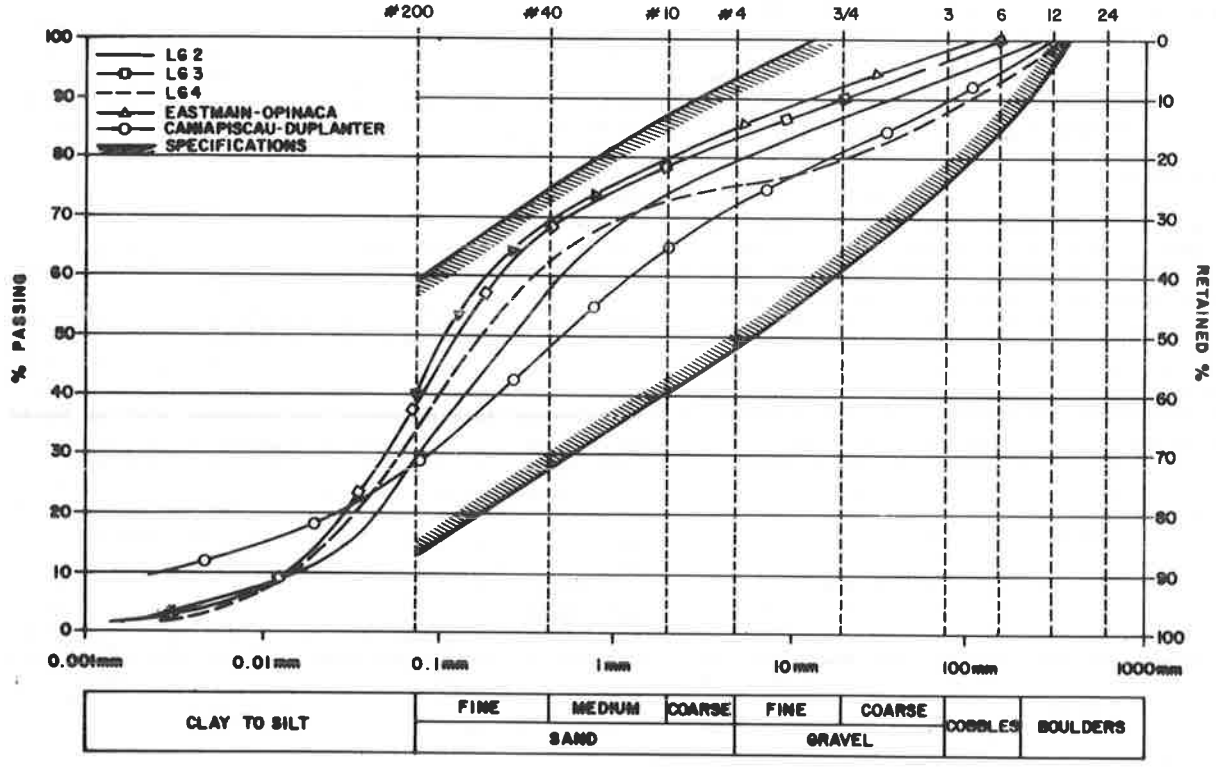

sities have been determined according to ASTM D698-70, A or D. Whereas the method A tests are easier and faster to perform, the method D tests are considered to be better suited to the overall gradation of the material. Table 3 and Figure 6 present a comparison of the method A results corrected for coarse fractions with the corresponding results determined in a large rigid box or by method D. These tests have demonstrated that both method D and method A (when duly corrected for the coarse fraction) as used for the till with oversize fractions not exceeding 30 percent of the total volume gave results that were considered to be in good agreement with reality. Some rapid estimation methods that involve relations between gradation characteristics and maximum density have also been developed in order to complement the standard Proctor tests.

The maximum dry density varies between 2.0 and 2.2 Mg/m³ and the corresponding optimum water content varies between 7.3 and 8.2 percent. The fill densities correspond to about 97 to 99 percent (percentage compaction) of the standard Proctor maximum density at LG3, LG4, and Caniapiscau. Somewhat high average compactions (99-100 percent) were observed at LG2 and EOL and are attributed to an overestimate of the in situ density determined by the sand-cone method.

GRANULAR MATERIAL

The specified gradation limits for the shell zones are well adapted to the broad range, which varies from uniform fine sands to coarse gravels, in the borrow areas. The material processing limited to scalping of the boulders of sizes in excess of 30 cm and to elimination of the zones of fine sand concentration has been adequate and satisfactory.

The granular materials used in the filter and transition zones required selective exploitation of borrow pits or special processing in order to meet the following filter design criteria (where B and F correspond to the base and filter materials, respectively):

1. $D_{15F} \geq 5D_{15B}$,
2. $D_{15F} \leq 5D_{85B}$,
3. Less than 5 percent of the filter material passes sieve no. 200, and
4. Parallelism of the gradation curves of both materials.

The gradation of the filter zones is designed with respect to the gradation of the till matrix (i.e., the fraction that passes sieve no. 4, which in fact is the material to be protected against erosion). Processing of sand and gravel deposits was performed when needed to produce material that meets these filter criteria, including screening, crushing, and mixing, while erecting stockpiles at the borrow pits. Typical gradation curves for a filter material as it existed in the borrow pit and as placed in the embankment are shown in Figure 7.

Since the sand and gravel deposits are relatively heterogeneous, a selective exploitation was employed to minimize the processing and maximize the homogeneity of the fill material. Segregation in the stockpiles was also significantly reduced by erecting stockpiles of limited height in layers less than 1-m thick. Gradation analyses are carried out on a regular basis before and after treatment of the material at the borrow pits, in the stockpiles, and on the embankments.

Placement

The construction problems encountered during the placement of the granular materials were generally related to segregation, contamination, and over com-

Figure 5. Comparison of till densities determined by sand cone and nucleodensitometer.

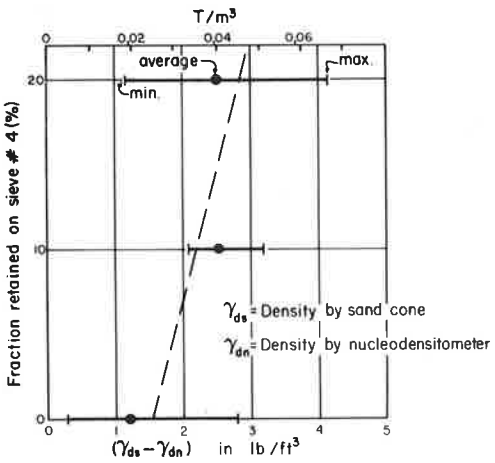

Figure 6. Accuracy of standard Proctor method A densities.

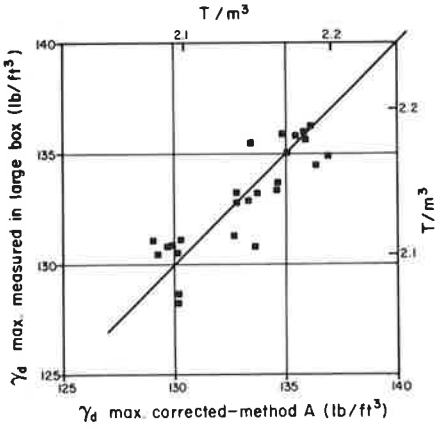

Table 3. Comparison between standard Proctor methods D and A with oversize gravel correction.

Site	Borrow Area	No. of Tests		Fraction Smaller Than		$\gamma_{d\,max}$ Method A (Mg/m³)	$\gamma_{d\,max}$ (A) Corrected (Mg/m³)	$\gamma_{d\,max}$ Method D (Mg/m³)	w_{opt} Method A (%)	w_{opt} Method D (%)
		Method A	Method D	19 mm	4.8 mm[a]					
LG 2	G and J	470	164	93	86	2.07	2.11	2.12	7.6	6.7
Caniapiscau	A2	20	20	96	88	2.11	2.15	2.16	7.8	7.5
	A1	4	17	91	82	2.12	2.16	2.16	8.0	7.6
	A8	8	20	90	80	2.18	2.21	2.19	7.5	6.9

Note: The results presented above represent average values based on tests carried out on materials of relatively similar gradation characteristics for each borrow area.
[a]Sieve no. 4.

Figure 7. Gradation filter material in borrow pits and embankment, dike TA-24 - LG 3.

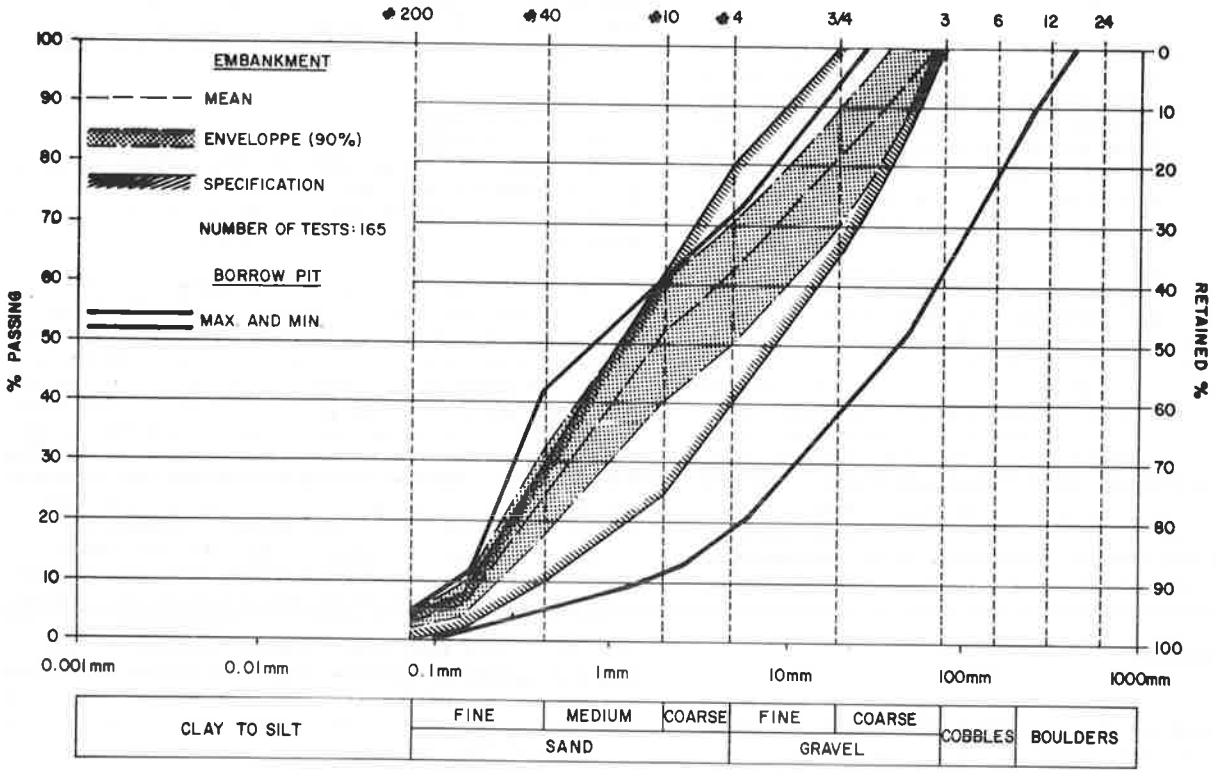

paction. Segregation that creates conditions conducive to internal erosion and piping has been curbed by limiting the maximum particle size to 75 mm in the filters and to 150 mm in the transitions, by pushing with grader blades the coarse fractions toward the outer limits of the zones, and by raking at the zone interface to produce progressively changing material.

In order to limit the contamination of the filter and transition zones with the till from the adjacent core due to traffic or due to washing during rainfall, the placement of the filter material with one layer in advance of the core material was adopted and has proven to be effective. The problem of over compaction, which is a result of the shape, size, and well-graded nature of the material rendering it easy to compact, has been handled by reducing the number of passes of the vibratory rollers by one and by restricting construction traffic over these zones.

Quality Control

Quality control for the granular materials involves visual inspection, which is aided and complemented with laboratory testing and surveying. The homogeneity of the fill is examined occasionally by excavations of trenches. Visual inspection is directed at controlling

1. Gradation with rapid determinations of the fraction that passes the no. 200 sieve,
2. Lift thickness,
3. Water content (wetting of the lift may be necessary), and
4. Number of passes, overlap, speed, and frequency of vibration of the rollers.

Testing is performed to determine the gradation characteristics, the in situ density of fill, and the corresponding maximum-minimum of a target maximum density. The in situ densities are measured by the water replacement method (by using 0.4 m and 1.3 m diameter rings for the filter and transition zones, respectively) or with a nuclear device. Based on the experience of the Société d'énergie de la Baie James as well as that of others (5), the results of relative density tests are prone to significant variations due to slight variations in testing procedures and materials. Thus, whereas this method was found to be satisfactory for relatively homogeneous materials of filter zones, its use for the shell materials that have a significantly wide range of gradation characteristics was considered unsatisfactory. The use of relative compaction (in situ density expressed as a percentage of a target density for material of similar gradation) has been found to be more suitable and has been employed for shell zones.

Target density represents the average of the upper 10 percent of a large number of density measurements and was determined with respect to the percentage of material that passes sieve no. 4. The empirical relation between the target density and the percentage of gravel fraction, as developed at LG4, is shown in Figure 8. A density that corresponds to 95 percent of the target density has been found to be equivalent to a relative density of about 70 percent.

Comparative tests were performed on the filter material at LG3 to ascertain the relative accuracy of the in situ density testing with a 0.5-m diameter ring and with the nuclear device by using four cross-wire reading positions and the probe lowered to 25-cm depth. As shown in Figure 9, densities obtained from the water replacement method are generally higher than those given by the nucleodensitometer, the difference increasing with density. Further investigations carried out on material of known

Figure 8. Embankment dry density (maximum 10 percent) versus percentage gravel.

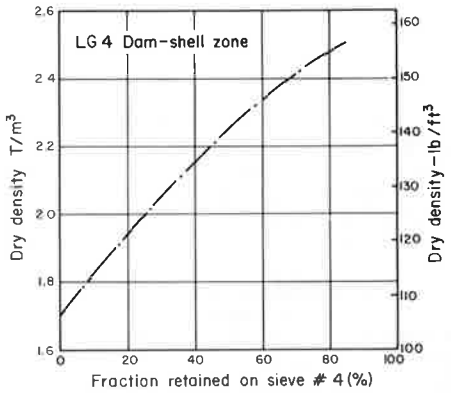

Figure 9. Comparison of water replacement and nucleodensitometer methods.

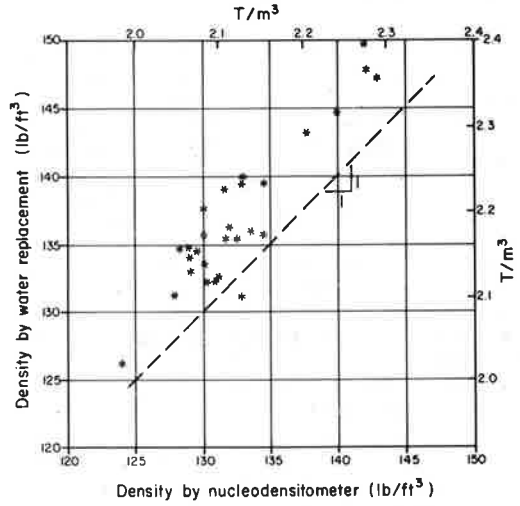

density (placed in a rigid box) showed that the wet density measured with the nuclear device increased with increasing depth of the probe up to a depth of 15 cm, and the variation diminished thereafter (Figure 10). Studies carried out in a test box revealed that, for a pit-run granular material, the mean density deduced from the water replacement method is approximately 1-2 percent higher than density based on direct measurements of the weight and size of the box. The use of the nuclear device with the probe lowered to 15 cm or more is thus considered a satisfactory method for rapid evaluation of the in situ density of granular material provided the results obtained are calibrated against the water replacement method.

Following the specified compaction procedures and this new approach of compaction evaluation, the granular materials at different project sites have been found to be at 95-97 percent relative compaction (2.0-2.2 Mg/m³). Statistical analyses for the transition material has shown that the specified compaction with heavy vibratory rollers (10 Mg, 3 passes) produces good results with a density of about 2.30 Mg/m³.

ROCKFILL

In addition to the visual inspection of particle sizes, lift thicknesses, and number of passes of the 10-Mg vibratory rollers, quality control of the

Figure 10. Density variation with depth of nucleodensitometer probe.

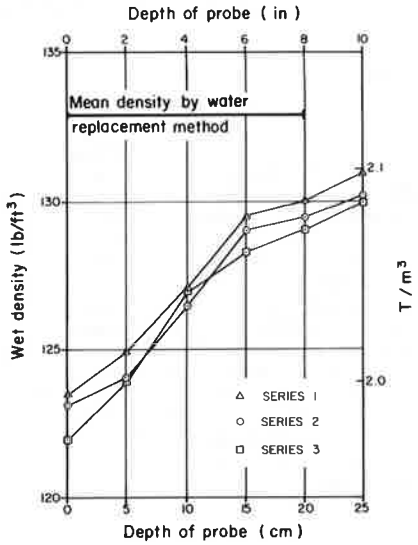

rockfill shell zones involved occasional measurement of the in situ density by the water replacement method in large-scale test pits and the determination of the distribution of grain size of the material excavated from these pits. Roller effectiveness tests were sometimes performed by measuring surface settlement with respect to the number of passes. The results of grain size analyses performed at LG2 and Caniapiscau are shown in Figure 2. In situ dry densities of 2.24 and 2.16 Mg/m³ were measured at LG2 and Caniapiscau, respectively.

ACKNOWLEDGMENT

We express our appreciation to La Société d'énergie de la Baie James for permission to publish this paper. The close collaboration among the society's engineering and construction departments, the consulting engineering firms, and the society's Board of Engineering Consultants is acknowledged. Thanks are due to the geotechnical laboratories (Laboratoire Ville Marie, Laboratoire de Béton, Terratech Ltd., and Laboratoire d'inspection et d'essais, Inc.) who performed the field tests.

REFERENCES

1. D.K. Murphy and J. Levay. Engineering Geology in the La Grande Complex, Quebec. ASCE National Convention, New York, 1981.
2. J.J. Pare, J.G. Lavalle, and P. Rosenberg. Frost Penetration Studies in Glacial Till on the James Bay Hydroelectric Complex. Canadian Geotechnical Journal, Vol. 15, No. 4, 1978.
3. J.J. Pare, G.S. Larocque, and C.E. Schneeberger. Design of Earth and Rockfill Dams for La Grange Hydroelectric Complex in Northern Quebec. Water Power and Dam Construction Journal, 1978.
4. A.D. McConnel, J.J. Pare, N.S. Verma, and D.A.B. Rattue. Materials and Construction Methods for the Dam and Dyke Embankments of the LG4 Project. 14th Congress of Large Dams, Rio de Janeiro, Brazil, May 3-7, 1982.
5. F.A. Tavenas, R.S. Ladd, and P. La Rochelle. Accuracy of Relative Density Measurements. Results of a Comparative Test Program. 75th Annual ASTM Meeting on Evaluation of Relative Density and Its Role in Geotechnical Projects Involving Cohesionless Soils, 1972.

Prediction of Roller Compaction Efficiency

R.N. YONG AND E.A. FATTAH

The usual procedure for specification of roller equipment, lift thickness, and number of passes to compact a soil fill material of prescribed water content to an optimum density is one that heretofore has traditionally depended on empirical relations and similitude modeling—the use of laboratory-derived test data on soil compaction. In this study, soil compaction under a towed roller is predicted by using the finite-element method (FEM) of analysis. The format of the analysis encompasses the transient loading nature of the tire or roller. By expressing the compaction effort exercised by the rigid roller in terms of the amount of compaction energy required to produce a resultant unit deformation of a particular soil lift thickness, FEM analysis allows one to obtain an evaluation of the influence of soil type, lift thickness, water content, and number of passes on compaction efficiency. In addition, the format for analysis is structured to incorporate compaction of additional soil layers through a layered soil-analysis procedure. The analysis of soil compaction efficiency is supported with corresponding laboratory experiments that involve wheel tow-bin tests.

The general procedure for specification of size and capability of roller equipment for compaction of soil fill material is one that depends on prior experience and assessment of results obtained from laboratory compaction tests on the soil fill material. The questions that need to be answered in a compaction program can be stated simply as follows:

1. What type and size of roller? and
2. What is the lift thickness? Number of passes? Soil water content?

The answers to the above questions are not always sought through rigorous analytical means because of the lack of analytical models that deal specifically with the coupled surface interaction between roller and soil. By and large, available analytical techniques generally regard the problem of compaction as a simple boundary value problem and thus concern themselves with soil deformation under load.

The problem of interest, because of present concern for energy conservation, is one that is posed in terms of roller compaction efficiency. [i.e., "How efficient is a particular roller in compacting a specified (known) soil?"] The input energy (work done) required by a roller to produce a specific degree of compaction is a function of the following:

1. Roller type--rigid or pneumatic tire;
2. Roller loading--speed, slip, towed or self powered, and arrangement of rollers (tires);
3. Tire properties and characteristics--diameter, width, cross-sectional shape, aspect ratio, inflation pressure, carcass stiffness and shape, tire structure, and tire material properties (note that, for this particular study, although tests were also performed with pneumatic tires, because of the very extensive data and results available, only the rigid roller results will be discussed); and
4. Soil--stress-strain behavior in loading and unloading composition and type, density, moisture content, saturation, soil structure, and confining pressure.

Efficient soil compaction matches the soil response (load or rebound) characteristics with lift thickness, number of passes, and roller loading features to produce the maximum soil density for the desired fill thickness with the least amount of input work (roller passes and energy input).

Compaction of layers of soil is increased by increasing the magnitude of roller-imposed normal stresses established at the roller-soil interface; however, note that, if the roller-imposed normal stresses exceed the local bearing capacity of the soil, the soil will extrude or flow under the rollers instead of compacting. This is obviously not an efficient compaction process.

In this study an analytical model is established (a) to calculate the amount of work done in compaction per unit distance traveled by a moving roller for every pass and (b) to determine the total work required to produce a certain soil density or permanent deformation of the soil layer. Soil compaction under a moving roller is predicted by using the finite-element method (FEM) of analysis. The format of the analysis encompasses the transient loading nature of the roller (or tire). By expressing the compaction effort delivered by the rigid roller in terms of the amount of compaction energy required to produce a specific resultant dry density of a particular soil lift thickness, FEM analysis allows one to obtain an evaluation of the influence of soil type, lift thickness, water content, and number of passes on compaction efficiency. Roller compaction efficiency is evaluated by comparing the work spent by the roller to produce certain density with that obtained in a standard Proctor test. Note that expression of compaction efficiency with reference to the standard Proctor test technique is arbitrary (i.e., the standard Proctor density is taken as optimum for a convenient reference state).

The experimental program in this study uses a soil tow-bin and, for roller soil, compaction that covers the range of soil from loosely placed soil to fully compacted soil (i.e., no further change in the density of the compacted soil with increasing number of passes). Because of the phenomenon of local shear failure in the first pass, the analytical portion of the study directs its attention to compaction of the soil layers beyond the first pass loose soil compaction.

METHOD OF ANALYSIS

The performance of a roller that moves with constant speed on a soil surface is analyzed by applying the principle of energy conservation. The energy balance relation equates the roller input energy (powered roller) or pull energy (towed roller) to the sum of the following energy components (Figure 1):

1. Energy spent in compacting the soil,
2. Energy dissipated at roller-soil interface through slip between roller and soil surface,
3. Energy dissipated because of distortion of the roller under load (this form of energy dissipation is negligibly small in the case of rigid rollers), and
4. Output energy (powered roller); i.e., drawbar pull. (In the case of a towed roller system, drawbar pull is zero and sometimes even negative.)

For convenience in presentation of the analysis, it is assumed that at any stage of roller compaction, the soil continuum consists of two layers, as shown in Figure 2 (1). The underlying soil layer (i.e., the previously compacted layer) has reached optimum or close to optimum density and can be as-

sumed to remain in the as compacted state. The top layer is the current soil layer to be compacted and is analyzed accordingly. If desired, a multilayered compaction analysis can be performed where the underlying layers are also analyzed and considered as undergoing further densification. However, by and large, the increases in densities in the underlying layers are small--if efficient compaction is achieved--and can be ignored as a first approximation in the analysis given here.

Figure 1. Roller-soil energy systems.

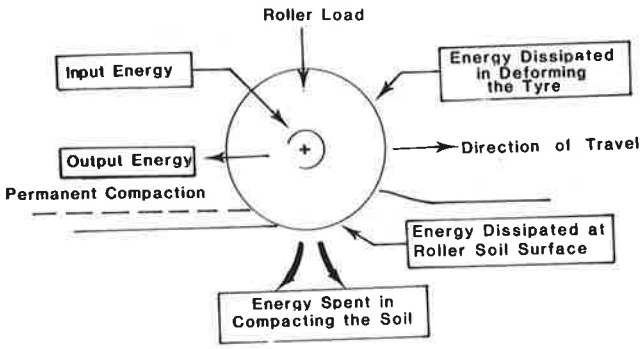

Figure 2. Idealized soil continuum showing a developed two-layer system.

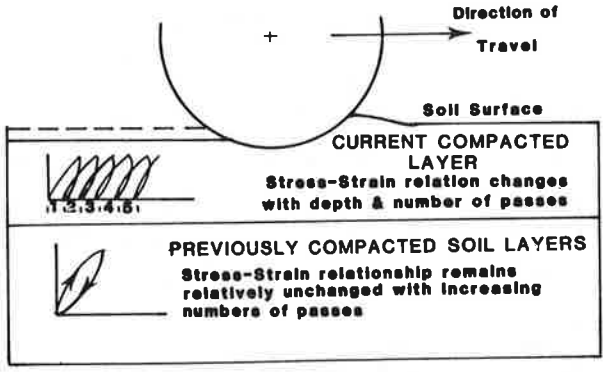

ANALYTICAL RELATIONS

The governing equations used for the FEM analysis developed for rigid wheel motion by Yong and Fattah (2) and extended for pneumatic tire motion on soft soil (3) has been adapted for soil compaction analysis (4) and need not be repeated here. Since the rollers (tires) used for compaction are relatively wide, a plane-strain type of analysis can be adopted and all calculations are given in terms of a unit width of the roller. The boundary conditions that satisfy the actual physical roller-soil interaction behavior can be specified in terms of loads or displacements. For this study, the load boundary condition was used.

Load Boundary Conditions

To specify the load boundary at the roller-soil interface two items are required: (a) stress-distribution due to roller load and forward motion and (b) contact area. The roller-soil interfacial stresses can be determined from continuum mechanics; however, the problem solution can be complex because of (a) the transient type of soil loading, (b) the nonlinearity of the soil stress-strain relations, (c) roller distortion under load and in motion, and (d) relative movements at the roller-soil interface due to slip. To simplify the problem solution, the interfacial stress distribution can be specified in terms of known distributions based on previously available, or reported, measurements (5).

Constitutive Relations

Since the roller load imposed in compaction is a transient type of loading, any point in the soil continuum is subjected to a state of loading or unloading according to its position with respect to the roller (i.e., for each roller pass the soil is subjected to a complete stress-reversal cycle). The constitutive relation should, therefore, encompass a complete stress-reversal cycle. Because of the nonlinear stress-strain behavior of the soil, a nonlinear elastic response was used to represent the

Figure 3. Finite element idealization.

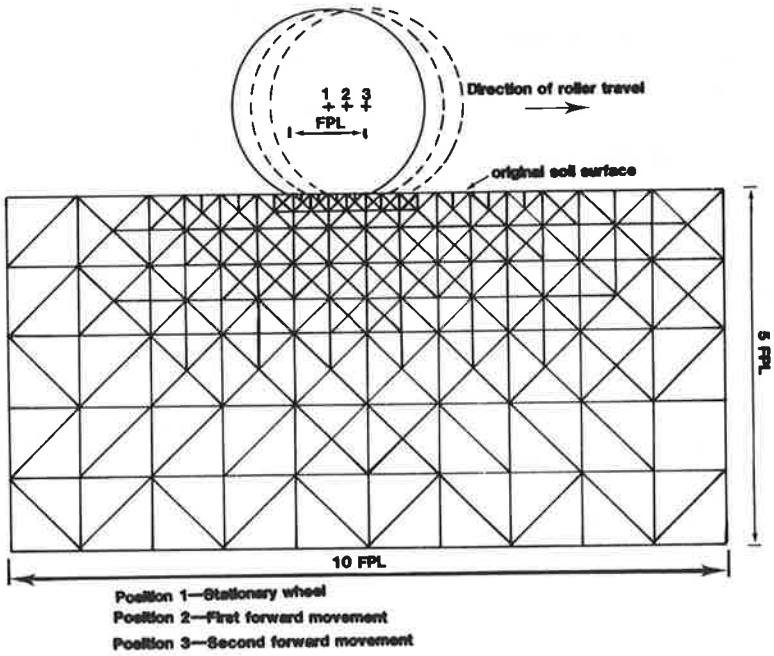

soil during loading and an elastic response was used for the unloading process. For loading and unloading of a soil element the following code was used in the analysis:

$$W = \sigma_{ij} de_{ij} \quad (1)$$

where

σ_{ij} = state of stress,
de_{ij} = incremental state of strain,
If $\Delta W < 0$ the element is unloading, and
$\Delta W > 0$ the element is loading.

ANALYTICAL SOLUTION

The finite element used in the problem solution is shown in Figure 3. For simplicity, the idealization, which is dimensionless, is essentially a function of the contact length of roller at the roller-soil interface. This is identified as the footprint length (FPL).

For this study the displacement and load boundary conditions were used and an incremental technique employed for problem solution. The complete solution, which covers roller motion from a stationary start to a constant travel speed, can be obtained by using the incremental displacement approach in two major steps.

The stationary roller position is considered first and the subsoil stresses, strains, displacements, and the roller-soil interfacial reactions are calculated accordingly. Displacement boundary conditions are applied in the form of vertical displacement increments and stresses calculated at the end of each increment by using the nonlinear stress-strain relations. These are then augmented to their previous values and the process continued until the augmented vertical reactions at the roller-soil interface reach the value of the roller load.

At the end of each vertical displacement increment the possibility of contact occurence of a new node with the roller is checked as follows:

$$\delta_o - \delta_i > Z_i \quad (2)$$

where

δ_i = vertical displacement of the soil surface at node i,
Z_i = initial gap between the roller and soil surface at node i, and
δ_o = vertical displacement increment of the roller.

The second step in the solution is to assume that the roller is moving with a constant speed. For a steady-state roller loading and homogeneous soil, any tracer object will describe the same particle path as any other placed at the same initial depth. Hence, the displacements of any nodal point on the soil surface can be determined with knowledge of the particle path and the original position of the nodal point with respect to the intersection of the roller centerline with the original soil surface.

By using equal increments of time or roller distances, the nodal displacements at the roller-soil interface can be determined, provided the shape of the particle path is known. The boundary displacements are used as the loading boundary required for calculating roller-soil interfacial stresses, subsoil stresses, and strains. This process is continued and the results are added to previous values until the summation of the vertical reactions at roller-soil interface remain constant with any incremental roller travel distance.

The technique for using the load boundary condition at roller-soil interface is similar to the second step used--the displacement boundary approach. The implementation of the analysis calls for one to determine the stresses and displacements in the soil beneath the roller with the roller center in position 1 (Figure 3). This computational procedure is repeated by moving the roller center to position 2. Note, however, that in moving the roller from position 1 to 2, unloading at position 1 occurs as loading in position 2 occurs. The solution is essentially applied in the continuous roller travel on the soil surface by taking successive roller positions. This procedure accounts for the transient motion of the roller (i.e., the solution format is a pseudo-kinematic procedure). Since the state of stress in the soil at the end of the increment depends on the initial state of stress established at the beginning of the travel increment, the incremental roller travel computational procedure is terminated automatically when the state of stress at any point in the soil at fixed coordinates with respect to roller center does not change significantly with the imposition of the next increment.

EXPERIMENTAL PROGRAM

The experimental program was designed to provide information to serve as input and to verify the predicted results of the analytical model.

Soil Properties and Roller Characteristics

The soil used in the experiments was a mixture of English paper clay kaolinite and fine silica sand that passes sieve no. 30 in the ratio of 1 to 4, respectively. Figure 4 shows the results of standard Proctor compaction tests for different soil mixtures, from which the ratio of 1 to 4 was chosen. The liquid limit for the kaolinite was 54 percent, plastic limit was 37 percent, and specific gravity was 2.62.

To obtain the relevant soil mechanical properties, soil samples were prepared at different initial densities and tested in plane strain compression. Typical stress-strain curves for the soils are shown in Figure 5. These are used as input to the analytical model.

The model rigid roller used was 35 cm in diameter, with a width of 9.5 cm.

Tow-Bin Tests

The moving roller tests were performed in a soil bin that was 200-cm long, 30-cm deep, and 10-cm wide to permit plane strain test conditions. The following parameters were considered:

1. Roller load was 31.75 kg and 45.81 kg,
2. Translational speed was 17.3 cm/s, and
3. Number of roller passes was a maximum of 16.

The following measurements were made:

1. Surficial, such as drawbar pull, input torque, and rut depth and
2. Subsurface, such as soil deformations as a function of time by using an automatic motor drive camera.

The soil properties such as density, vane shear strength, water content, and unconfining compressive strength, were measured before and after roller-soil compaction.

Figure 4. Standard Proctor test.

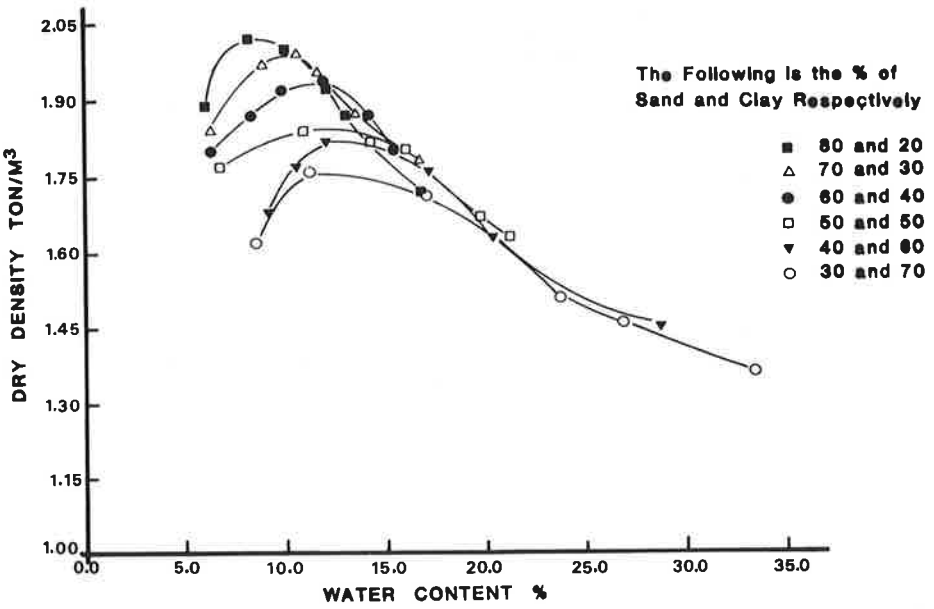

Figure 5. Stress-strain curve of clayey sand.

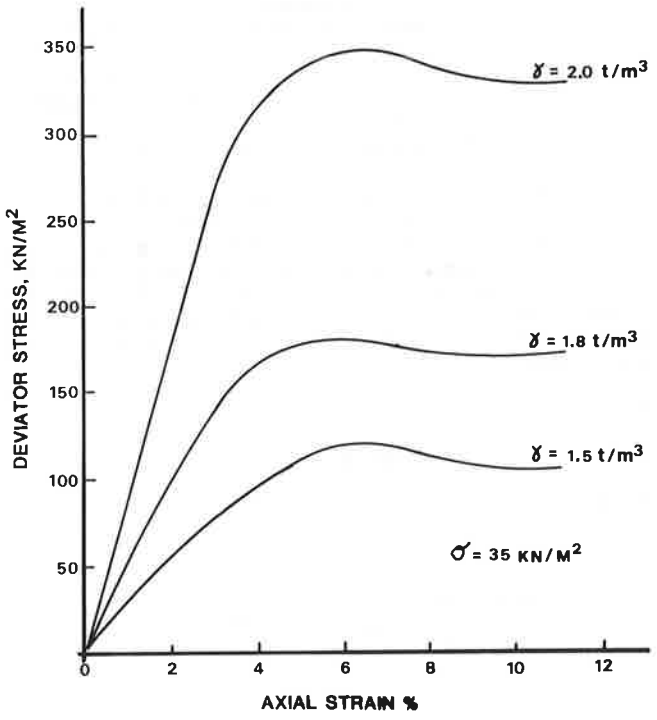

Figure 6. Effect of number of passes on soil surface deformation.

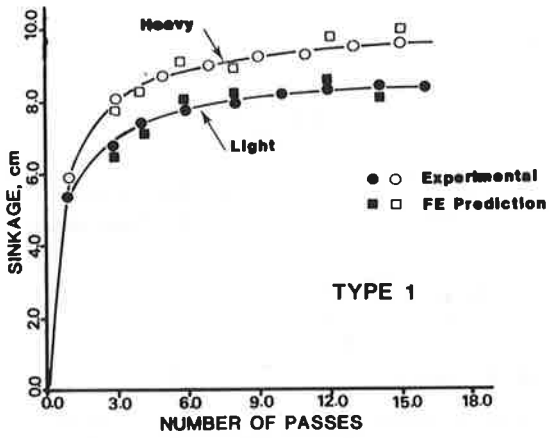

RESULTS AND DISCUSSION

Since the analytical model used in this study is basically a continuum mechanics approach for solving a boundary value problem, the FEM solution predicts the subsoil stresses, strains, deformations, and deformation energies that result from roller motion on the soil in the compaction process. The calculation procedures also allow for determination of surface deformations, roller motion resistance, changes in the roller-subsoil densities, and hence the work done.

Figure 6 shows the effects of the number of passes on soil surface permanent deformation for the case of smooth towed rigid roller. As expected, the initial sinkage is high and decreases as the number of passes increases, to the point where the sinkage becomes relatively constant after a certain number of passes, according to the type and initial condition of the tested soil. The results show good agreement between the finite-element prediction and the measured sinkage values. Note that the analytical model is used to predict the performance of the roller after the first pass.

Figure 7 shows the finite-element predicted and measured density profile after 16 passes. The change in density is determined by calculating the change in the area of every finite element after every pass. The predicted values agree with the measured values.

Figure 8 shows the predicted and measured roller rolling resistance (towed force) as a function of number of passes. The rapid decrease in the rolling resistance with increasing number of passes is expected because of the increase in density of the soil. The stiffness and strength of the soil layer will increase correspondingly, and surface deformations will decrease with the increasing number of passes.

Figure 7. Dry density versus depth after 16 passes.

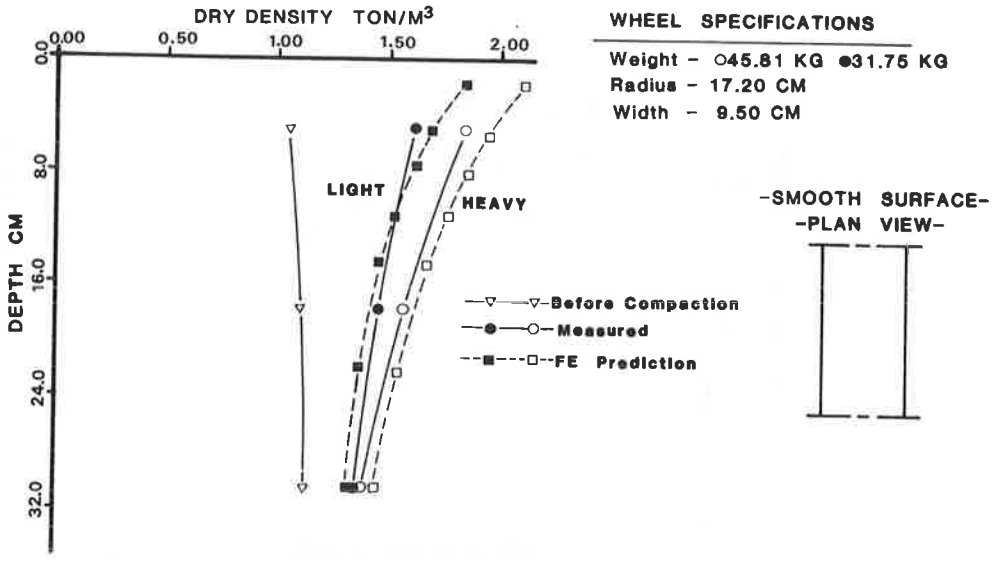

Figure 8. Effect of number of passes on towed roller motion resistance.

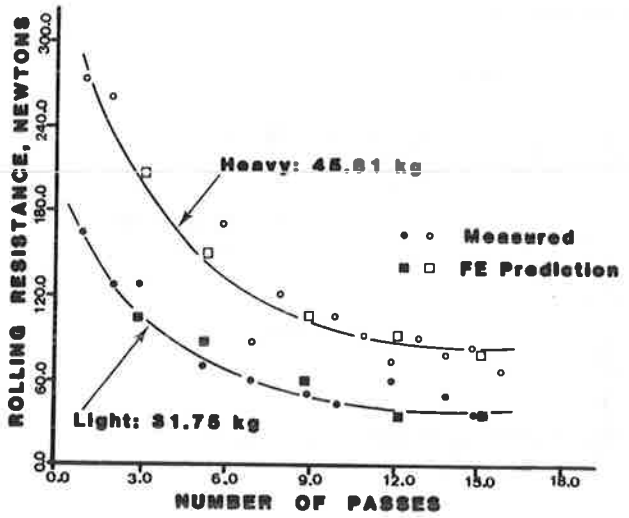

Figure 9 shows the relations for the energy spent in compacting the soil versus dry density. In this figure the finite-element-predicted results are compared with those calculated from the roller multipass tests and the Proctor mold and ram tests. Note that the increasing density is an average of several values obtained throughout the soil density profile.

In the FEM, the energy spent in compacting the soil is calculated at each incremental roller travel distance in each finite element by using the following formula.

For the constant strain triangular element,

$$W = (1/2\Delta X)\,[\sigma_{x_1} + \sigma_{x_2})\,d\epsilon_X + (\sigma_{y_1} + \sigma_{y_2})d\epsilon_y + (\tau_{xy_1} + \tau_{xy_2})\,d\epsilon_{xy}]\,dA \quad (3)$$

The total compacting energy per unit of travel distance can be calculated by

$$D = \sum_{1}^{N} W \quad (4)$$

where

$\sigma_{x_1}, \sigma_{y_1}, \sigma_{xy_1}$ = states of stress at the start of the increment,
$\sigma_{x_2}, \sigma_{y_2}, \sigma_{xy_2}$ = states of stress at the end of the increment,
$d\epsilon_x, d\epsilon_y, d\epsilon_{xy}$ = incremental states of strains,
ΔX = incremental roller travel distance, and
N = number of finite elements.

The energy spent in compacting the soil is calculated by using the surficial measurements of the two bin tests as follows: It is assumed that the towed roller input energy is equal to the energy spent in compacting the soil; therefore, the energies dissipated at roller-soil interface and in deforming the roller are vanishingly small. The soil compacting energy can be calculated as

$$P * L = D \quad (5)$$

Work per unit travel distance

$$P = D/L \quad (6)$$

where

P = drawbar pull (N),
D = compaction energy (N-m), and
L = travel distance (m).

Thus, in the case of a towed rigid roller, the energy spent in compacting the soil per unit of travel distance is numerically equal to the drawbar pull. If one assumes that the energy is spent uniformly over the depth of the soil layer, the energy spent per unit volume of the soil at a certain pass is equal to:

$$P/d = D/L * d \quad (7)$$

where d is the depth of soil layer.

The compacted energy per unit volume of the soil after a certain number of roller passes is calculated as,

$$E = \sum_{i=1}^{N} P_i/V_i \quad (8)$$

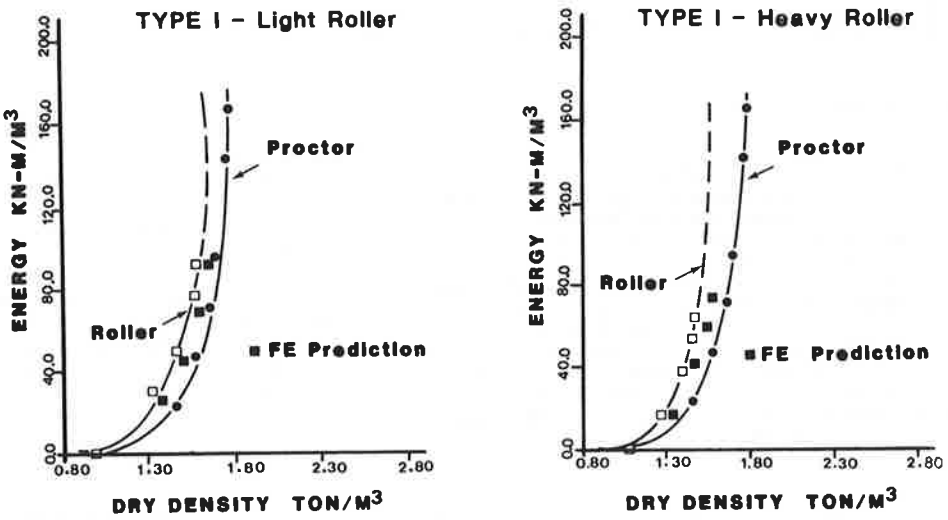

Figure 9. Compacting energy-dry density relation.

where

E = input energy per unit volume,
V_i = cross-sectional area of the compacted soil at pass i,
P_i = roller towed force at pass i, and
N = number of passes.

In calculating the input energy as a function of the dry density in the case of the Proctor test, different samples were subjected to a varying number of blows, so that the varying applied input energy could be related to the different obtained dry densities. The initial density with respect to state of zero energy was obtained by filling the Proctor mold loosely. The testing procedure used was the same as that used in the standard Proctor test. The input energy per unit of volume for the Proctor test can be calculated as

$$E = W * L * N_B * N_L / V \quad (9)$$

where

E = input energy per unit of volume,
W = weight of hammer,
L = height of hammer drop,
N_B = number of blows per layer,
N_L = number of layers = 3.0, and
V = volume of the mold.

Figure 9 shows that the finite-element prediction for the compaction energy-soil density relation compares well with that calculated from the results of the tow bin tests but differs slightly from that obtained from the Proctor tests.

Theoretically, the change in soil density should be a function of the compacting energy and its rate of application to the soil. Thus, the difference in the energy relations shown in Figure 9 may be due to the difference in the rate of application of the soil-compacting energy or the method of averaging the soil dry density and not to the method of compaction. The results also show that the soil density does not change after a certain level of compacting energy. The magnitude of this energy is a function of its rate of application, the initial physical and mechanical properties of the soil, and the roller parameters. This energy value may be called the compaction energy limit.

The efficiency of the roller can be evaluated as the ratio between the density predicted by using FEM and that of the Proctor test at the roller-limiting compacting energy.

CONCLUSION

The comparison between predicted and experimentally computed values of compaction energy for the case of towed roller show that the analytical model presented can be used to evaluate the compactibility of the soil in terms of the minimum energy required to produce a certain permanent density. This model takes into account the effect of the successive roller passes and the changes in the soil properties with depth from pass to pass provided the soil stress-strain relations at different dry densities are used to generate the required constitutive relations for the model.

ACKNOWLEDGMENT

The experimental assistance provided by S. Ng is acknowledged. This study was supported under an NSERC grant.

REFERENCES

1. R.N. Yong and E.A. Fattah. Analysis of Soil Compactibility by Rollers. ASCE Convention, Hollywood, FL, 1980.
2. R.N. Yong and E.A. Fattah. Prediction of Wheel-Soil Interaction and Performance Using the Finite Element Method. Journal of Terramechanics, No. 13, 1976, pp. 227-240.
3. R.N. Yong and B.P. Warkentin. Soil Properties and Behaviour. Elsevier Scientific Publishing Company, New York, 1975.
4. R.N. Yong and E.A. Fattah. Analysis of Soil Compactibility by Rollers. Proc., ASCE Symposium on Generalized Stress-Strain Applications in Geotechnical Engineering, 1981.
5. R.N. Yong, P. Boonsinsuk, and E.A. Fattah. Tyre Flexibility and Mobility on Soft Soils. Journal of Terramechanics, No. 17, 1980, pp. 43-58.

Undrained Failure of Compacted Plastic Embankments

RAYMOND L. GEMME

This paper deals with the effectiveness of the New York State Department of Transportation earthwork compaction specifications, which are based on a percentage of standard Proctor maximum density as they relate to overall embankment stability. A number of failures have occurred in recent times within moderate to low plastic soil fills in New York State. These failures have been traced to the placement of plastic materials in a condition where the moisture content exceeds the optimum moisture content for standard compaction. Although the percentage of standard Proctor maximum density that is required by New York State construction specifications was equaled or exceeded, the resulting shearing strength of the fill was inadequate to support the additional proposed fill loads. Two detailed case studies are shown to identify the nature of the problem. A discussion of potential alternative methods of compaction control is given.

New York State Department of Transportation's specifications require embankment lifts to be compacted to 90 percent of standard Proctor maximum density. Several plastic glacial till embankments up to 40-ft high have failed in recent times where the density of the fill was found to be as high as 94 percent of standard Proctor. Laboratory tests on samples of fill obtained from two such areas have confirmed that undrained failures of plastic fills can take place when they are placed at standard compaction and at greater than optimum moisture contents.

The two embankment areas reported in this paper are located on the Interstate highway system, one on the Genesee Expressway near Mount Morris, and the other on I-88 at Suits Ravine (see Figure 1).

Figure 1. Site locations.

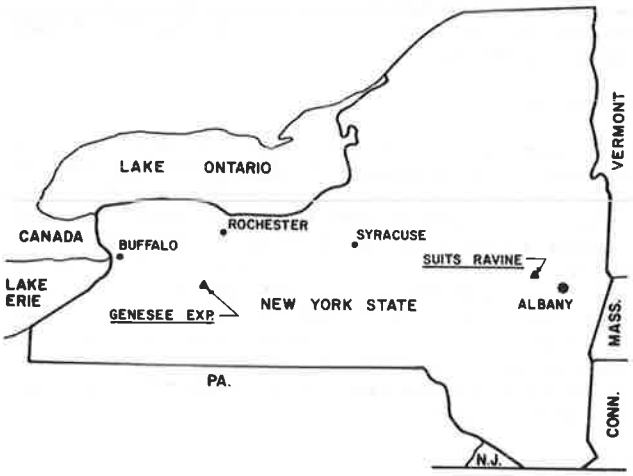

GENERAL BACKGROUND OF FAILURES

Genesee Expressway, SB 549+ to SB 555+

In May 1978, shortly after embankment construction reached subgrade (65- to 70-ft high fill), a crack developed in the surface of the Genesee Expressway and a bulge appeared on the embankment slope 40 or more ft below subgrade. The first 45 ft of fill was a brown plastic glacial till, which possessed an average plasticity index (PI) of 13. It was placed in the fall 1977. The remainder of the fill was constructed of broken shale to subgrade in the spring 1978. After several days this crack opened up to ±1-ft wide (see Figure 2). Approximately 10 ft of fill was then removed to relieve the embankment stresses. The fill was eventually stabilized by flattening the side slopes to 1 on 3 with shale.

I-88 - Westbound East Abutment, Suits Ravine

The abutments on I-88 at Suits Ravine were constructed and backfilled in the fall 1979. Bridge movement records over the winter indicated 0.35 ft of vertical downward movement and 0.14 ft of horizontal outward movement. The fill was constructed

Figure 2. Typical side slope section of Genesee Expressway.

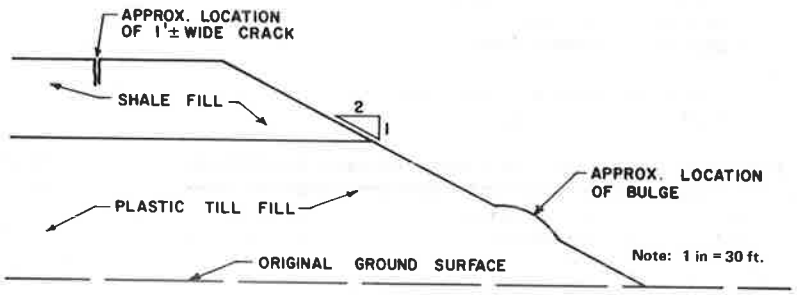

Figure 3. Section at bridge end slope of Suits Ravine, I-88.

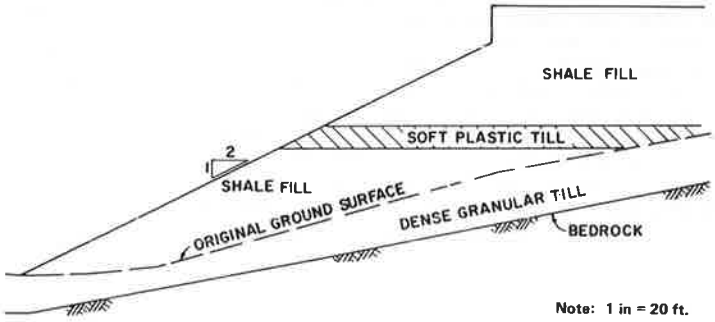

mostly of broken shale with some layers of brown plastic glacial till (PI≈8) benched into shallow till (original ground) over bedrock. Subsequently a slope inclinometer installation indicated horizontal movements to be occurring in two thin soft till layers located 14 and 18 ft below footing level, which was ±16 ft below the theoretical grade line. Cracks were not evident at the surface of this fill (see Figure 3). This fill was eventually stabilized with 20-ft wide side berms and 40-ft wide end berms.

Testing Program and Results

Both failures were apparently due to undrained displacements (overstress) of relatively thin layers of moderate-to-low plastic glacial till. A review of the compaction records indicated that the soils that were moving passed the state's minimum 90 percent standard density requirement. This prompted our testing program, which was progressed to compare unconsolidated undrained shear strength results with percentage of standard density wet of optimum and to relate this percentage of density to maximum allowable fill height via slope stability analysis. Samples of the fill were obtained from large diameter borings. The samples from each site were mixed into batches and dried to below optimum. During this process the large stones (i.e., +1/4-in stones) were removed from each batch. The materials were then compacted at standard effort and at successively higher moisture contents to produce the compaction curves shown in Figure 4. The full diameter (3.375 in ϕ) soils were then extruded from the compaction molds and were subjected to failure at an unconsolidated undrained (UU) confining pressure (σ_3) of 25 psi (see Figure 5). Information from a report by Weitzel and Lovell (1) on a highly plastic St. Croix clay (PI≈31) is also shown in Figures 4 and 5 for comparison. Note that the shear strength curves are plotted directly below the compaction curves between optimum moisture content and the moisture contents at 90 percent density for comparison purposes. Very low shear strengths were obtained for all three soils at 90 percent density.

The Genesee Expressway till was also compacted to modified effort and failed at UU strengths above optimum moisture contents. The results are compared with standard effort and are shown in Figures 6 and 7. These plots show that the moisture content has more of an influence on shear strength of samples compacted over optimum than the actual compaction effort. This is also verified in Figures 8 and 9, which show results for the St. Croix clay. Others (1-3) have found the same to be true in relating California bearing ratio or undrained shear strength to moisture content at various compactive efforts.

Figures 10 and 11 were obtained from and quantify the information shown in Figures 4 and 5. These figures show that only a ±200 psf shear strength is obtained at 90 percent standard density and at 7 percent moisture content over optimum. The shear strength increases to ±1000 psf at 95 percent standard density and at 3.5 percent moisture content over optimum. These curves show that the increase in shear strength and the percentage of moisture content over optimum decreases are sensitive to small changes in the percentage of standard density over optimum moisture content.

Slope Stability Analysis

Slope stability analyses were run to equate safe and equilibrium fill heights to shear strength with the use of the simplified Bishop circle analysis. In addition, overstress analyses were run to more accurately simulate a squeeze-type failure that appears to be the governing criteria. The results of these analyses are shown in Figure 12.

Figure 13 shows the relation of percentage of standard density versus equilibrium fill heights for both fill areas by using information from Figures 11 and 12. This figure also shows that only 10-15 ft of fill can be safely constructed if the soil is compacted to 90 percent of standard density at over optimum moisture content. Of major significance is that these curves indicate that 93-95 percent of standard density at over optimum moisture content is required for most grade crossing embankment fills constructed of plastic fill materials (i.e., embankment fills between 23 and 40 ft high).

Compaction Control

Figure 13 shows that a fill height of 23 ft is marginally safe if it is constructed to 93 percent of standard density at greater than optimum moisture content and a fill height of 40 ft is marginally safe if it is constructed to 95 percent of standard density at greater than optimum moisture content. Figure 10 indicates that the percentage of moisture content over optimum is relatively insensitive to the degree of plasticity of the soil in the 93-95 percent of standard density range. In other words, in order to safely construct a 40-ft high fill for a soil of any plasticity the moisture content should not be greater than 4 percent greater than optimum.

This information indicates a need for more than the normal degree of control for plastic fills placed over optimum moisture content. It indicates that the control can be placed either on the degree of compaction or on the percentage of moisture content over optimum, depending on the fill height. The question is what would be the easier way to control the operation for adequate safety of these fill materials? Since statewide compaction control curves are available for most soils in New York State, percentage compactions could be performed routinely on these types of soils and a minimum 95 percent standard dry density be required of these soils for all embankments up to ±40 ft high. The determination of moisture content is still a requirement. Greater percentage of standard densities would be required for embankments that exceed this fill height.

The above information on stable embankments is based on the fills being field compacted with standard effort. The heavy compaction equipment that is available today produces compactive efforts that exceed the normal. Based on the information in Figures 6 and 7 (i.e., an increase in the compaction effort at a constant moisture content over optimum decreases the undrained shear strength), greater field compactive efforts will require even greater percentage standard densities than are recommended for stability. For instance, from these curves the maximum allowable percentage of moisture content over standard optimum is 2 percent for the modified effort as compared with the 4 percent for the standard effort to provide a stable embankment. This is equivalent to requiring a 98 percent standard density at greater than optimum moisture content. At greater field compactive efforts than the modified effort the stable standard density approaches 100 percent at greater than optimum moisture contents. This condition further complicates the method of field compaction control.

Based on the above discussion concerning the current use of heavier-than-standard compaction equipment, soils of low-to-moderate plasticity should be compacted to at least 98 percent standard density at greater than optimum moisture contents or be compacted to at least 90 percent standard density at

Figure 4. Moisture content versus dry density: standard compactive effort.

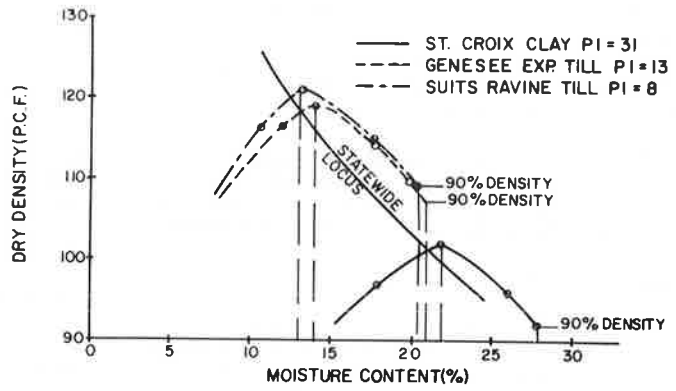

Figure 5. Moisture content versus shear strength: standard compactive effort.

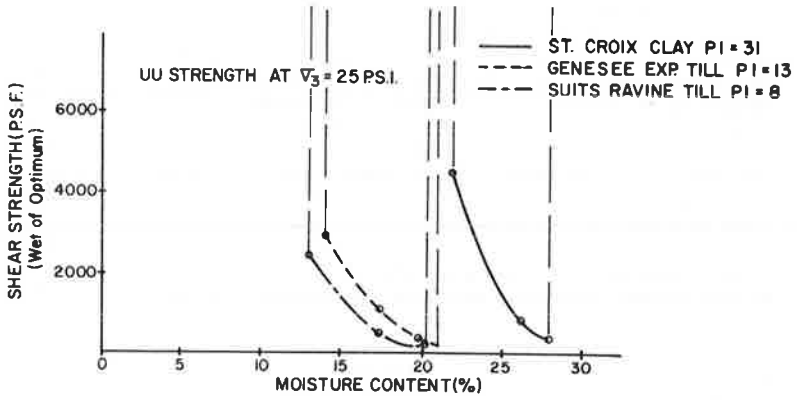

Figure 6. Moisture content versus dry density: Genesee Expressway till.

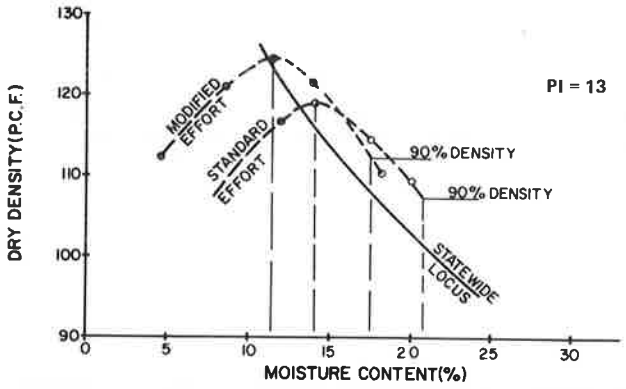

Figure 7. Moisture content versus shear strength: Genesee Expressway till.

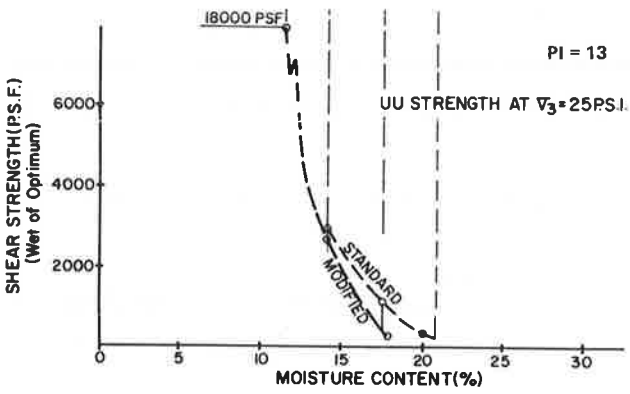

Figure 8. Moisture content versus dry density: St. Croix clay.

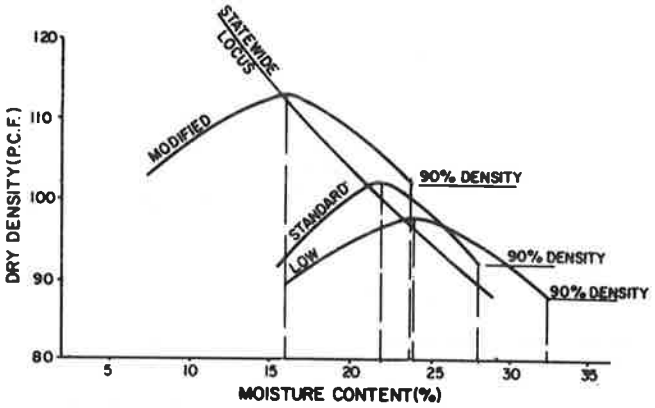

Figure 9. Moisture content versus shear strength: St. Croix clay.

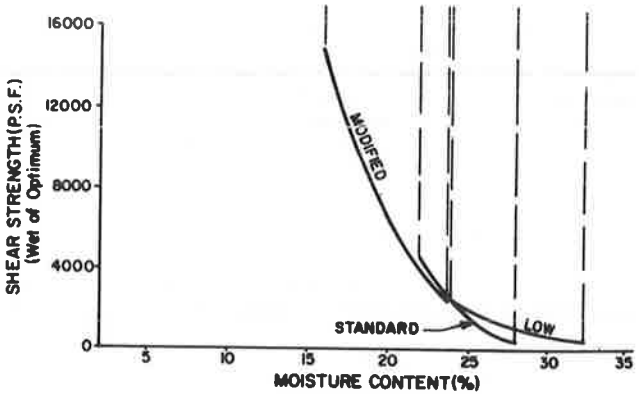

below optimum moisture contents. To be on the safe side for all conditions, these soils should not be compacted at greater than standard optimum moisture content.

The above comments are based on properties of plastic soil in their final states in an embankment. Compaction of an embankment to between 2 and 4 percent over standard optimum moisture content would require the use of light equipment. An embankment could be compacted with heavy equipment and subsequently become over optimum relative to the standard effort with precipitation. However, if the embankment surface becomes too wet it is either removed or allowed to dry back and be recompacted prior to placement of subsequent lifts. Initially placing an embankment below standard optimum moisture content could become a problem by using heavy vibratory equipment. This equipment could draw moisture from lower lifts into the lift being compacted and cause it to become over optimum. However, this and other similar conditions are usually rectified during construction.

Figure 10. Moisture content over optimum versus PI: standard compactive effort.

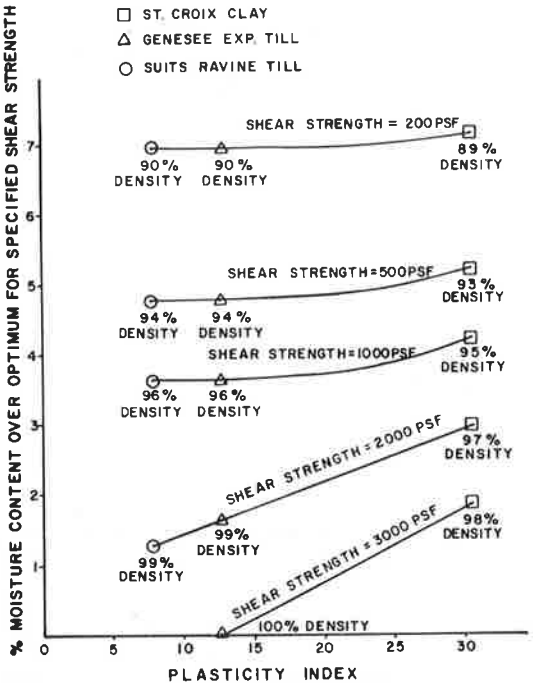

Figure 11. Shear strength versus percentage of standard density.

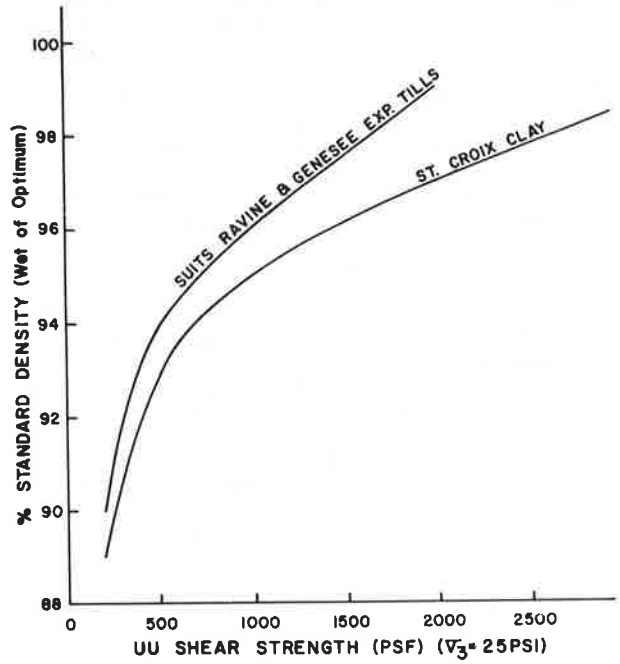

Figure 12. Shear strength versus fill height.

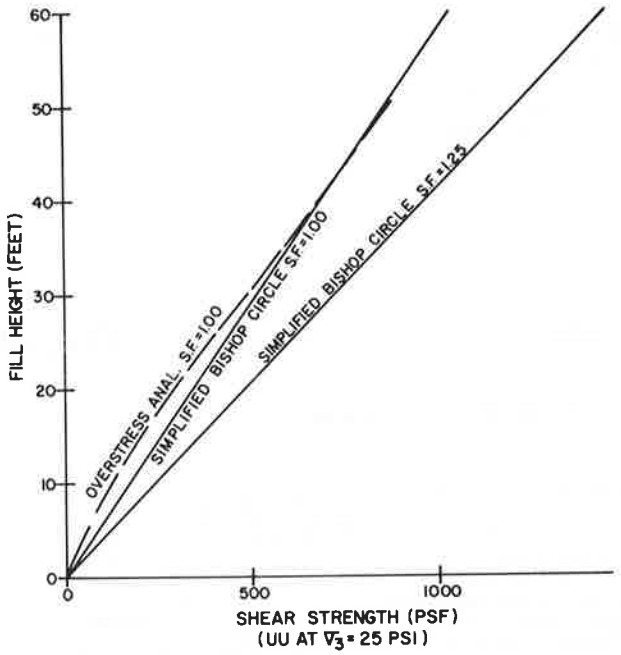

Figure 13. Safe fill height versus percentage of standard density: Suits Ravine and Genesee Expressway tills.

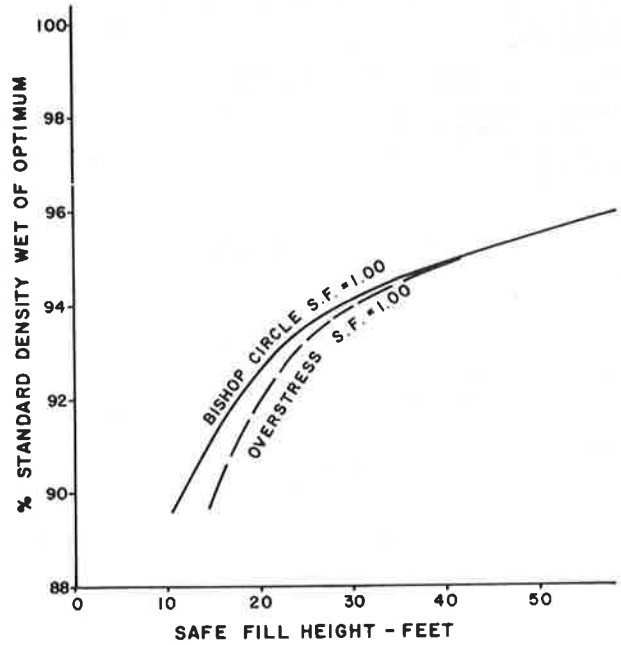

CONCLUSIONS

Moisture content over optimum has more of an influence on shear strength than does the actual compaction effort (Figures 6 and 7). An increase in the compaction effort at a constant moisture content over optimum decreases the undrained shear strength (Figures 6 and 7). Both the shear strength increase and percentage of moisture content over optimum decrease are sensitive to small changes in percentage of standard dry density greater than optimum moisture content (Figure 10).

Plastic embankment fills placed over optimum at standard effort should be compacted to at least 95 percent standard Proctor to ensure stable fill placements up to 40 ft high. Greater percentage densities will be necessary for fills that exceed this height. This was found to be true of plastic soils that have PIs in excess of 8 percent. Additional investigation is required to determine whether this is a problem for the lower PI soils.

In reality, with the use of heavier-than-standard field compaction equipment the stable degree of compaction for plastic embankment fills is at least 98 percent of standard density at greater than optimum moisture contents or 90 percent of standard density below optimum moisture contents. To be on the safe side for all conditions of compactive effort and fill heights, these soils should not be compacted at greater than standard optimum moisture contents.

REFERENCES

1. D.W. Weitzel. The Effect of Laboratory Compaction on the Unconsolidated-Undrained Strength Behavior of a Highly Plastic Clay. Purdue Univ. West Lafayette, IN, Joint Highway Research Project Rept. 79-21, Aug. 1979.
2. W.P.M. Black and N.W. Lister. The Strength of Clay Fill Subgrades: its Prediction in Relation to Road Performance. Transport and Road Research Laboratory, Crowthorne, Berkshire, England, Rept. 009, 1979. ISSN 0305-1293.
3. W.T. Mills and J.M. DeSalvo. Soil Compaction and Proof Rolling. Soils, Converse Ward Davis Dixon, Newsletter, Fall 1978.

Compaction Effects of Oscillating Rollers

ERNEST T. SELIG AND TAI-SUNG YOO

Studies of vibratory compaction with smooth-drum rollers have indicated that the amount of compaction is highly dependent on two parameters: the magnitude of the vertical oscillatory displacement of the drum and the number of oscillations per unit of distance of travel. Model tests with small-scale rollers were carried out in the laboratory to study the effects of these parameters on the amount of compaction. The roller had a 12-in diameter. Applied compaction forces and soil layer thicknesses were scaled down appropriately. The frequency of oscillation was reduced to eliminate the vibration effects but maintain the number of oscillations per unit of distance of travel within the range representative of full-size rollers. The mean and oscillatory components of the force applied to the soil were varied as well as the number of passes and the number of oscillations per unit of distance. The test soils were a coarse- to medium-graded silica sand and a fine clayey sand prepared with several initial density states. The results of the tests showed the relations of the test variables to the amount of compaction and to the soil stiffness and the internal damping. The stiffness and damping observations were valuable in explaining the soil-machine interaction of full-scale vibratory rollers and led to the development of an analytical model for predicting the magnitude of drum oscillation during vibration. The paper describes these model tests and presents the experimental results. The implications of the results in compacting soil with vibratory rollers are also discussed.

Some basic concepts relating to vibratory roller behavior have been presented elsewhere (1). The reference suggested that

1. One of the major mechanisms of compaction with such rollers was volumetric strain caused by the cyclic nature of the loading;
2. Key parameters that control the amount of compaction include the number of drum oscillations per unit of travel distance (equal to vibration frequency divided by travel speed) and the amplitude of drum displacement during vibration;
3. Drum displacement is a function of the dynamic soil-roller interaction, which may be modeled as a mechanical system of masses, springs, and damping elements; and
4. Soil stiffness and damping characteristics relevant to a moving roller are quite different from those that would be measured in any soil property test.

The dynamics of the soil-roller system have also been described in detail (2). The interaction between the soil and machine parameters was shown and the influence of these parameters on the magnitude of drum displacement was illustrated.

This paper uses model roller tests to investigate the relation between the amount of compaction and the controlling parameters, which are oscillations per unit of distance and drum displacement. The effects of the test parameters on soil stiffness and internal damping for a moving roller are also shown.

The test apparatus consisted of a moving soil box, with a vertically oscillated roller in which the forces, motions, forward speed, and oscillation frequency could be controlled and measured. The roller model was approximately 1/5 scale, and the compaction forces were scaled down appropriately.

PRELIMINARY LABORATORY TESTS

A preliminary series of laboratory tests was carried out to illustrate the stress-strain relation of soils associated with vibratory compaction so that it can be properly used in the analytical model. Another reason for the tests was to postulate a possible way to relate the calculated motions from the analytical model to the amount of compaction so that the analytical results become meaningful for prediction of compaction.

The roller was modeled by a 12-in diameter drum positioned over a moving box of soil. The drum was raised and lowered at a prescribed deformation rate during horizontal sliding of the soil box to simulate sinusoidal drum motion with the desired amplitude and wave length. The vertical contact force

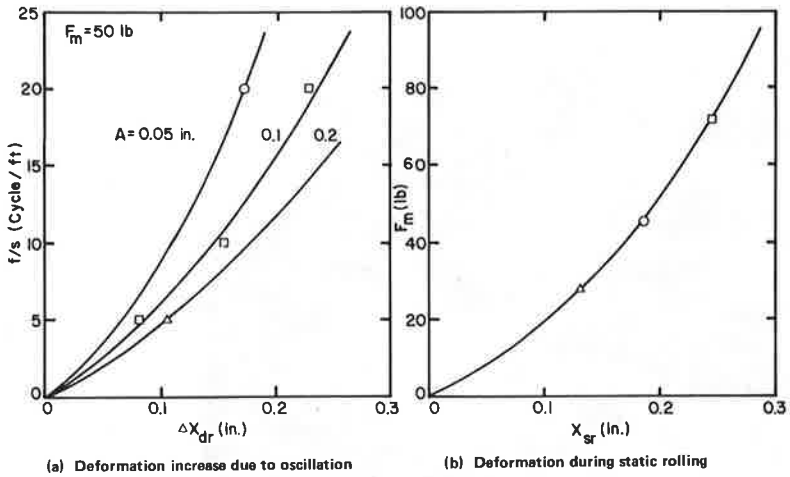

(a) Deformation increase due to oscillation (b) Deformation during static rolling

Figure 1. Separation of soil deformation into components during preliminary laboratory tests on kaolin clay.

between the soil and the drum was measured by using a proving ring. The vertical soil deformation was determined by calculating the average of the readings of two deflection dial gauges located on the ends of the drum axle.

Two different types of soils were used. One was a coarse- to medium-graded silica sand and the other was a kaolin clay. These soils were mixed with a nonvolatile plasticizer liquid instead of water to maintain constant moisture during repeated tests. The liquid contents of the silica sand and kaolin clay were 6.8 and 38.0 percent by weight, respectively. The clay-plasticizer combination had a liquid limit of 61 percent and a plasticity index of 14 percent. More information on the properties of these materials is given elsewhere (3).

At the start of each test, one of these soils was placed loosely in the test box. The resulting densities were 86 lb/ft³ for the silica sand and 75 lb/ft³ for the kaolin clay. A typical test began with the lowering of the roller into the prepared soil bed at a constant rate of deformation while the soil box was moved at a constant speed. The speeds of roller and soil box motions were kept low (on the order of 0.1 to 0.6 in/min) so that the response of the roller during the above sequence was considered to be in static equilibrium at all times. After the desired peak deformation was reached, oscillatory deformation of a desired amplitude was superimposed while the constant rolling motion was maintained. The oscillation frequency was on the order of 0.05 cycles/min so that vibration effects were not present. In comparison tests, oscillatory loads were applied with zero travel speed, so that the roller remained at a fixed soil location.

The results showed that a much smaller drum load was needed to produce a given deformation during rolling than when stationary. Also, oscillations during rolling produced closed load-deformation loops with no progressive permanent settlement into the soil. In contrast, oscillations without rolling showed increased permanent settlement with each repeated cycle of loading.

These tests also showed that the superimposing of oscillation causes greater settlement of the drum during rolling than when rolling occurs under a constant load, as in static compaction. This response is similar to the behavior of soil under cyclic shear strain.

Silver and Seed (4) studied the densification characteristics of dry sands in terms of repeated shear strain as part of research on ground surface subsistence induced by seismic loadings. The simple shear tests they conducted indicated that cyclic shear strains deformed the sample and allowed the soil particles to move into a denser packing. They further demonstrated that the vertical strain due to compaction was only dependent on the shear strain amplitude, not the vertical stresses, especially when the shear strains exceed 0.05 percent. Vertical settlement due to compaction was a logarithmic function of number of cycles, but most of the change occurred during the first 10 cycles.

Based on the test results mentioned previously, Youd (5) developed an analytical expression that related the shear strain to the amount of compaction of granular materials, assuming that the shear strain is the primary factor in controlling compaction. He hypothesized that a sequence of small to moderately sized strain pulses would produce a finite density increase through the contraction-expansion sequence with continuous cycles, since contraction predominates at those strain amplitudes. Examples of the compaction prediction were presented by using the void ratio-shear strain relation obtained in the laboratory and simple analytical method of estimating shear strain under a given load.

The model tests suggested that the total settlement (x_{dr}) might be divided into a static component (x_{sr}), which represents the compaction solely due to the dead weight of rolling compactor without oscillatory motion, and a dynamic component (Δx_{dr}), which represents the compaction increase due to the superimposed oscillatory dynamic force.

The compaction results for the tests in kaolin clay are shown in Figure 1 divided into the analogous static and dynamic components. As the mean roller load (F_m) increases, the deformation from compaction increases, but at a decreasing rate (Figure 1b). For a constant mean load of 50 lb, the component of compaction from oscillation increases with an increase in the number of cycles per unit of distance of roller travel [equal to ratio of oscillation frequency (f) to travel speed (s)] and an increase in peak-to-peak oscillation amplitude (A).

MAIN SERIES OF LABORATORY MODEL TESTS

Based on the findings of the preliminary model tests, improved apparatus was developed to permit a more extensive evaluation of the effects of the test parameters. The main emphasis was directed toward the variation of the loading conditions, as represented by (a) the mean or static component of vertical force (F_m) applied to the roller, (b) the amplitude of the superimposed oscillatory force (F_d), and (c) the number of loadings per unit of distance represented by the frequency speed ratio

Figure 2. Model roller in moving soil box for main test series.

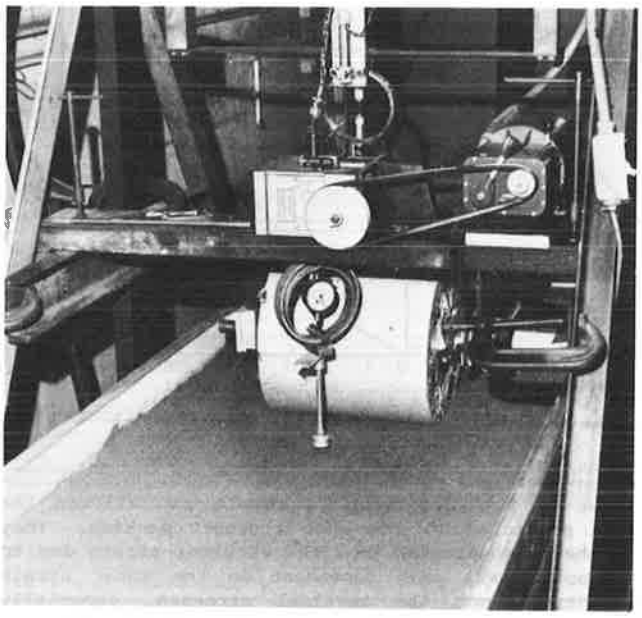

Figure 3. Diagram of model test apparatus.

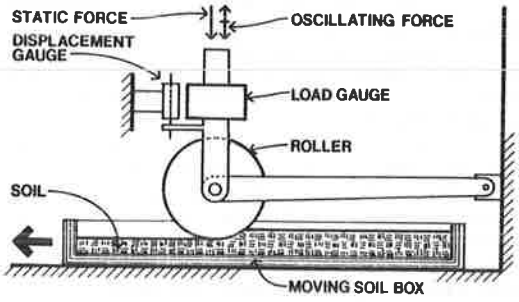

(f/s). Two different soils were used in the tests, but primarily with one initial lift thickness and one initial density. Some tests were conducted at other initial densities and layer thicknesses and, in many tests, measurements were made with more than one roller pass to observe the effect of changing soil conditions caused by compaction.

Apparatus

The facility (Figure 2) constructed for these tests had controlled vertical force instead of controlled deformation, as in the preliminary tests. The fundamental components are shown in Figure 3 and are as follows:

1. Moving soil box,
2. Small-scale roller,
3. Reaction frame,
4. Servo-controlled hydraulic load cylinder,
5. Force and displacement sensors,
6. Hydraulic power supply, and
7. Instrumentation for controls and measurements.

The roller was approximately a 1/5-scale model of typical full-scale vibratory rollers. The other parameters, such as the applied forces and soil layer thickness, were scaled down appropriately. The mean vertical force, the amplitude and frequency of the oscillating force, and the forward speed of soil box movement could be controlled independently. The instrumentation was capable of measuring the static and dynamic components of the vertical force as well as sinkage of the roller as a function of time.

The roller was made of 12-in diameter plywood discs bonded together to provide a 12-in width. It had a relatively light weight (about 30 lb) to minimize the inertial resistance of the roller that may develop at the higher operating frequencies. This was important because the force applied to the roller was used as a measure of the force applied to the soil.

The soil box, which was 2-ft wide, 6-ft long, and 6-in deep, was built to contain and to move the test soil sample. The box was chain-driven on supporting guide rails by an electric motor, and its speed was varied by using different combinations of sprocket teeth. The speed range provided with such combinations was 1.1 to 0.3 in/s.

Two different soils were used in the tests. One was the silica sand plasticizer mixture used in the preliminary laboratory tests. The other was a clayey sand, composed of 94 percent medium to fine sand and 6 percent kaolin clay. The nonvolatile plasticizer liquid was used to provide the moisture. Compaction tests were performed by using ASTM D698 procedures (AASHTO T99). Optimum moisture content was about 10 percent by weight, and maximum dry density was about 122 lb/ft^3. The dry side of optimum was thought to be the most desirable for the tests because the soil yields a higher strength and sustains a greater compaction effort on the dry side of optimum moisture than on the wet side. Thus, the test soil was prepared at a moisture content of 7 percent.

Experimental Procedures

The placement of the soils in the test box was achieved by allowing the material to fall from a wide shovel being shaken gently while maintaining about a 6-in falling distance. Pouring was continued until a uniform layer approximately 1/4-1/2 in thicker than the desired bed thickness had been placed. Then the uneven soil surface was gradually and carefully shaved to make it flat and smooth. The resulting initial layer thickness was normally 2 in.

After preparation of each test bed, several in situ density measurements were made to check uniformity. The results indicated that the initial soil conditions were reasonably uniform within a test bed and from one test bed to another. The average values of initial loose wet density for the silica sand and clayey sand layers prepared by this method were 86 and 84 lb/ft^3, respectively.

When a denser test bed was desired, the loose layer prepared as above was precompacted with the model roller under a prescribed constant vertical force. Then the compacted surface was again leveled off with a multitoothed scarifier to provide the desired thickness. An average wet density of 95 lb/ft^3 was obtained with the clayey sand mixture when a loose layer was rolled five times under a vertical force of 25 lb.

Both single-coverage and multiple-coverage tests were conducted. The single-coverage test consisted of applying only one roller pass to the test bed under the selected conditions of mean force, amplitude and frequency of oscillating force, and roller speed. These tests were conducted so that general relations among roller sinkage, final density, and soil characteristic changes could be developed for the same initial soil conditions. The multiple-coverage test involved repetition of the rolling

tests on the same bed to extend the relations developed during the single-coverage tests and to simulate successive roller passes in the field.

The normal sequence of steps for the single-coverage test was as follows:

1. Apply a prescribed vertical force to the roller while the soil box is stationary and allow the roller to settle into the soil,
2. Move the box at a constant speed to simulate drum rolling until an equilibrium sinkage is reached at the given constant vertical force, and
3. Add the desired vertical oscillating force while maintaining the same mean force and rolling speed, and continue rolling to reach another equilibrium condition.

This procedure provided information on three different characteristic phenomena:

1. Stationary load-penetration relations of the roller,
2. Compaction under constant vertical forces as in static roller compaction, and
3. Compaction caused by drum oscillation.

Test procedures for the multiple-coverage case were the same as those for the single-coverage test, except that the oscillating force was applied when rolling was initiated.

The principal measurements taken throughout each test were the vertical load and roller sinkage. These were monitored as a function of time on a strip-chart recorder, and load was plotted as a function of sinkage on an x-y recorder. In addition, data on in situ density and soil strength for various conditions were accumulated during the single-coverage tests.

LOAD-DISPLACEMENT RELATIONS

Figure 4 illustrates a sample chart recording during a single-coverage test. It illustrates the sequence of load-displacement relations for three different situations that take place during the entire period of a test. It clearly shows the three distinctive equilibrium states. As the vertical force was gradually increased to the selected mean value while the roller remained stationary, the deformation gradually grew to a value indicated by x_{ss}. Then, the initiation of rolling increased the deformation to another equilibrium value (x_{sr}) under the same mean vertical force. For all the tests on both soils, the ratio of x_{sr} to x_{ss} was about 1.4 to 1.6. Additional deformation was observed when oscillation of the vertical force was imposed. The final deformation value during oscillation (x_{dr}) was taken as the mean of the motion whose peak-to-peak amplitude was defined as A. All of the three equilibrium displacements were constant over a sufficient period of time to indicate that they were not transient values. The deformation increase due to oscillation (Δx_{dr}) equals $x_{dr} - x_{sr}$.

To show that the deformations x_{sr} and x_{dr} represent compaction, penetration tests were performed before and after rolling by using a 1-in² flat circular bearing plate, shown in Figure 2. Typical results indicate an increase in bearing resistance by a factor of 3.5 from rolling without oscillation compared with the initial uncompacted state, and an increase by a factor of 7 from rolling with oscillation compared with the uncompacted state. This confirms the effectiveness of oscillation in compacting soil.

Figure 5 illustrates the roller force plotted as a function of vertical deformation as measured by the x-y recorder. A well-defined, repeated, closed hysteretic loop was formed during oscillation after a few initial cycles. The soil stiffness during stationary penetration is the slope of the curve following initial sinkage. The corresponding stiffness during oscillation is the average slope of the steady state hysteresis loop. This stiffness represents the soil behavior as felt by the moving roller. The stationary soil elements, in contrast, experience large plastic deformation represented by x_{dr}, which is essentially unrecovered after the roller passes. Hence, x_{dr} is a measure of the soil compaction.

A typical x-y recording during the multiple-coverage tests is shown in Figure 6. By controlling the recorder pen, only one cycle of the equilibrized loop was recorded for each roller pass, so that comparison of the change in deformation during each pass was possible. As expected, Figure 6 shows that the deformation (compaction) increment for each pass decreased with each additional roller pass. Simultaneously, the stiffness during oscillation increased and the hysteretic damping decreased.

Because changing soil stiffness that results from compaction can cause a change in the dynamic force applied by a vibratory roller, two tests were performed in which the oscillatory force was changed for each pass. Figure 7 represents a test with increasing oscillatory force for each roller pass, and Figure 8 is the counterpart for decreasing force. In both cases, the mean force was maintained constant at about the same value as in the constant force amplitude test. Clearly, the changes in stiffness and damping are different for these cases.

COMPACTION DEFORMATION

The component of compaction caused by rolling without oscillation (static component) is shown in Figure 9 for dense clayey sand and for loose silica sand in terms of soil deformation (x_{sr}). As expected, the amount of compaction increases at a decreasing rate with increasing compaction force.

The additional component of compaction caused by the oscillation is shown in Figures 10-12 in terms of the deformation increment (Δx_{dr}) for three soil conditions. The oscillation is represented by the peak-to-peak vertical displacement amplitude (A) rather than by the oscillatory force (F_d) for two reasons: (a) previous research has indicated that cyclic strain is a better measure of expected compaction than cyclic stress and (b) oscillation amplitude can be easily measured on vibratory compactors, whereas the dynamic force applied to the soil cannot be determined easily.

For the initially loose soils (Figures 10 and 11), the dynamic component of compaction (Δx_{dr}) increases at a decreasing rate with increasing oscillation amplitude (A) and with the number of oscillations per unit travel (f/s). For the initially compacted clayey sand (Figure 12), Δx_{dr} increased linearly with A, but increased at a decreasing rate with f/s. Although the value of mean force (F_m) is expected to affect the magnitude of Δx_{dr} obtained for any f/s and A, within the range of conditions tested this effect was not a major one.

MULTIPLE PASS COMPACTION

The effect of number of roller passes on the amount of compaction produced by rolling without oscillation is shown in Figure 13. Compaction is represented by the percentage of soil layer compression, which is equal to the soil deformation divided by the initial layer thickness. The percentage of

Figure 4. Force and deformation relation from strip chart recording during test.

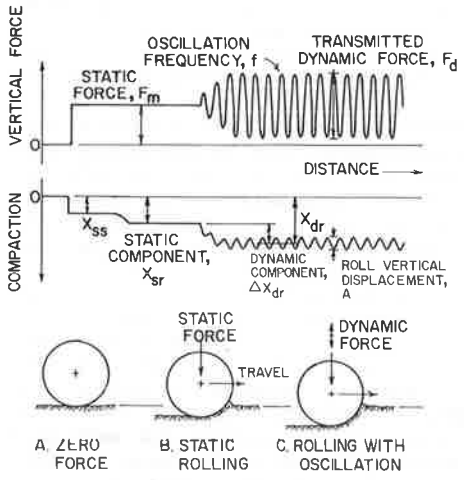

Figure 5. Roller force compared with soil compression as observed by X-Y recorder.

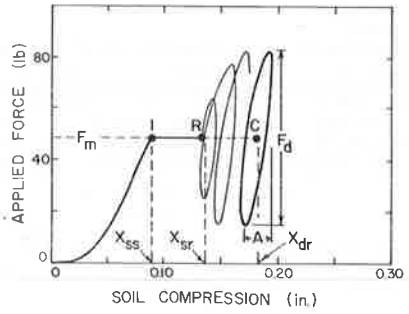

Figure 6. Oscillatory force-compression relation for repeated passes of constant force amplitude.

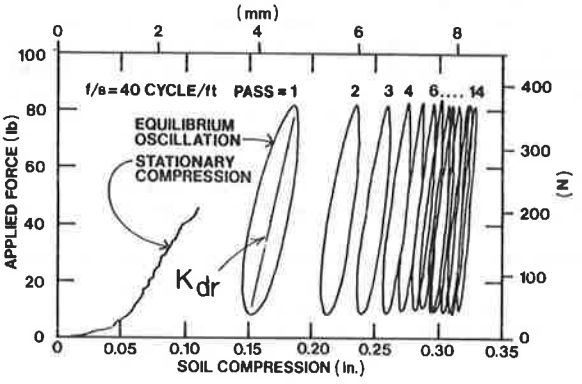

density change is approximately the same in magnitude as the percentage of compression. The compaction growth curves in Figure 13 are characteristic of those observed in the field (6).

The effect on the compaction growth curves of adding oscillation is illustrated in Figure 14. Two passes without oscillation were made first, followed by repeated passes with a constant oscillatory force (F_d) and a constant f/s ratio. The addition of oscillation not only increased the compaction for any number of passes but also increased the rate of compaction compared with the results with no oscillation.

The compaction growth curves for the cases of constant F_d (Figure 6), increasing F_d (Figure 7), and decreasing F_d (Figure 8) after each pass

Figure 7. Oscillatory force-compression relation for repeated passes of increasing force amplitude.

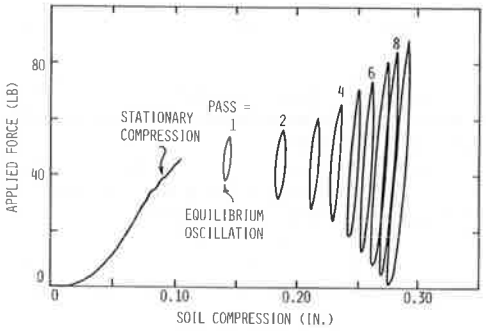

Figure 8. Oscillatory force-compression relation for repeated passes of decreasing force amplitude.

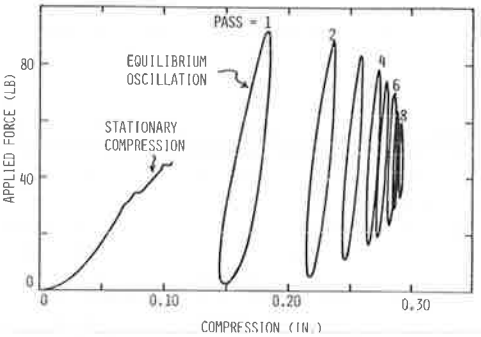

are compared in Figure 15. The decreasing F_d case, which had the highest F_d initially, had the highest rate of compaction growth for the first four passes, but only a small increase after that. The constant F_d case, which had a lower F_d than the decreasing F_d case initially but a higher average over 9 passes, showed a smaller amount of compaction, but compaction continued to increase up to 12 passes, when it then equalled that from the decreasing F_d case. The increasing F_d case had about the same average F_d over 9 passes as did the decreasing F_d case but much lower values for the first 4 passes. The amount of compaction achieved remained well below that of the other two cases for the entire test. The results in Figure 15 indicate that the amount of compactive effort applied during the first few passes is a primary factor in determining the total amount of compaction that will be achieved after a reasonable number of passes, such as 8.

STIFFNESS AND DAMPING CHARACTERISTICS

The average soil stiffness as felt by the moving roller is the slope (k_{dr}) of the line that connects the maximum and minimum points on the force-deformation hysteresis loops, as shown in Figure 6. Soil stiffness was observed to decrease with increasing F_d, decreasing f/s, and decreasing F_m (Figure 16).

The hysteretic damping felt by the moving roller was represented by the area within the hysteresis loops, which is expressed as foot-pounds per cycle of oscillation. This damping factor (c) was observed to increase with increasing F_d and decreasing f/s (Figure 17). The magnitude of F_m did not appear to influence the damping.

The stiffness changes observed in the multiple-

pass tests are shown in Figure 18. For constant F_d, the stiffness increased each pass in a manner similar to the compaction growth. For the decreasing F_d case, the stiffness increased rapidly with each pass. For the increasing F_d case, the stiffness only increased for the first three passes, after which the stiffness remained constant for three passes and then decreased for the remaining passes. For this case, the tendency for increased stiffness from compaction was offset by the tendency for decreased stiffness from the F_d increase.

Accumulation of roller passes under a constant dynamic force produced a decrease in damping and displacement amplitude with each successive cycle. For the case of decreasing F_d, both parameters decreased much more rapidly. In contrast, the case of increasing F_d caused a gradual increase in both damping and displacement.

The trade-off between the effects of stiffness and damping increases suggests the possibility that

Figure 9. Compaction produced from rolling without oscillation.

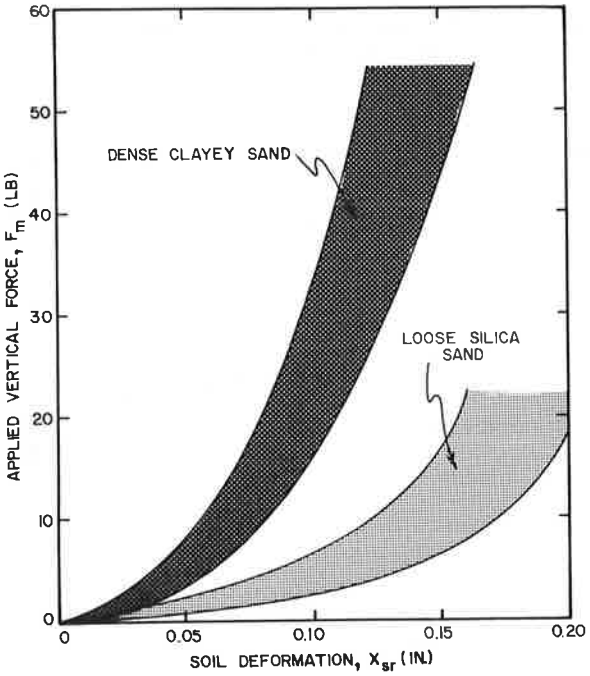

Figure 10. Roller sinkage increase due to oscillation for loose silica sand.

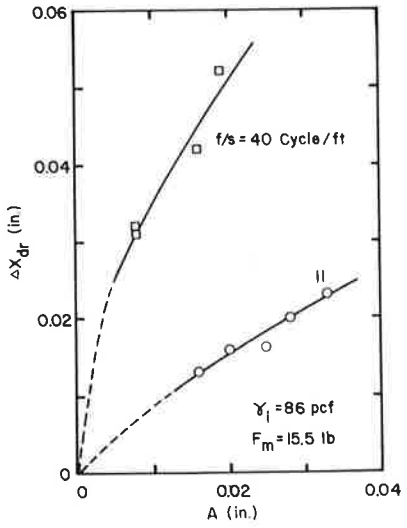

Figure 11. Roller sinkage increase due to oscillation for loose clayey sand.

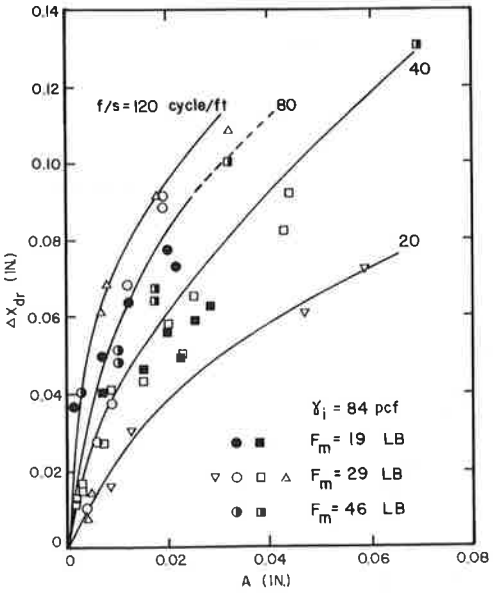

Figure 12. Roller sinkage increase due to oscillation for dense clayey sand.

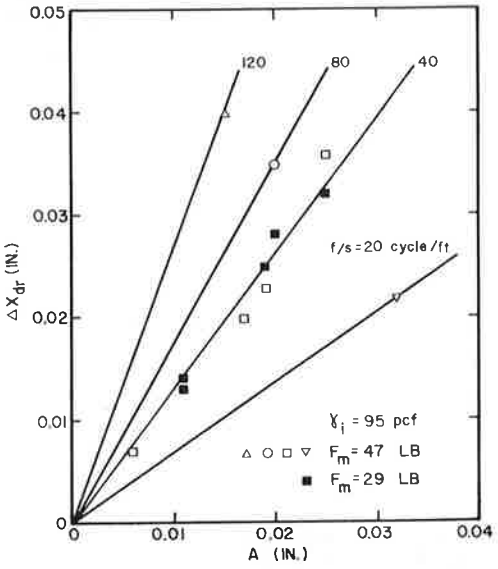

Figure 13. Compaction growth curves during rolling without oscillation under various vertical mean forces in loose clayey sand.

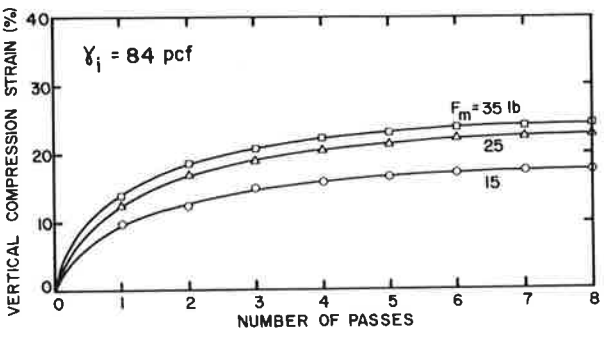

the amplitude could either remain constant, decrease, or increase with additional passes of a vibratory roller, depending on which effect is greater. When the trade-off is about the same, the amplitude would remain constant, which is what many investigators have observed in the field (7-10).

Figure 14. Influence of oscillation on compaction growth curves for dense clayey sand.

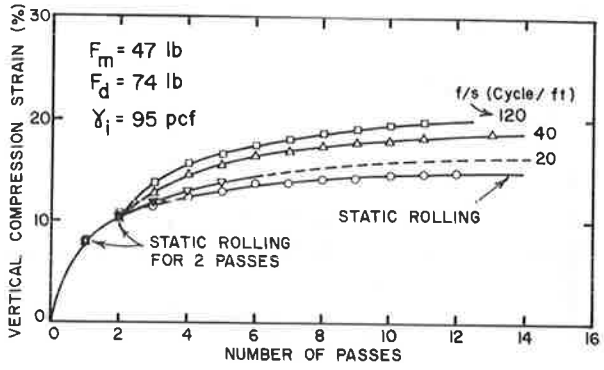

However, when effects of the stiffness are predominant compared with the damping effect, the amplitude would increase. The reverse trend would also be true when the damping effects play the major role.

CONCLUSIONS

Small-scale model roller tests were performed in the laboratory with the cyclic force applied to the soil at low enough frequencies to avoid dynamic effects such as soil particle vibration and wave propagation. These tests showed that the amount of compaction can be represented by a static component that is a function of the static roller weight and a dynamic component that is a function of the vibration frequency to travel speed ratio and the magnitude of drum vertical displacement during oscillation. The repeated strain caused by the drum vertical oscillation appears to be one of the principal causes of the compaction with vibratory rollers. Other suggested mechanisms such as impact, particle acceleration, and strength reduction during vibration are not required in order to achieve compaction.

Stiffness and damping behavior for the soil associated with the moving and oscillating roller are quite different from the behavior during stationary

Figure 15. Comparison of soil strain growth curves for various oscillatory force trends in dense clayey sand.

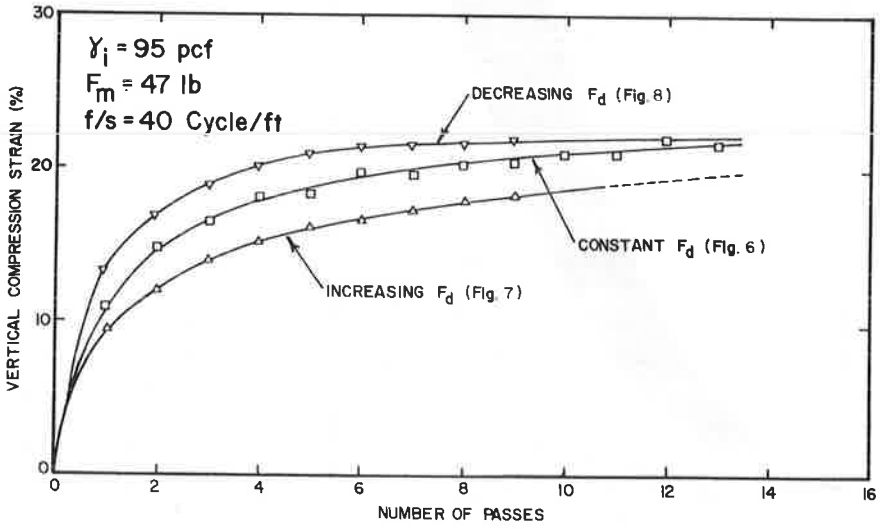

Figure 16. Variation of soil stiffness during oscillation under different mean forces in loose clayey sand.

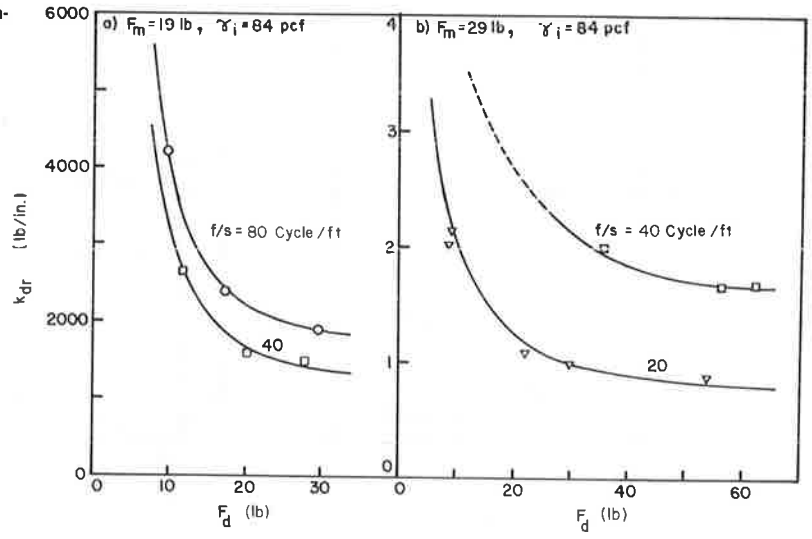

Figure 17. Soil hysteresis damping loss during oscillation in dense clayey sand.

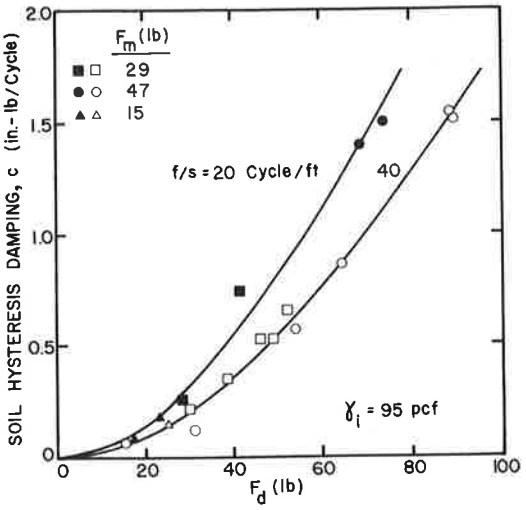

Figure 18. Variation of soil stiffness during oscillation with number of passes under different dynamic loading conditions in dense clayey sand.

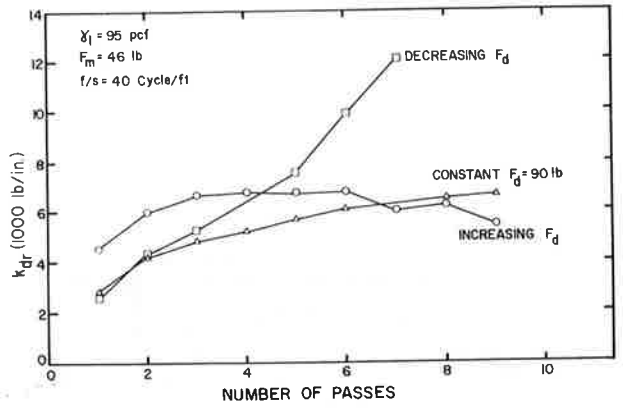

soil loading. Although the soil behaves as a plastic material during compaction, it appears to the moving roller to be elastic and exhibits no permanent strain. The stiffness and damping properties cannot be measured directly with any of the common methods such as the field plate load test and the laboratory triaxial test. Thus, the soil properties used in dynamic roller analysis must be derived indirectly from measurements with a moving roller.

ACKNOWLEDGMENT

The instrumentation and the control system for the model tests were developed by Adam C. Bell, then at the State University of New York at Buffalo. Partial support for the research was provided by Rexnord, Inc., of Milwaukee, Wisconsin.

REFERENCES

1. E.T. Selig and T.-S. Yoo. Fundamentals of Vibratory Roller Behavior. Proc., 9th International Conference on Soil Mechanics and Foundation Engineering, Vol. 2, Tokyo, Japan, 1977, pp. 375-380.
2. T.-S. Yoo and E.T. Selig. Dynamics of Vibratory Roller Compaction. Journal of the Geotechnical Engineering Division, ASCE, Vol. 105, No. GT10, Proc. Paper 14907, Oct. 1979, pp. 1211-1231.
3. E.T. Selig and A.C. Bell. A Study of Soil Disaggregation and Displacement Using High-Pressure Gas. U.S. Army Engineer Waterways Experiment Station, Vicksburg, MS, Contract Rept. S-73-1, Aug. 1973.
4. M.L. Silver and H.B. Seed. Volume Changes in Sands During Cyclic Loading. Journal of the Soil Mechanics and Foundations Division, ASCE, Vol. 97, No. SM9, Sept. 1971, pp. 1171-1182.
5. T.L. Youd. Compaction of Sands by Repeated Shear Straining. Journal of the Soil Mechanics and Foundations Division, ASCE, Vol. 98, No. SM7, July 1972, pp. 709-725.
6. E.T. Selig and W.B. Truesdale. Properties of Field Compacted Soils. HRB, Highway Research Record 177, 1967, pp. 77-97.
7. D.J. D'Appolonia, R.V. Whitman, and E.D. D'Appolonia. Sand Compaction with Vibratory Rollers. Journal of the Soil Mechanics and Foundations Division, ASCE, Vol. 95, No. SM1, Jan. 1969, pp. 263-264.
8. J.W. Hall. Evaluation of Vibratory Rollers on Three Types of Soils. U.S. Army Engineer Waterways Experiment Station, Vicksburg, MS, Soil Compaction Investigation Rept. 10, Tech. Memo No. 3-271, March 1968.
9. D.A. Tiedemann. Ground Motions for Vibratory Roller Compaction of Cohesive Soil. U.S. Bureau of Reclamation, REC-OCE-70-28, June 1970.
10. A.C. Whiffin. The Pressures Generated in Soil by Compaction Equipment. ASTM, STP No. 156, 1953, pp. 186-210.

Building on Mine Spoil: New Approach Using Dynamic Consolidation and Pressuremeter Testing

CHRISTIAN GUYOT

A combination of two well-known techniques of soil testing and soil improvement was used on an experimental section to test its ability to improve and test recent mine spoils. These techniques are pressuremeter testing and Dynamic Consolidation. The mine spoil is composed of 100 ft (33 m) of shales, tills, and loesses that were transformed by weathering action into a silty clay matrix. This silty clay holds in its mass an extremely large number of limestone boulders. The spoil, 10-15 years old, exhibits poor engineering characteristics and has not yet reached its self-bearing level. Pressuremeter tests were performed at all stages of the work. The depth of the boreholes was generally 50 ft (15 m), and a test was performed every 3 ft (1 m) down. The pressuremeter probe was protected by a slotted steel casing. The Dynamic Consolidation was performed with light equipment in order to test the technique economically on the top 35 ft of the spoil. Two trial areas were compacted and results were compared with those of a 20-ft (6-m) high earth-fill load test. Results show that improvement due to the Dynamic Consolidation is dramatic and two to eight times larger than the improvement induced by the earth-fill load test. The analysis of the results enabled the determination of a program to improve the entire mass of the fill so it can be used as a good foundation to support heavy construction on shallow foundations.

The construction of a large industrial plant with heavy loads and limited settlement tolerances on 100 ft (33 m) of a silty clay material with large boulders of limestone raises some serious foundation problems, both technical and economic. A new approach for testing and improving the engineering characteristics of the soil was developed and tested on site. The techniques involved were essentially pressuremeter testing and Dynamic Consolidation, both developed and performed in the field by Menard, Inc.

SITE GEOLOGY

The soil consisted of a heterogeneous mixture of shales, tills, and loesses transformed by weathering action into a silty clay material. It holds in its mass a large amount of big angular blocks of limestone. These materials were originally the overburden of a series of coal strata that were strip mined approximately 12 years ago. During the operation, the above mine spoils were dumped erratically on the site. The water table at the time was situated 35-ft (10.5-m) deep.

PROGRAM OF OPERATIONS

The test included three major activities:

1. Pressuremeter testing before, during, and after the Dynamic Consolidation work,
2. Execution of Dynamic Consolidation, and
3. Pressuremeter testing through an earth-fill load test to calibrate the results.

Pressuremeter Testing

The pressuremeter is an instrument for in situ measurements of soil load and deformation parameters. It consists of two main components (Figure 1):

1. The probe is a cylindrical metal body covered by a radially deformable cover. It is formed of three cells (see Figure 2). The central or measuring cell is filled with water under controlled pressure.
2. The control unit regulates volumes and pressures applied on the different cells.

The probe is placed within a previously drilled borehole or driven into the ground at the desired elevation. Pressure is then applied in equal increments and the corresponding volume variations are noted at 30- and 60-s intervals. By plotting volumes versus pressures at each increment, an in situ stress-strain curve is obtained (see Figure 2). Some of the engineering characteristics of the soil that are derived from the test are the limit pressure Pl, or the pressure at which failure occurs. It reflects directly the bearing capacity of the soil. The test also gives the modulus of deformation (E) from which settlements can be calculated.

All tests were carried out by using a GA-type Menard pressuremeter. In order to avoid frequent puncture, the probe was inserted into a slotted casing. The casing was driven into the ground by using an Atlas Copco Roc 601 drilling rig and O.D. method. Boreholes were usually terminated at 50-ft (15-m) depth. Tests were carried out every 3 ft (1 m).

Dynamic Consolidation

Dynamic Consolidation is a method patented and developed in 1969 by the late French engineer Louis Menard. It improves the engineering properties of in-place soils at depth, both above and below ground water table, both onshore and offshore. The method consists of providing large energy impacts at the ground surface. This is done by dropping steel tampers 10-200 tons in weight from heights of 60-120 ft.

In any type of unsaturated material, the shock waves cause compaction as in a Proctor test. In submerged soils, P-wave first causes partial-to-full liquefaction and the S-wave and the Raleigh wave rearrange the soil grains structure into a denser state. Improvement has been achieved in materials that range from rock fill to clayey silt and building or domestic refuse. The results of treatment by Dynamic Consolidation are dramatic and immediate. Strength in terms of bearing capacity is typically improved by a factor of 2-4. Compressibility in terms of total and differential settlements can be reduced by a factor of 3-10. An essential part of the Dynamic Consolidation service is an intensive program of field and laboratory tests. On the basis of these tests energy requirements and construction sequences are planned.

The budget available for the test section did not allow for the mobilization of special heavy rigs capable of improving the soil down to 100 ft (33 m). Therefore, the test was carried out with a modified 150-ton crawler crane dropping a 15-ton pounder from 65 ft (see Figure 3). That type of equipment can usually treat the ground down to 30 ft (9 m). Careful analysis of results enables determination of the improvement that could be obtained at a greater depth by using heavier equipment. This is done by using empirical formulas established on numerous sites around the world.

Earth Fill Load Test

An earth fill load test 22 ft (6.7 m) high and 80x80 ft (24x24 m) square top was available on the site. Settlements of the soil below the embankment had been monitored by using 15 settlement gauges dropped in four different boreholes at different elevations. The deepest gauge was located at 75 ft (22.5 m) below the original ground surface. At that point a pressuremeter boring was made in the mine spoil through the embankment. Tests were carried out every 3 ft (1 m) down to a depth of 106 ft (38 m).

Figure 1. Pressuremeter equipment.

Figure 2. Typical pressuremeter curve.

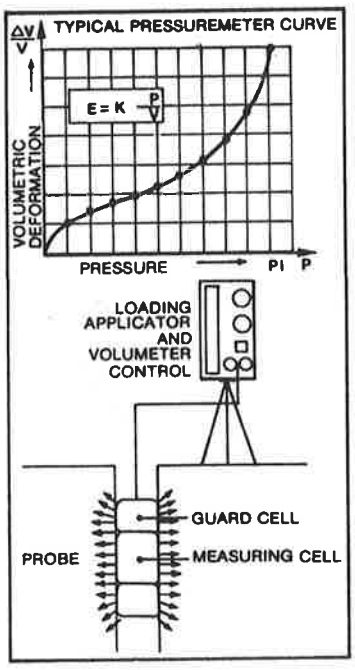

RESULTS OF EARTH FILL LOAD TEST

Settlements measured under the earth fill are plotted on Figure 4. They indicate that compression occurred down to 113 ft (34 m). The pressuremeter profile, especially the modulus of deformation, shows that, in fact, the improvement due to the static load was limited to 36 ft (11 m). Immediately underneath the foundation the stress applied on the surface induces a volume change in the soil and, therefore, the development of a consolidation process (increases of the three principal stresses). Below that area, only angular deformations occur to induce settlements but no consolidation (only one principal stress increases with the load).

Compariso between the settlements that occurred underneath the earth fill load test and those calculated for the same load by using the pressuremeter results enables the determination of some important parameters, such as the so-called structure coefficient, which varies according to the type of soils and its degree of consolidation. This parameter also represents the ratio between the pressuremeter deformation modulus and the constrained modulus. The structure coefficient was found to be equal to 0.55.

DYNAMIC CONSOLIDATION

The Dynamic Consolidation technique was tested in two different areas. They were approximately 500 ft (150 m) apart and were both cleared of vegetation and leveled prior to the treatment.

Area A

Treatment on area A was performed in five phases. Phases 1 and 2 consisted of pounding a 20x20 ft (6x6 m) square grid. Phases 3 and 4 consisted of pounding a 20x20 ft intermediate grid (prints in between prints of the primary grid). Phase 5 consisted of

Figure 3. Dynamic consolidation rig.

an ironing phase where the pounder was dropped once on a 10x10 ft (3x3 m) square grid. A total energy of 304 Mg•m/m² was necessary to compact this area. (The energy consists of the weight of the hammer in megagrams multiplied by the drop height in meters and divided by the grid surface in square meters.)

Area B

Treatment of area B was performed in four phases. Phase 1 was done on a 40x40 ft (12x12 m) grid; Phase 2 on a 40x40 ft intermediate grid. Phase 3 was done on a 20x20 ft (6x6 m) grid superimposed on the previous ones. Phase 4 was an ironing phase on a 10x10 ft (3x3 m) grid. The energy necessary to compact this area was equal to 330 Mg•m/m².

Results

The clayey nature of the mine spoils necessitated the presence of a 2-ft (0.6-m) thick rock-fill working platform on both areas. This rock fill was used primarily to backfill the craters created by the treatment in order to provide a good transmission of energy between two subsequent subphases in the same prints. The settlements induced during the Dynamic Consolidation treatment are an average of 50 percent higher than those induced by the earth-fill load test. A great many pressuremeter tests were performed before, during, and after treatment of both areas. Results showed that the treatment on area B was more successful. The improvement in terms of pressuremeter results is shown on Figure 5, where it is also compared with the original characteris-

Figure 4. Settlements measured under earth fill.

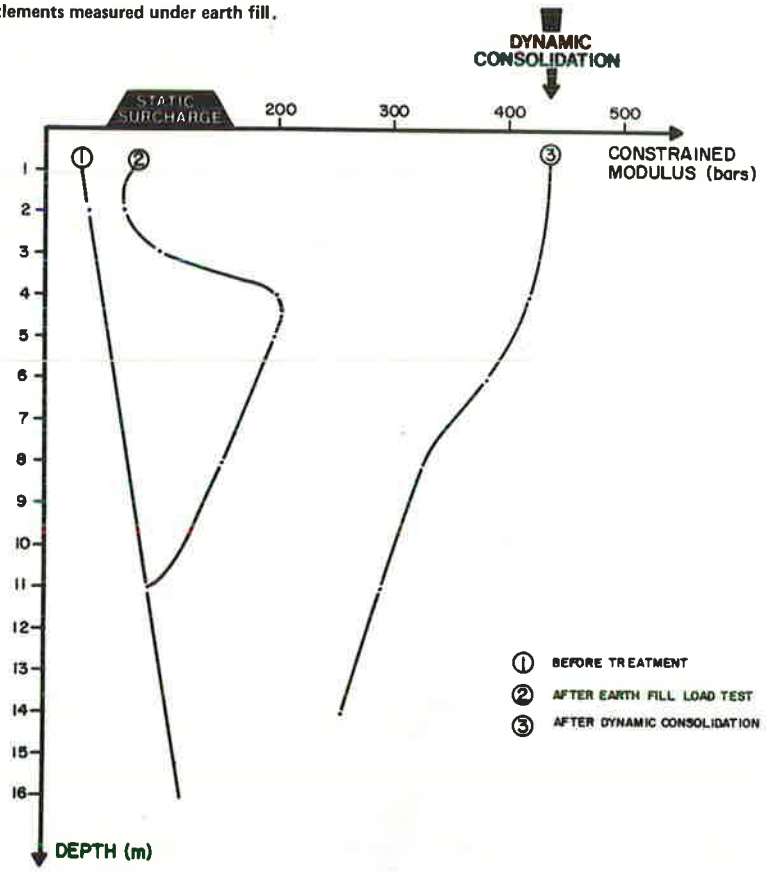

Figure 5. Energy-limit pressure relation.

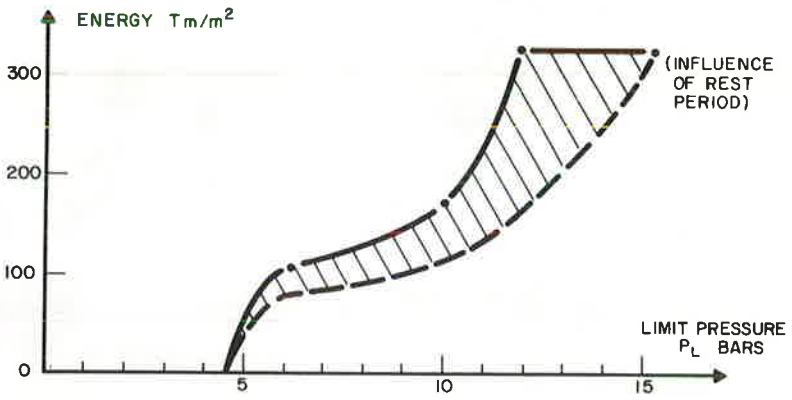

tics of the soil and those after the load test. The observation of the limit pressures shows three different zones in the treated ground:

1. From 0-30 ft (9 m) very high densification with average limit pressures in excess of 16 tons/ft² (1.6 MPa)
2. From 30-37 ft (11 m) slightly lower results with average around 10.5 tons/ft² (1.0 MPa), and
3. Below the water table 37 ft (11 m) down, a regain of the characteristics with limit pressure around 15 tons/ft² (1.5 MPa).

Tests immediately after treatment and two weeks after treatment showed that the characteristics are improving with time (Figure 5). This is explained by the very fine composition of this material and, therefore, the time required for the water pressure to dissipate.

The analysis of results obtained after treatment enabled the determination of the parameters that govern the relation between energy and depth. The equation used is

$$H = cd\sqrt{E} \quad (1)$$

where

H = depth of influence of the treatment (m);
c = coefficient depending on soil conditions;
d = coefficient determined as follows, for free drop d = 1 or for crane drop d = 0.9; and
E = energy per blow (Mg•m).

For the very high densification zones described above, c is 0.6. For the lower densification below that zone, c is 1.

By using all these parameters, a 40-ton pounder can be calculated to highly densify 60 ft (18 m) and collapse 100 ft (30 m) of mestastable soil. These numbers for a 150-ton pounder would be 107 ft (32 m) and 173 ft (52 m), respectively.

CONCLUSIONS

The extensive efforts that were put into the design, treatment, and control of this test section have largely improved the knowledge and understanding of the behavior of mine spoils. The pressuremeter tests were found to be a reliable and practical method of evaluating the engineering characteristics of this material, which are usually difficult to assess due to their heterogeneities.

The Dynamic Consolidation treatment improved this very fine and heterogeneous material dramatically. Depending on the type of construction and depth of the mine spoil, different machines with different energies per drop can be used. Densification of soils 30- to 100-ft deep can be achieved. Postconstruction total and different settlements are largely reduced to tolerable levels.

A Dynamic Consolidation treatment on mine spoils can be successfully completed for a fraction of the cost of other conventional techniques, such as overexcavation and backfill or piles.

Wick Drains, Membrane Reinforcement, and Lightweight Fill for Embankment Construction at Dumbarton

JOSEPH B. HANNON AND THOMAS J. WALSH

The use of special features to permit embankment construction over soft bay mud is reported. These features included reinforcing fabric, lightweight fill (sawdust), and vertical wick drains, a system that allows construction to proceed on schedule without major foundation failures. An instrumented test embankment that incorporates these features was constructed by the California Department of Transportation (Caltrans) in 1979 at the bridge head of the east approach to the new Dumbarton Bridge. The successful performance of the test embankment provided data for developing specifications for construction of the 2.4-mile embankment contract across the soft bay mud deposits. The fabric provided initial support over the bay mud, lightweight fill reduced loading to ensure ultimate stability, and vertical wick drains accelerated foundation consolidation, which allowed up to 7 ft of settlement to occur in 1 year as opposed to about 50 years under the same loading with normal drainage conditions. Polyvinyl chloride (PVC) wick drains were found to be 40-50 percent as efficient as Alidrains in accelerating consolidation. Their efficiency increased with greater hydrostatic pressures. Instrumentation monitored and controlled the rate of embankment placement. These special features were successful in maintaining stability during construction that would not have been possible by the use of conventional construction techniques.

Embankment placement over soft compressible foundation soils has caused many perplexing problems for the transportation engineer, both during construction and in long-term pavement maintenance. The selection of a particular foundation treatment to aid construction and reduce future maintenance depends on the extent and character of the soft foundation deposits. (i.e., Can they be removed and replaced with more competent material or improved by consolidation and resultant strength increase?)

The soft muds in the San Francisco Bay area have presented a challenge to California Department of Transportation (Caltrans) engineers on a number of occasions. The most recent challenge is the embankment construction for the approaches to the new Dumbarton Bridge. The existing low-level lift span bridge carries traffic for CA-84 across the southern portion of San Francisco Bay between Alameda and San Mateo Counties, in Caltrans district 4. The new 1.6-mile long, high-level bridge structure, which is under construction, should be open to traffic through detour connections in 1982. The approach embankments to this facility are also under construction. The east approach embankment extends from the bridgehead across the Newark salt ponds to Thornton Avenue, a distance of 2.4 miles. The west approach embankment construction covers a distance of 1.6 miles (Figure 1).

This paper discusses the construction and performance of a test fill, the east approach embankment construction, and the development of specifications for special features in embankment construction used

Figure 1. Project location.

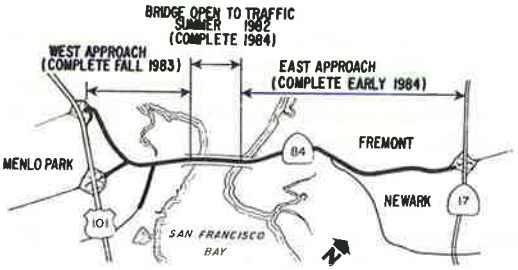

Figure 2. Cross section 04-ALA-84-PM 0.7/3.1.

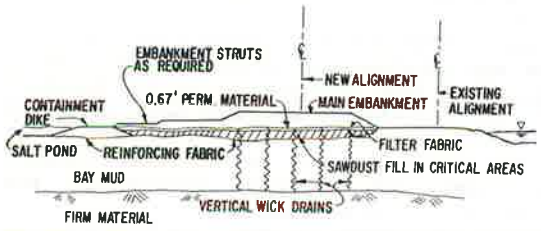

to successfully execute the work within the contract schedule.

BACKGROUND AND ANALYSIS

The salt ponds through which the east approach alignment traverses lie over former marshlands. The average depth of water in the salt ponds is about 2.5 ft. The entire area is underlain by San Francisco Bay mud, which ranges in thickness from 20 ft near the toll plaza to 40 ft at the bridgehead. This material has an undrained shear strength of less than 100 lb•f/ft² near the surface and increases to more than 300 lb•f/ft² at greater depths. The proposed embankment, including surcharge, will reach a height of approximately 14-16 ft above mean sea level during construction. The bay mud foundation will not provide sufficient support without special foundation treatment and controlled rates of embankment loading.

As originally conceived, the approach roadway to the new bridge was to be built by conventional methods by allowing about four years of settlement time prior to pavement placement. However, local demands dictated that the bridge construction be undertaken first, followed by the approaches at intervals of one to two years. These time constraints and the need for a planned roadway profile at elevation +10 presented new stability and settlement problems.

To accomplish the embankment construction within the contract time, several features were incorporated that have had minimal prior use in the United States:

1. Reinforcing fabric to distribute embankment loading and prevent failure of soft foundation soil during construction and reduce differential settlement,
2. Lightweight fill (sawdust) to reduce total embankment loading,
3. Vertical wick drains to accelerate the consolidation process to less than one year, and
4. Filter fabric to prevent contamination of a permeable drain blanket for removal of pore water as part of the consolidation process (Figure 2).

Stability analyses of critical cross sections revealed only marginal to failure conditions by using conventional fill placement. The above features were needed to preclude multiple shear failures and the development of an extensive mud wave. Shear failure, long-term differential settlement, and inordinate maintenance requirements would result from the use of conventional construction techniques. The maximum heights attainable with conventional fill, based on previous Caltrans experience, would also be limited to about 8 ft. Laboratory studies indicated that normal consolidation would also require up to 50 years for ultimate settlement of about 6 ft to occur in a 40-ft depth of bay mud. Reinforcing fabrics have been successfully employed by Haliburton (1) and others to bridge soft materials. The use of fabric at Dumbarton would provide the uniform support necessary over the soft bay mud during the early stages of embankment placement. From computer analyses we estimated that the fabric would add about 10 percent to the overall stability of the embankment foundation system through additional unit cohesion provided by fabric tensile strength.

The sawdust would be incorporated in the main embankment as lightweight fill below elevation +5, which would keep it in a saturated state free from oxidation and, thus, deterioration. The experience of others (2,3) suggests that this condition, or a condition free from continuous wetting and drying within an embankment, will ensure long-term service life. After settlement of the bay mud foundation at Dumbarton, the sawdust would be submerged below the adjacent salt ponds.

The lightweight fill would be placed in areas of questionable stability and would require no compaction other than that provided by spreading equipment. Design parameters assumed for the sawdust were drained angle of internal friction (ϕ = 31°), drained cohesion (c = 0), and wet unit weight (γ = 40 lb•f/ft³) based on experience (2). The conventional earth fill compacted wet density was specified at 145 lb•f/ft³ maximum.

Wicks or band-shaped drains were proposed for this project to accelerate consolidation and strength gain and to minimize postconstruction settlement. Wick drains are made of paper, plastic, or other synthetics and conduct water upward by excess hydrostatic pressure. They are about 4-in wide and vary in thickness from 1/16 to 1/4 in. With a wick spacing of 4 ft, we estimated that the settlement period could be reduced to less than a year.

Barron's method (4) was employed by assuming an equivalent sand drain diameter of 6 in for the wick drains based on work by Fellenius (5) and Hansbo (6). Values of site soil permeability were estimated from reference data and other project performance records. For design, the project was divided into units A, B, and C according to approximate depths of bay mud. Unit A had 40 ft of bay mud and required a wick spacing of 4 ft. Wick spacings of 5 ft for unit B with 30 ft of mud and 6 ft for unit C with 20 ft of mud were a compromise based on economics and similar postconstruction settlements in the three units.

TEST FILL

A 300-ft long test fill to a maximum height of 16.5 ft was constructed in 1979 at the east bridge abutment, prior to the main embankment contract. The test fill provided an evaluation of the applicability of the proposed special features prior to incorporation in the main contract. It was constructed by change order under the ongoing bridge contract.

Caltrans installed extensive instrumentation to

monitor construction loading and prevent potential embankment failures. Instruments were located on two cross sections and at the corners of the embankment struts (buttress fills). The instrumentation consisted of settlement platforms, anchor postsettlement gauges, horizontal settlement profile gauges, piezometers, heave stakes, and inclinometers. In addition to the instrumentation, six test areas with different reinforcing fabrics were established.

Construction of the test fill was accomplished in the following sequence (see Figure 3):

1. Construct both longitudinal and cross-containment dikes by first placing reinforcing fabric across the salt ponds and end dumping and compacting earth fill to strut elevation +6,
2. Dewater area contained by dike and existing roadway embankment,
3. Place reinforcing fabric on bay mud for main embankment within containment area,
4. End dump lightweight fill (sawdust) and earth fill as required to establish a working table to elevation +5,
5. Place layer of filter fabric on working table,
6. Place permeable drainage layer,
7. Place layer of filter fabric on drainage layer,
8. Place 0.5-ft layer of earth fill,
9. Install wick drains,
10. Advance remaining fill at a controlled rate of 1-ft maximum/7 calender days to elevation +10 and 1-ft maximum/14 calender days for elevations above +10, and
11. Allow for settlement period whose exact length of time will be determined from instrumentation.

The test fill was constructed without serious problems and was considered a major success based on settlement performance. It also produced valuable information from which to develop specifications for the main east and west approach embankments.

The reinforcing fabrics placed under the test embankment included woven and nonwoven materials. A wide variation in the handling characteristics of these materials was noted. On the basis of strength, elongation, and handling characteristics, a woven reinforcing fabric of either polyester, nylon, or polypropylene was specified for the main approach embankment. Test requirements were a minimum grab strength of 200 lb, an elongation at failure of 35 percent maximum, and a minimum joint strength of 160 lb.

One-foot of earth cover was required over the sawdust for the main approach fill to prevent wind blown losses during long periods of exposure and to provide additional support. The first level of filter fabric was placed directly over this earth layer followed by the permeable drainage rock blanket.

For maximum efficiency of the wick drains, cutoff of the wicks was provided within the drainage blanket. Therefore, specifications were that approximately one-half thickness of the drain rock be placed, that the wicks be driven and cut off at this working table surface, and that the remaining portion of the drain rock then be placed.

The relief of the test fill drainage blanket by outletting at the toe of slope did not function as anticipated. In fact, the pore water that exuded up the wick drains from the bay mud foundation never appeared at the planned outlet although it was encountered in test holes at depths of 1-2 ft. This may be explained in part by the construction of the wick drains (Alidrains) that allowed pore water to exude at any vertical elevation, collect in the sawdust fill, and possibly escape along the plane of the reinforcing fabric.

The drainage relief plan for the main fill was changed to include a longitudinal underdrain system that would discharge into vertical riser pipe pumping stations at 500-ft intervals on centerline. The longitudinal collector used was a 1.5-in diameter slotted plastic pipe.

At the time of the test fill construction, only two wick drain materials were available in California: the polyvinyl chloride (PVC) wick, a Japanese product with no local installer, and the Alidrain wick, a product of Canada distributed in the United States through Vibroflotation Company of Pittsburgh. Vibroflotation was engaged in a wick drain project in southern California and so was selected by the contractor to perform the work for the test fill due to their availability. The wicks had to be driven through 1 ft of earth fill, 8 in-1 ft of drain rock, two layers of filter fabric, 3-5 ft of sawdust, a reinforcing fabric, and ±40 ft of bay mud to a total depth of 46 ft (see Figure 2).

The hydraulic powered wick driving machine, a Swedish design, was mounted on a backhoe. The installation proceeded smoothly with only normal delays and was completed in about three weeks. The test embankment was then placed to the planned height by using the controlled rates of loading previously described. The maximum fill height attained was 16.5 ft, including a surcharge.

Instrumentation was placed during the early stages of construction and was monitored continuously during embankment placement. The consolidation process accelerated immediately following installation of the wick drains in October 1979. Eleven feet of additional fill material was then placed above the wick level by using the controlled loading rates. By mid-February 1980, five months after the wick installation, nearly 100 percent of the primary settlement had occurred. Six months later the total recorded settlement was approximately 6.5 ft and the settlement curve was flattening (Figure 4).

As shown in Figure 4, which compares actual field settlement to the theoretical settlement curve with normal consolidation drainage, the wick drain performance met expectations. Figure 4 also shows a reasonably close comparison between predicted and actual settlement performance with wick drainage. The overall performance and appearance of the test fill was excellent. Two small cracks appeared in the first terrace of the embankment, which were probably the result of differential settlement between the main embankment and the outer strut. A small crack also appeared near the catch point between the new embankment slope and the existing roadway, which probably represented drawdown and rotation of the existing roadway.

The reinforcing fabric under the fill prevented the development of a mud wave in the soft bay mud foundation. High pore pressures were recorded during construction, which probably would have caused failure if reinforcing fabric had not been used. By contrast, an adjacent staging area constructed to elevation +6 by the end dumping method with no special treatments or controlled rates of loading produced a large mud wave.

EAST APPROACH EMBANKMENT

The east approach construction went to contract in June 1980. The original construction sequence, amended through experience with the test fill, was incorporated in its entirety. However, to facilitate the operation, the contractor was given the op-

Figure 3. Construction sequence for test fill.

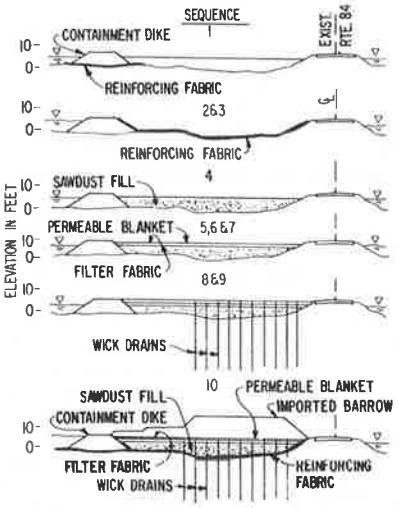

Figure 4. Actual versus predicted settlement for Dumbarton test fill.

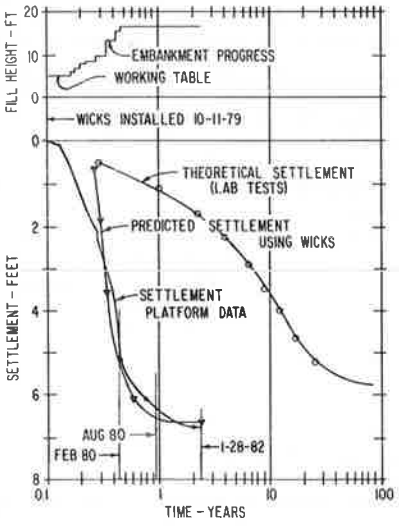

tion of diking off subareas, which he elected to do (see Figure 3).

Reinforcing fabric was first placed by hand with the aid of a row boat across the open water, longitudinally with the dike. The salt ponds had conveniently been drawn down to about 1- to 2-ft depth, which aided placement. Imported borrow for the dikes was hauled in 10-wheelers, end dumped on the fabric, and pushed and advanced by D-6 dozers. The specified grading required a minimum of 20 percent passing the no. 200 sieve to ensure an impermeable dike.

Dewatering of the containment areas was accomplished by using 6-in trailer-mounted pumps supplemented by smaller suction pumps. Following dewatering of the subponds, reinforcing fabric was placed with stitched seams transverse to the main embankment. The woven Mirafi-500X reinforcing fabric was supplied by Celanese Corporation. It was floated on air in large sheets to cover the diked off subponds. Lead corners of the fabric were tied to light trucks that pulled the fabric over the dewatered ponds. One truck operated on the dike and the other from the shoulder of existing CA-84. This kite was about 200 ft wide and 800 ft long.

Complete evacuation of all the fluid muds near the surface was impractical. Consequently, much of this material was trapped as mud boils under the fabric. Loading and pushing of the fill materials on the fabric eventually forced the fluid mud out of the fill area, across the dike, and into the adjacent main pond. During this operation the fabric was able to contain mud boils up to several feet in thickness and a hundred or more feet on a front.

Earth fill for the embankment was hauled primarily in bottom dumps and pushed and spread by D-6 dozers. Sawdust for lightweight fill was trucked in from various saw mills in the Sierra foothills and northern logging counties. Sawdust was pushed and spread by D-6 dozers equipped with flotation tracks and side boards attached to the dozer blades. Drain rock for the permeable blanket was supplied locally and the nonwoven filter fabric was Mirafi 140S supplied by the Celanese Corporation.

The wick installation was done by Malcolm Drilling Company of South San Francisco. Malcolm elected to use the Japanese-manufactured PVC drain. For this project Malcolm built up two wick-drain-driving machines, which consisted of dual mandrels suspended from wide-tracked 70-ton cranes. Each pair of mandrels was driven by a single vibratory hammer powered off a generating package mounted at the rear of the cab. The mandrels could be adjusted to any drain field pattern.

The engineer's estimate called for 1 887 000 linear ft of vertical drains. On completion of the item approximately 95 percent of the estimated quantity had been installed. A portion of the remaining wicks was used through a change in contract order that required the contractor to drive additional wicks in an area where considerable amounts of fluid to very soft surface muds were encountered. The additional wicks were to provide early stabilization of the area and to the minimize damage potential to the adjacent KGO radio tower facility. This also provided wick spacings of 2.5, 4, and 5 ft for comparison within the same depth of bay mud (30 ft). The vertical drain work was done over a period of slightly more than four months, between October 1980 and February 1981.

The embankment was placed at the prescribed controlled rate to elevation +10 and excess pore pressures were monitored by piezometers in the 30- and 40-ft deep sections of bay mud. The contractor's embankment placement operation above elevation +10 required close control as a result of the slow dissipation of these excess pore pressures. Pore pressures were also monitored in the 20-ft section of bay mud, but only localized problems were experienced.

The waiting period required for dissipation of pore pressure exceeded eight weeks in some areas between placement of each additional 1-ft lift of embankment. The excess pore pressures in this case represented more than 50-60 percent of the total applied embankment load. A typical plot is shown in Figure 5.

Measured total settlement through November 1981 averaged about 3.5 ft in the 40-ft bay mud section. This represents about 55 percent of the predicted ultimate settlement in the deepest bay mud section. Figure 6 shows a comparison of settlement produced in the main east approach foundation by the PVC wicks and that produced in the test fill foundation by the Alidrains. The PVC wicks are not functioning as efficiently as the Alidrains; however, the rate of consolidation is accelerated somewhat with the PVC wicks driven on closer-than-normal spacings. This is illustrated in Figure 7, which compares field settlement with PVC wicks on spacings of 2.5, 4, and 5 ft.

Even though pore pressures were critical, with most of the embankment load being carried by pore water, no failures occurred in the 2.4-mile east ap-

proach embankment. However, one area did exhibit evidence of potential failure. A slope indicator located beyond the containment dike measured about 2 in of lateral movement. The outer portion of the main fill in the same area also subsided up to 1 ft over a distance of about 200 ft. No other signs of distress were observed other than settlement cracking. Failure would have occurred in this area and possibly other areas had the reinforcing fabric not been used.

A determination of strength gain of the underlying bay mud foundation was accomplished by in situ vane shear tests. The results suggested an average shear strength gain of 0.1 tons/ft² (200 lb•f/ft²) after 40-50 percent consolidation in the 40-ft bay mud section (see Figure 8). Based on these results and some dissipation of excess pore pressure, a decision was made to resume embankment loading.

The PVC wick drains were observed to function more efficiently with additional embankment loading and greater hydrostatic pressure, which was consistent with laboratory wick drain performance test results. The problem of slow pore pressure dissipation minimized with the additional loading. However, waiting periods in excess of two weeks were still required for each additional 1-ft embankment lift. The east approach embankment was completed in January 1982.

Figure 5. Typical time plot for embankment progress, pore pressure, and settlement response in critical PVC wick drain area.

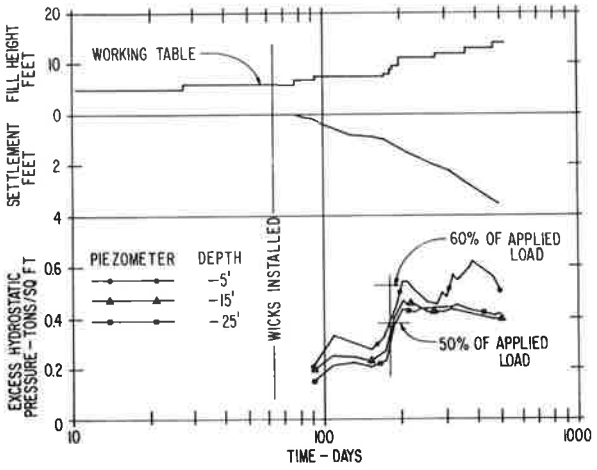

Figure 6. Settlement comparison, PVC wick drains versus alidrains.

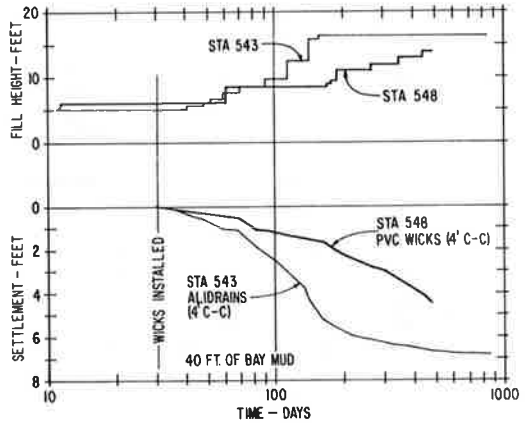

Figure 7. Settlement with PVC wicks on three spacings.

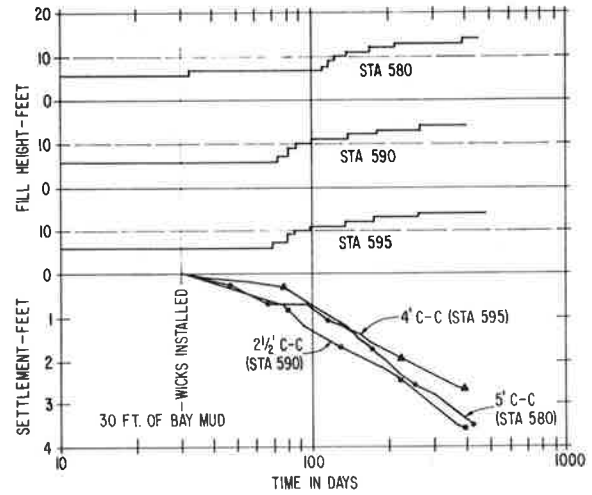

SUMMARY

This project provided the opportunity to introduce and evaluate various special features for construction of embankments over soft compressible bay mud deposits. The embankment construction was termed a major success because all previous construction experiences over bay muds were plagued with difficulty and embankment failures. These features comprised a system that, when carefully applied and controlled, resulted in successful construction. The system solved the problem of regulated construction approach, short-term stability, and long-term consolidation.

The reinforcing fabrics successfully bridged across the soft compressible bay mud foundation and provided adequate initial support for embankment construction. During the loading process, the reinforcing fabric held the fill together and prevented failure during critically high pore pressure conditions. Appropriate fabric specifications are now available as a result of this project.

Sawdust proved effective as lightweight fill and served to reduce both the initial and ultimate loading on the bay mud foundation and provided satisfactory support for construction equipment. Wick drains were effective in accelerating consolidation and proved to be an economical alternative to sand drains. The Alidrains in the test fill reduced the settlement period from 50 years under normal consolidation drainage to less than 1 year. The PVC drains in the main east approach fill were found to be 40-50 percent as efficient as the Alidrains in accelerating consolidation. The efficiency of the

Figure 8. In situ vane shear strength of bay mud.

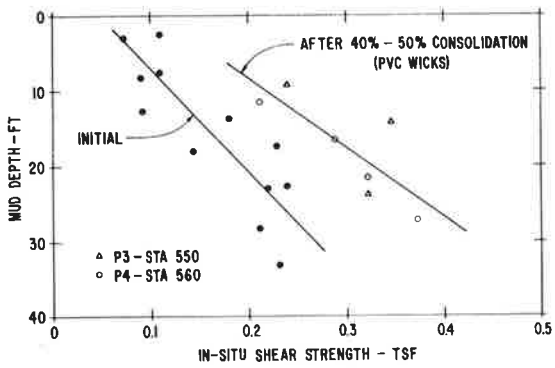

wick drains increased with greater hydrostatic pressure due to embankment loading.

This project introduced the use of wick drains in California and several wicks are now available. Their application on other projects is proposed.

REFERENCES

1. Haliburton Associates. Design of Test Section for Pinto Pass Dike, Mobile, Alabama. U.S. Army Corps of Engineers, Mobile District, Mobile, AL, June 1978.
2. D. Nelson and W. Allen. Sawdust as Lightweight Fill Materials. Public Roads, Vol. 39, No. 2, 1975.
3. J.D. Robinson. Sawdust Embankment. Highway Focus, Vol. 8, No. 3, Oct. 1976.
4. R.A. Barron. Consolidation of Fine Grained Soils by Drain Wells. Transactions, ASCE, Paper 2346, 1947.
5. B.H. Fellenius. The Background and Theory of Vertical Drains with Particular Reference to the Alidrain. Notes for lecture in Skelleftea, Montreal, Aug. 24, 1977.
6. S. Hansbo. Consolidation of Clay by Band-Shaped Prefabricated Drains. Ground Engineering, Vol. 12, No. 5, July 1979.

Determining Maximum Void Ratio of Uniform Cohesionless Soils

JOHN E. WALTER, WILLIAM H. HIGHTER, AND ROBERT P. VALLEE

A testing program was conducted to evaluate several methods of determining the maximum void ratio of cohesionless soils. Preliminary test results indicated that a new procedure called the tube method was consistent in attaining reliable maximum void ratios. In performing the tube method, a long narrow tube or cylinder opened at both ends is placed upright in a mold of known volume. A quantity of dry sand sufficient to fill the mold is placed in the tube and then the tube is slowly extracted to allow sand to trickle into the mold until the mold overflows. The sand is then screeded level with the top of the mold and the void ratio is calculated from measured masses and volumes and the specific gravity of the sand. To evaluate various methods of determining maximum void ratios, a test series was carried out by using eight different test procedures on four sands. Statistical analyses of the data indicated that the tube method yielded higher values of maximum void ratio than did the other procedures. In addition, a testing program involving nine inexperienced operators demonstrated that by using the tube method an individual operator was able to reproduce results consistently and the operators were able to replicate one another's results well within limits mandated by practical applications.

Relative density (density index) is used to describe the state of compactness of cohesionless soils as a function of the loosest and densest states that the soil can attain. Knowledge of the density index (I_D) can give engineers valuable insight into the engineering behavior of a soil. However, since a particular soil can have different fabrics or arrangements of particles at the same void ratio, additional descriptors are required to characterize the soil.

The density index or relative density (D_r) of a soil at void ratio e and dry weight γ_d is defined in terms of void ratio as

$$I_D = D_r = [(e_{max} - e)/(e_{max} - e_{min})] \times 100\% \quad (1a)$$

and in terms of corresponding dry unit weight as

$$I_D = D_r = [\gamma_{d_{max}}(\gamma_d - \gamma_{d_{min}})/\gamma_d(\gamma_{d_{max}} - \gamma_{d_{min}})] \times 100\% \quad (1b)$$

where the subscripts refer to maximum and minimum states.

Dry unit weights or void ratios of the soil in the densest and loosest states are determined by laboratory tests. Errors in determining these values lead to significant errors in the estimation of the density index (1) and can mislead the engineer in an assessment of the likely in situ behavior of the soil under service loads. The determination of the loosest state of soil compactness has been particularly troublesome. The research reported here focuses on the procedures used in the determination of maximum void ratio for clean, medium to fine, uniform sands.

The choice of sands to use in the testing program was influenced by the findings of previous investigators. Burmister (2,3) reported the effects of particle shape, size, and gradation on limiting void ratios. Kolbuszewski (4) also studied parameters that controlled limiting void ratios in granular soils and found that particle shape and pluviation height have a strong influence on maximum void ratio. Youd (5) found particle size to have minimal effect on maximum void ratio. Studies by Dickin (6) and Norris (7) found particle shape to be the most influential soil factor in controlling maximum void ratio. Youd (5) prepared a plot from which maximum void ratio can be estimated from gradational and particle shape characteristics.

PROPERTIES OF SOILS TESTED

The four soils used in the investigation were medium to fine sands. The selection was based on particle shape, size, and gradation characteristics. Each sand contained less than 5 percent of particles finer than the no. 200 sieve and no more than 5 percent coarser than the no. 4 sieve. Because of the important effect of particle shape on limiting void ratio, a major criterion in selecting the soils was their shape characteristics.

Microphotographs of each candidate soil were obtained and, based on the method suggested by Wadell (8), the roundness of each soil was obtained. Wadell (8) defined roundness (ρ) as

$$\rho = (1/R)\left[(1/N)\sum_{i=1}^{N} r_i\right] \quad (2)$$

where the term within brackets is the arithmetic mean of the sum of N internal radii of the projected particle shape and R is the radius of the maximum

Table 1. Index properties of four soils.

Soil	Specific Gravity (G_s)	Particle Size: Effective [D_{10} (mm)]	Particle Size: Mean [D_{50} (mm)]	Coefficient of Uniformity (C_u)	Coefficient of Curvature (C_c)	Roundness[a] (ρ)
F-70 banding sand	2.65	0.10	0.15	1.5	1.1	0.30
ASTM C109 sand	2.65	0.22	0.38	1.9	1.0	0.42
ASTM C190 sand	2.65	0.56	0.75	1.4	1.0	0.60
Garnet mine tailings	3.16	0.06	0.19	3.3	1.2	0.19

[a]Results based on equations by Wadell (8) and charts by Powers (9).

Figure 1. Grain size distribution curves for four sands.

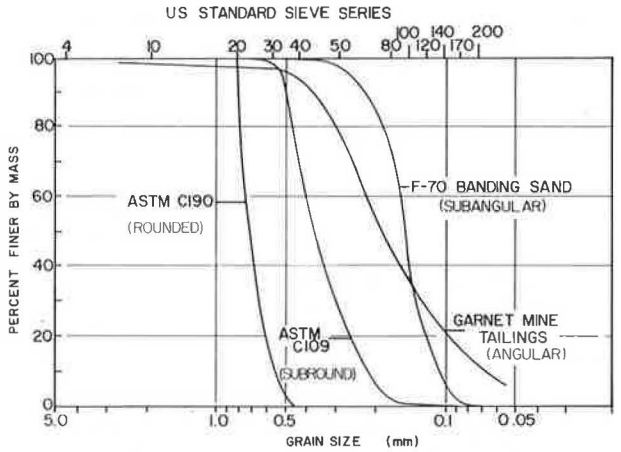

Table 2. Mean maximum void ratios from initial pluviation tests.

Funnel Diameter (in)	Pluviation Height (in)	Mean Max Void Ratios by Mold Diameter: 2.0 in	2.5 in	3.0 in	3.5 in	4.0 in	4.5 in
0.117	6	0.831	0.835	0.833	0.835	0.830	0.836
	12	0.800	0.808	0.815	0.822	0.818	0.821
	24	0.622	0.664	0.702	0.709	0.730	0.705
0.275	6	0.831	0.831	0.838	0.837	0.831	0.839
	12	0.827	0.824	0.836	0.835	0.825	0.824
	24	0.818	0.814	0.818	0.818	0.806	0.803
0.435	6	0.816	0.813	0.815	0.814	0.814	0.817
	12	0.812	0.811	0.809	0.811	0.807	0.814
	24	0.807	0.805	0.804	0.803	0.799	0.804

inscribed circle within the projected area. Based on its value of ρ, each soil was then classified according to angularity by using the system developed by Powers (9).

So that a wide range of particle shapes was represented in the study, the soils chosen were ASTM C190 sand (rounded), ASTM C109 sand (subrounded), F-70 banding sand (subangular), and (angular) mine tailings from a garnet mining operation.

Index properties of the four soils are given in Table 1 and in Figure 1 are the grain size distribution curves for each soil.

INITIAL TESTING SERIES

Deposition by pluviation involves the free fall of soil particles through a fluid median (air or water) so that the particles come to rest in a loose configuration. The rate of deposition is controlled by the aperture through which the soil flows. To determine the void ratio, the soil is pluviated into a mold of known volume and weighed. A preliminary series of dry pluviation tests that used air as the median was carried out to determine the effects of height of free fall, diameter of aperture (funnel) opening, and mold diameter on the void ratio. In these tests dry soil flowed through a funnel into a mold of known volume. The funnel was supported by a ring clamp, and when the center of the funnel and the center of the mold were aligned a stopper was held to the tip of the funnel while a quantity of banding sand sufficient to overflow the mold was placed in the funnel. The stopper was then removed and the soil rained down.

The excess soil was gently struck off flush with the top surface of the mold by using a straightedge or screed that had an edge bevelled at approximately 45°. The screeding procedure consisted of three steps.

The first step was to place the bevelled edge of the screed on a small area of the lip of the mold. This was sometimes difficult, depending on the size and shape of the soil particles. If possible the screed was pushed horizontally into the first layer of sand grains. Alternatively, the screed was held at an angle of 30°-45° to the horizontal, which caused the sand grains to separate slightly and allowed the screed to rest on the lip of the mold.

In the second step the bevelled edge of the screed was held approximately 30° to the horizontal. Application of a slow, continuous foreward motion to the screed caused the excess sand to overflow the mold and created the desired horizontal plane behind the screed. During this step care was taken to limit any vibration. Occasionally, to release particles wedged between the screed and the lip of the mold, a small side to side motion was applied to the screed as it was advanced across the top of the mold, but the screed was never reversed in its forward progress or raised.

The third step in the screeding procedure was necessary only if particles became wedged between the screed and lip of the mold. This occurred infrequently with angular particles only. Side to side motion usually freed trapped grains, but extraction of a particle was sometimes necessary. The void left in the surface was filled by lightly depositing sand with a spoon. The first two steps of the screeding procedure were then repeated to eliminate minor surface irregularities.

In the initial series of pluviation tests, 54 combinations of funnel opening size (3), pluviation height (3), and mold diameter (6) were chosen to examine the effects of these variables on the resulting void ratio. The results given in Table 2 are the average of five tests for each combination. The data show that the largest void ratio was obtained when the soil was pluviated from a 0.28-in diameter funnel through a 6-in free fall into a 4.5-in diameter mold.

The tube method evolved from the results of the initial testing series, which used the pluviation method and the research reported by Lucks (10) and Kolbuszewski (4). In the tube method a tube or right cylinder opened at both ends is positioned within the center of a mold that has one end supported by the bottom of the mold. A quantity of dry soil sufficient to fill the mold is placed in the

tube and the tube is then extracted to allow the soil to flow into the mold. Excess soil is then screeded off.

An initial series of tests that used tubes was run to determine which combination of radius ratio (tube radius to mold radius) and extraction speed yielded the largest void ratio. For each of the four soils, a total of 30 combinations, each repeated 10 times, was performed. The following observations were made from a study of the data from all tests: the largest void ratio was obtained by using a tube-mold combination that had a small radius ratio (RR), and higher void ratios were obtained with the slower extraction rate than with the faster rate. Based on these observations, it was decided to use a tube-mold combination with a RR of 0.44 (2-in tube, 4.5-in mold) with a slow extraction speed in the evaluation test series designed to compare the results obtained from several published methods of determining maximum void ratio.

EVALUATION TESTS SERIES

The evaluation test series provided data and information so that comparisons could be made between several methods of determining the maximum void ratio of granular material. Of the eight procedures selected, four are variations of methods suggested by Kolbuszewski (4). In the notation of the listing that follows, the Kolbuszewski procedures are differentiated by the diameter of the cylinder used (2 or 3 in) and the fluid in which the soil particles are suspended--air (A) or water (W). The eight procedures were performed on each of the four soils in the following order:

1. Kolbuszewski 3A,
2. Modified ASTM D2049-69,
3. Kolbuszewski 2W,
4. Tube method,
5. Kolbuszewski 3W,
6. Castro method,
7. Kolbuszewski 2A, and
8. Mulilus, Chan, and Seed method.

The testing sequence was organized so that the data could be analyzed statistically and to separate similar procedures to minimize the influence of operator proficiency on the results. All eight procedures were carried out on one soil before another soil was tested. Each method was performed 30 times for each soil. Except for the two Kolbuszewski procedures, which used water as a medium, the soil used was air dry.

Procedures

ASTM D2049-69 Modified Method

A pouring device or funnel, with an inner spout diameter of 0.5 in was used to deposit the soil, as illustrated in Figure 2. The modification to ASTM D2049-69 (11) was that a 0.046 ft^3 rather than a 0.1 ft^3 mold was used. The decreased mold volume had no significant effect on the resulting e_{max} values. While the funnel was held firmly against the base of the mold, a quantity of soil sufficient to fill the mold was placed in the funnel. The funnel was then raised, which allowed a steady stream of soil to free fall 1 in into the mold, as shown in Figure 2. The pluviation (free fall) height was kept constant as the mold filled and the funnel was rotated in a spiral motion from the center to the edge of the mold to form a soil layer of uniform thickness. The excess soil was screeded from the mold.

Tube Method

As a result of the preliminary study, a 2-in inner diameter tube and a 4.5-in inner diameter mold (RR = 0.44) were used to perform the tube method test. The extraction rate was approximately 0.2 in/s. This method is illustrated in Figure 3.

Castro Method

The procedure used by Castro (12) is similar to ASTM D2049. The differences involve use of a dispersion plate, smaller diameter mold, and decreased height of pluviation. The dispersion plate was 0.5 in in diameter and was attached 0.2 in below the tip of the funnel by a thin wire harness (see Figure 2). Castro used a 2.9-in mold; however, a 3-in mold was used in this study. The same funnel motion used in the ASTM method was used.

Mulilus, Chan, and Seed Method

The ASTM method was modified by Mulilus, Chan, and Seed (13) to achieve a very loose soil structure within a 2.8-in diameter triaxial mold. This method of pluviation involved a larger free fall and a smaller mold than in the ASTM method. A variable pluviation height of from 6-20 in was used by Mulilus and others, but in this study, because the preliminary test results showed that a 6-in free fall yielded larger void ratios, a constant height of 6 in was used. This method is illustrated in Figure 2 with the 3-in diameter mold used in this study.

Kolbuszewski Methods

Whereas other methods used in this study involved the placing of an unknown mass of soil in a known volume and then measuring the mass, Kolbuszewski's approach (4) is to place a known mass of soil in an unknown volume and then measure the volume occupied by the soil.

A kilogram of soil was placed in a calibrated right cylinder 18-in high that was closed at one end. A rubber stopper was attached to the open end and the cylinder was inverted several times so that all sand particles were free from one another. An immediate inversion allowed the grains to settle into a loose soil structure. By use of a special apparatus developed specifically for the task (14), the unoccupied volume of the cylinder above the soil was measured. This volume was then subtracted from the known total volume of the cylinder to obtain the volume occupied by the soil.

Kolbuszewski (4) reported that the diameter of the cylinder influenced the void ratio obtained, so in this study cylinder diameters of 2 and 3 in were used. Another variable that affected the results was the fluid through which the soil pluviated. Both air (A) and water (W) were used in combination with the 2- and 3-in diameter cylinders. Hence, the method designations 2A, 3A, 2W, and 3W.

When using Kolbuszewski's method to deposit soil through water, care must be taken to eliminate entrapped air within the soil. This was done by tilting the cylinder slightly and pouring small amounts of deaired water down the cylinder wall, which allowed the water to percolate through the soil. When the soil was completely immersed, larger amounts of deaired water were added until the cylinder was full.

DISCUSSION OF RESULTS

The results of the testing program are given in the order that the soils were tested beginning with the

banding sand. In the tables in which the results are tabulated the listing begins with the method that gives the highest value of void ratio and continues in decreasing order.

The data obtained from the Kolbuszewski 2W and 3W tests are not given because these methods gave unrealistically high values of void ratio due to arching or tridimensional bridging of particles and entrapped air bubbles. Frequently, after final inversion of the cylinder, air bubbles became entrapped and unable to escape the falling soil particles. A second phenomenon noted by Kolbuszewski (4) was arching in the soil, which caused the soil to form a local honeycomb structure (Figure 4). This structure may have been formed by the collapse of soil grain columns that were formed as the soil pluviated through the water medium. Although the entrapped air and arching phenomenon are similar in effect (both give inflated e_{max} values) the granular structures are quite different. In the case of entrapped air bubbles, the soil grains rested against the air-water interface and were supported by surface tension. In contrast, the granular structure of the arch was self-supporting.

The soil grain columns whose collapse probably was responsible for the arching observed was caused

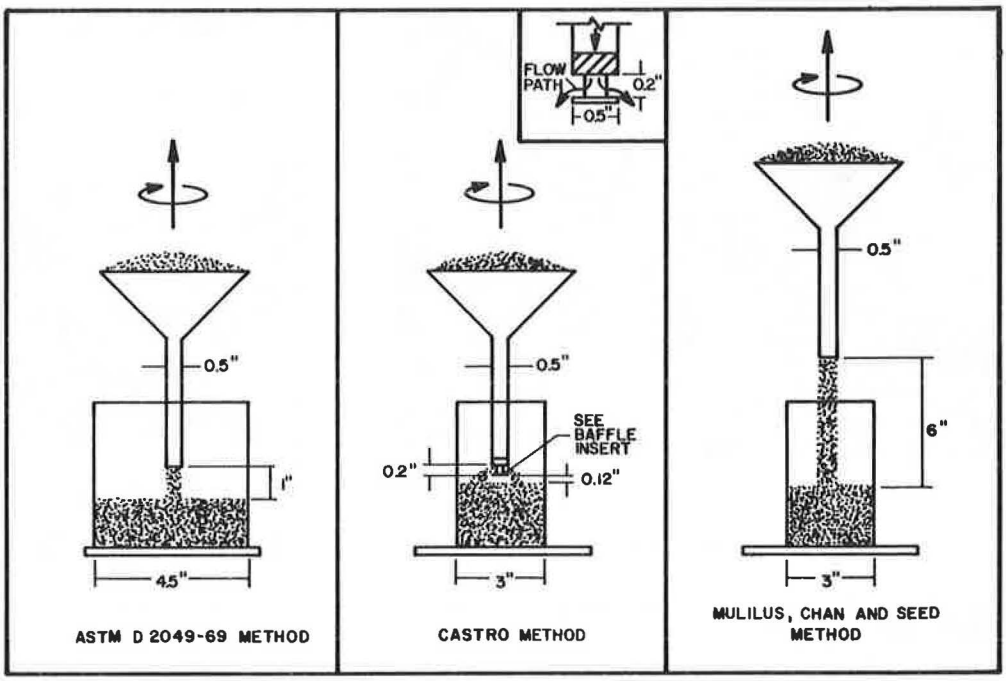

Figure 2. Schematic of three funnel methods.

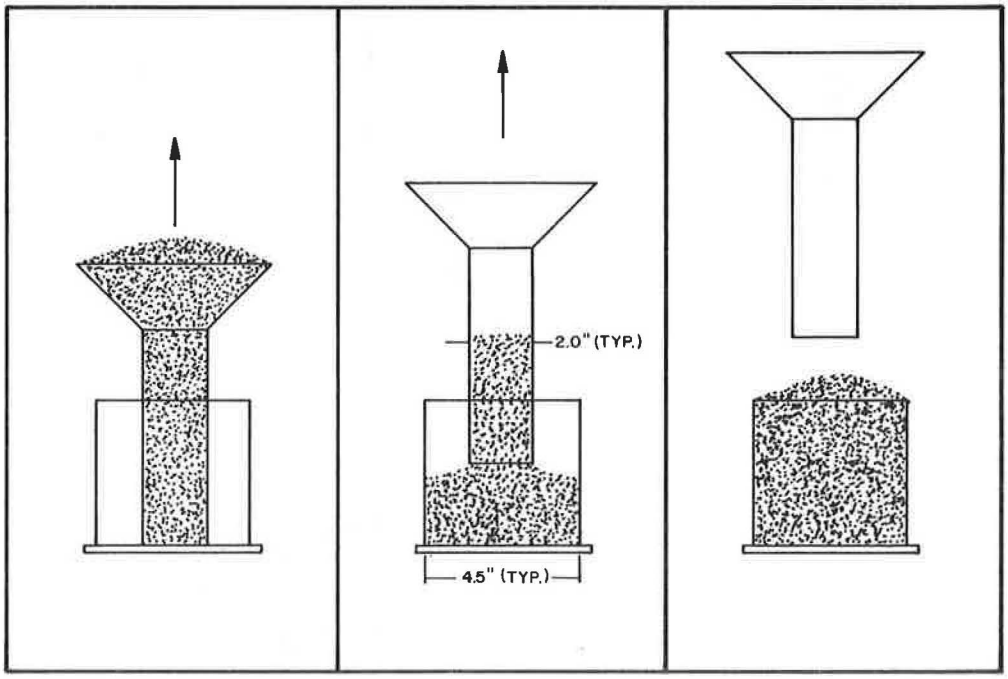

Figure 3. Schematic of tube method.

Figure 4. Honeycomb structure developed when water is used as the medium in Kolbuszewski method.

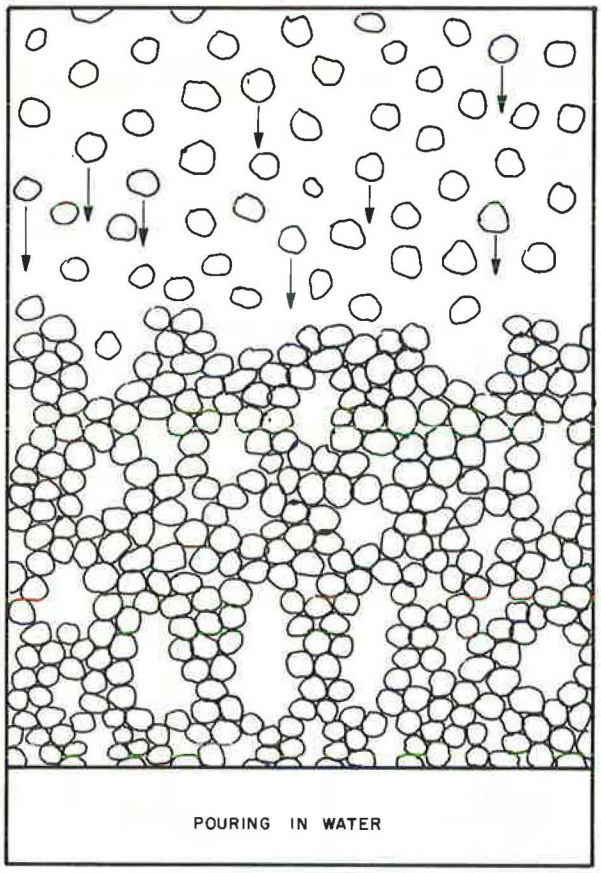

Figure 5. Soil structure from vertical channel currents when water is used as the medium in Kolbuszewski method.

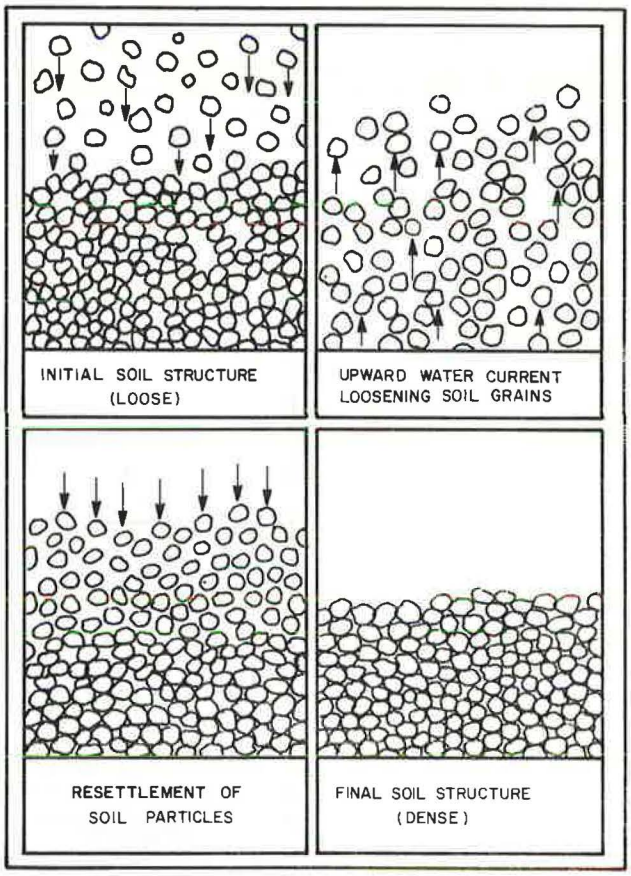

Figure 6. Range, mean, and coefficient of variation of e_{max} for C190 sand from eight test methods.

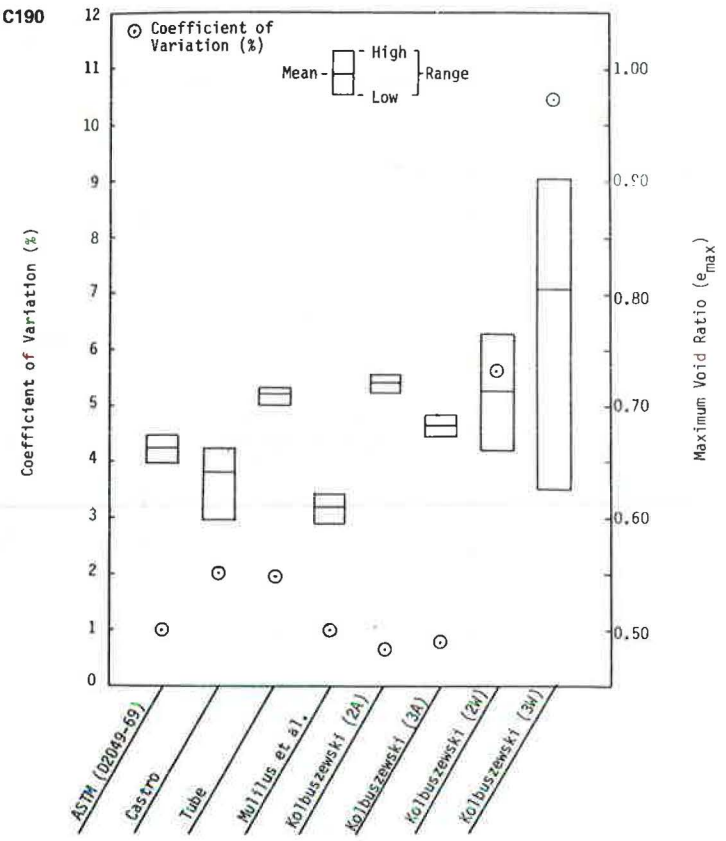

by the effect of water flowing upward on the settling soil particles. The vertical water currents caused a disturbance of the soil particles during pluviation, which forced the grains upward and caused them to resettle in columns (Figure 5). Kolbuszewski noted that the number of water channels increased for a given soil as the cylinder diameter decreased in size.

Air entrapment and soil arching result in wide scatter in the data obtained from tests that use these methods. This is shown in Figure 6. Because of the problems associated with the Kolbuszewski 2W and 3W methods, these procedures were not reported in the evaluation of methods for determining maximum void ratio. Results obtained from these methods are given by Walter (14).

The results from the six other test procedures were analyzed statistically to determine if the differences among mean e_{max} values obtained for each method were statistically significant. The statistical analysis examined the null hypothesis that there was no significant difference between the mean values of the maximum void ratio values obtained from any two test procedures. Rejection of the null hypothesis indicated that there existed a statistically significant difference between the mean values at a given level of confidence (95 percent was used). If the null hypothesis could not be rejected, then the analysis indicated there was no statistically significant difference between the mean values and, therefore, both methods gave the same mean e_{max}.

Banding Sand

Test results for the banding sand (subangular grains) are given in Table 3 arranged by method from the highest to the lowest mean value of maximum void ratio. The tube method gave the highest mean value of e_{max} and had the lowest standard deviation and coefficient of variation, which indicates that the method allowed the operator to reproduce results very closely. All methods had coefficients of variation of less than 2 percent.

Table 3 gives mean e_{max} values ranged from 0.836 for the tube method to 0.763 for the Kolbuszewski 3A method. Figure 7 shows the results of the statistical analysis to test the null hypothesis that the mean e_{max} from each method is not significantly different. The tube method gave a significantly higher mean e_{max} value than did each of the other methods (the null hypothesis that the means were the same was rejected).

C109 Sand

The results of the tests for this sand with subrounded grains are tabulated in Table 4. Once again the tube method gave the highest value of maximum mean void ratio and had the lowest coefficient of variation. The Castro method gave the second highest results for the C109 sand but had the largest coefficient of variation. Results for the statistical test on the mean e_{max} values for this sand are given in Figure 8. The mean value of maximum void ratio obtained from the tube method was statistically different (greater than) the mean values obtained from each of the other methods.

C190 Sand

A summary of the results of the six methods for the C190 sand that has rounded particles is given in Table 5 and Figure 6. The Kolbuszewski 2A method, which uses a 2-in diameter cylinder and pluviates the grains through air, gave the highest value of maximum void ratio. It was followed by the tube method. Statistical tests on the null hypothesis were carried out for each pair of data and in all cases the null hypothesis that the means were not statistically significantly different was rejected. Data from the Kolbuszewski 2W and 3W methods are included in Figure 6, which illustrates the effects of soil arching and air entrapment on the mean and range of the e_{max} values obtained in the 30 trials. Visual observation of the soil structures in the laboratory indicated the high mean value of e_{max} was mostly due to arching. The wide range of e_{max} values obtained in the tests and the high coefficient of variation indicate that arching did not occur in all of the 30 trials.

Mine Tailings

The mean maximum void ratio for each method for mine tailings with angular particles is given in Table 6. The mean e_{max} values ranged from a low of 0.966 (Kolbuszewski 3A) to a high of 1.044 (tube method). The coefficients of variation for all methods were less than 1.5 percent. The results of the statistical tests for significant differences between means are given in Figure 9. The mean of e_{max} obtained from the tube method is statistically significantly different from the mean of e_{max} obtained from the other five methods. However, the mean values of e_{max} obtained from the second and third ranking methods for the mine tailings, Kolbuszewski 2A method, and Castro method, respectively, were not significantly different.

Comments on the Test Methods

The tube method required no special preparation and was easy to perform. Visual inspection of the soil after deposition indicated a homogeneous structure if the tube was raised steadily. Soil layering resulted if the tube was extracted with a jerky stop and go motion. The tube method gave highly consistent results.

The Kolbuszewski method that used pluviation through air was easy to perform and gave consistent results. The soil structure was homogeneous. Special equipment was needed to measure the volume occupied by the soil so that the void ratio could be calculated accurately. For each soil tested the e_{max} obtained was higher for the 2-in diameter cylinder than for the 3 in and the means were statistically significantly different. This effect of cylinder diameter was also observed by Kolbuszewski (4).

Objections with the Kolbuszewski method that used water as a pluviation median were discussed previously. The soil structure obtained was heterogeneous and coefficients of variation obtained from the data for the four soils ranged from 10.8 to 13.9 percent compared with a maximum of 2.6 percent for any of the other methods (14).

Of the three pluviation methods employed in this study that used a funnel, controlling the height of fall while maintaining a continuous spiral motion was easiest by using the modified ASTM D2049 method. No special preparation was needed and the results were consistent.

It was difficult to duplicate test results by using the Castro method. This was because the dispersion plate, located just below the funnel, made it difficult to maintain the height of free fall (0.1 in) suggested by Castro (12). Even with special care, this invited operator error.

The 6-in pluviation height was difficult to maintain by using the Mulilus, Chan, and Seed method. Comparatively low values of e_{max} were obtained

Table 3. Results for F-70 banding sand.

Method	Mean ($\bar{x}$)	SD[a] (S)	Coefficient of Variation[b] [V (%)]
Tube	0.836	0.003 12	0.37
Castro	0.818	0.008 77	1.07
ASTM D2049-69	0.810	0.010 21	1.26
Mulilus, Chan, and Seed	0.800	0.006 50	0.81
Kolbuszewski, 2A	0.799	0.005 18	0.65
Kolbuszewski, 3A	0.770	0.010 89	1.41

Note: For each method, 30 tests were run.

[a] $S = \sum_{i=1}^{N} (x_i - \bar{x})^2/(N-1)$. [b] $V = (S/\bar{x})(100\%)$.

Table 4. Results for C109 sand.

Method	Mean ($\bar{x}$)	SD (S)	Coefficient of Variation [V (%)]
Tube	0.737	0.001 88	0.26
Kolbuszewski, 2A	0.709	0.003 97	0.56
ASTM D2049-69	0.696	0.006 20	0.89
Mulilus, Chan, and Seed	0.683	0.006 54	0.96
Kolbuszewski, 3A	0.681	0.006 12	0.90
Castro	0.677	0.017 76	2.62

Note: For each method, 30 tests were run.

Figure 7. Results of null hypothesis on mean values for F-70 banding sand, $\alpha = 0.05$.

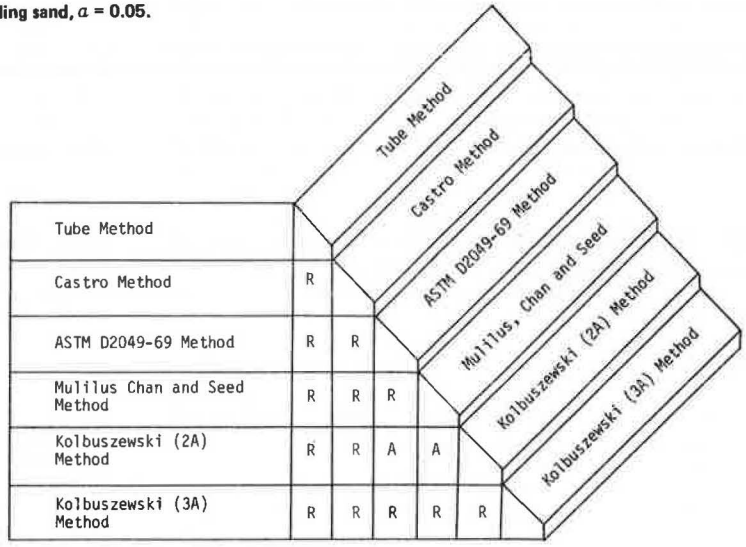

R-Rejection of the null hypothesis that the e_{max} means are equal

A-Acceptance of the null hypothesis that the e_{max} means are equal

Figure 8. Results of null hypothesis on mean values for C109 sand, $\alpha = 0.05$.

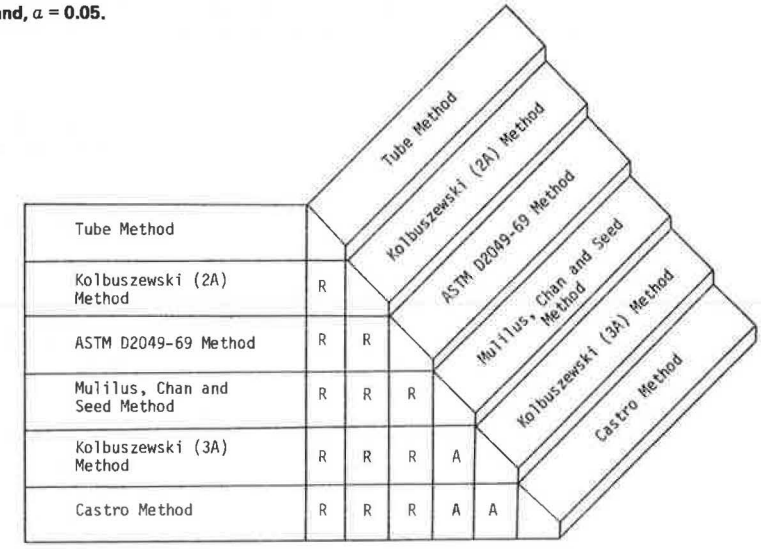

R-Rejection of the null hypothesis that the e_{max} means are equal

A-Acceptance of the null hypothesis that the e_{max} means are equal

because of compaction of the material already in the mold by the impingement of particles that dropped through a relatively large (6 in) pluviation height.

Operator Effect of Using the Tube Method

All the test results reported to this point were obtained by a single operator. Because of the encouraging results obtained with the tube method, the results of several operators were compared. After having 15 min of instruction that described the tube method and a demonstration, nine undergraduate students each ran 25 trials that used C109 sand. Each student was asked to complete the 25 trials without interruption within a 10-day period. Unreduced data were collected as soon as each student had finished 25 trials. Data reduction was not performed until all results were in and the students were asked not to discuss their data with others during the 10-day period.

The results of this study are given in Table 7. Students are differentiated by the order in which they completed their trials. Each student was able to reproduce his or her results extremely well. Coefficient of variation of all nine students was less than 0.5 percent and, with two exceptions, the range in data for each of the 25 trials was less than 1 lb•f/ft³.

Even though each student's mean of 25 trials was within 0.8 lb•f/ft³ of one another's, because of

Table 5. Results for C190 sand.

Method	Mean ($\bar{x}$)	SD (S)	Coefficient of Variation [V (%)]
Kolbuszewski, 2A	0.721	0.004 54	0.63
Tube	0.710	0.013 87	1.95
Kolbuszewski, 3A	0.682	0.005 61	0.82
ASTM D2049-69	0.662	0.006 66	1.01
Castro	0.640	0.013 22	2.07
Mulilus, Chan, and Seed	0.610	0.006 20	1.02

Note: For each method, 30 tests were run.

Table 6. Results for mine tailings.

Method	Mean ($\bar{x}$)	SD (S)	Coefficient of Variation [V (%)]
Tube	1.044	0.006 44	0.62
Kolbuszewski, 2A	1.013	0.005 71	0.56
Castro	1.012	0.012 85	1.27
ASTM D2049-69	0.995	0.010 66	1.07
Mulilus, Chan, and Seed	0.982	0.013 26	1.35
Kolbuszewski, 3A	0.968	0.003 60	0.37

Note: For each method, 30 tests were run.

Figure 9. Results of null hypothesis on mean values for mine tailings α = 0.05.

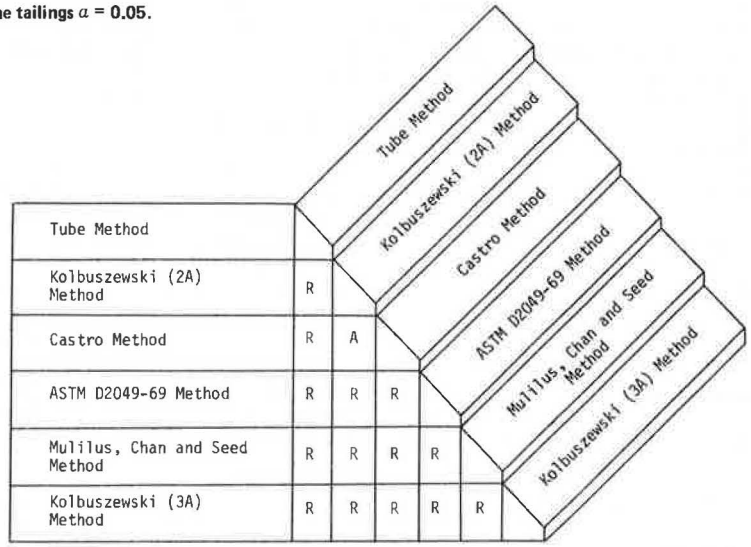

R-Rejection of the null hypothesis that the e_{max} means are equal

A-Acceptance of the null hypothesis that the e_{max} means are equal

Table 7. Results for student operators using C109 sand.

Operator	Mean (lb·f/ft³)	SD (lb·f/ft³)	Coefficient of Variation (%)	Maximum (lb·f/ft³)	Minimum (lb·f/ft³)	Range (lb·f/ft³)
Student S5	95.5	0.16	0.17	96.0	95.2	0.8
Student S7	95.4	0.16	0.17	95.9	95.2	0.7
Student S1	95.3	0.22	0.23	95.5	94.4	1.1
Student S8	95.3	0.13	0.14	95.5	95.1	0.4
Student S6	95.1	0.16	0.17	95.4	94.8	0.6
Student S3	94.9	0.41	0.43	96.1	94.4	1.7
Student S9	94.7	0.14	0.15	95.1	94.5	0.6
Student S4	94.7	0.13	0.14	95.0	94.5	0.5
Student S2	94.7	0.10	0.11	94.9	94.5	0.4
Overall[a]	95.1	0.36	0.38	96.1	94.7	1.7

[a] 225 trial runs.

Figure 10. Value of α required so that null hypothesis on mean values for different operators cannot be rejected, $\alpha = 0.05$.

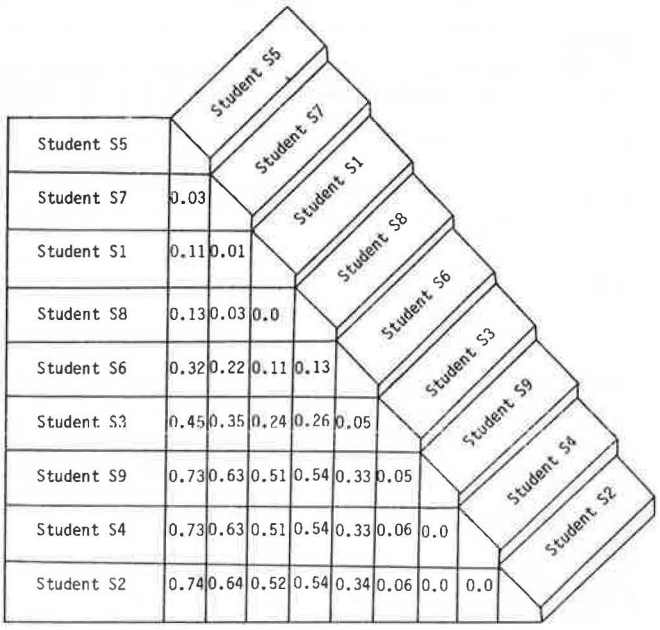

each student's ability to reproduce his or her own results so closely, statistical analysis indicated that in most cases each student's mean value was statistically significantly different from others (at the 95 percent level of confidence).

To get a clearer idea of the magnitude of the numbers involved, a statistical analysis was carried out to see how much smaller the difference in mean values of dry unit weight of two students need be so that the difference between them was not statistically significant. The results of the analysis, for the 36 combinations of nine students, is given in Figure 10. This figure shows, for example, that if students S1 and S9 had obtained means 0.51 lb•f/ft³ closer to one another the means would not have been statistically signficantly different.

The magnitude of the differences in means of the nine students is not believed to be of practical significance. The maximum difference that a change in $\gamma_{d_{min}}$ of 0.8 lb•f/ft³ makes in the density index (Equation 1) is about 8 percent.

SUMMARY AND CONCLUSIONS

The following observations and conclusions can be made as a result of this study, which used eight methods of determining the maximum void ratio of four soils.

1. In a preliminary series of tests where soil pluviation was used, larger values of maximum void ratio were obtained by decreasing the free fall height. An intermediate funnel diameter yielded the largest void ratios. Mold diameter was not found to be important.
2. In a preliminary series of tests that used tube extraction as a means of determining e_{max}, the highest void ratios were achieved when the tube was extracted slowly and a tube-mold radius ratio equal to 0.44 was used. This was the smallest radius ratio used in this study.
3. The Kolbuszewski method that used water as a pluviation medium resulted in a heterogeneous soil structure with some soil arching. This method is not recommended for obtaining e_{max} values.
4. The Kolbuszewski method that used air as a pluviation median in a 2-in diameter cylinder gave high, consistent values of e_{max}. The only drawback of this procedure is the difficulty and care that must be taken to measure the volume of the soil. Special equipment is needed for this purpose.
5. The method that gave the highest values of e_{max} for three of the four soils tested and the second highest for the fourth soil is the tube method. A 2-in diameter tube extracted slowly from a 4.5-in diameter mold gave consistent values of e_{max} in successive trials. Coefficients of variation of less than 0.7 percent were calculated from data from three of four soils; a value of 1.95 percent was obtained from the fourth.
6. The tube method of determining e_{max} produces very similar results for different operators. The range in γ_d for nine operators running 25 trials was 1.7 lb•f/ft³; the overall coefficient of variation was less than 0.5 percent.
7. For the soils tested in this study, the tube method is an excellent method of determining maximum void ratio of granular material.

ACKNOWLEDGMENT

The research reported in this paper was undertaken while we were affiliated with Clarkson College of Technology, Potsdam, New York. Feng-Bor Lin of Clarkson assisted in the statistical design and analysis of the experiment. Timothy Hartzell managed and analyzed the investigation dealing with operator effect while an undergraduate at Clarkson.

REFERENCES

1. F.A. Tavenas, R.S. Ladd, and P. LaRochelle. Accuracy of Relative Density Measurements: Results of a Comparative Test Program. ASTM, Special Tech. Publication 523, 1973, pp. 18-60.
2. D.M. Burmister. Grading-Density Relation of Granular Materials. Proc., ASTM, Vol. 38, 1983, pp. 587-596.
3. D.M. Burmister. Importance and Practical Use of Relative Density in Soil Mechanics. Proc., ASTM, Vol. 48, 1948, pp. 1249-1268.
4. J.J. Kolbuszewski. An Experimental Study of the Maximum and Minimum Porosities of Sands. Proc., 2nd International Conference on Soil Mechanics and Foundation Engineering, Rotterdam, Vol. 1, 1948, pp. 158-165.
5. T.L. Youd. Factors Controlling Maximum and Minimum Densities of Sands. ASTM, Special Tech. Publication 523, 1973, pp. 98-112.
6. E.A. Dickin. Influence of Grain Shape and Size upon the Limiting Porosities of Sands. ASTM, Special Tech. Publication 523, 1973, pp. 113-120.
7. G.M. Norris. Shape and Surface Roughness Effects on Maximum and Minimum Void Ratios of Sand. Annual Symposium on Engineering Geology and Soils Engineering, Boise, ID, 1980.
8. H. Wadell. Volume, Shape, and Roughness of Quartz Particles. Journal of Geology, Vol. 43, 1935, pp. 250-280.
9. M.C. Powers. A New Roundness Scale for Sedimentary Particles. Journal of Sedimentary Petrology, Vol. 23, No. 2, 1953, pp. 117-119.
10. A.S. Lucks. The Influence of Particle Shape on the Strength of Granular Materials. Massachusetts Institute of Technology, Cambridge, Ph.D. thesis, June 1970.
11. D2049-69 Standard Test Method for Relative Density of Cohesionless Soils. In 1980 Annual

Book of ASTM Standards, ASTM, Philadelphia, Part 19, 1980, pp. 311-319.
12. G. Castro, Liquefaction of Sands. Harvard Soil Mechanics Series, Cambridge, MA, No. 81, 1969.
13. J.P. Mulilus, C.K. Chan, and H.B. Seed. The Effects of Method of Sample Preparation on the Cyclic Stress-Strain Behavior of Sands. Earthquake Engineering Research Center, Univ. of California at Berkeley, Berkeley, July 1975.
14. J.E. Walter. A Study of the Methods for Determining the Maximum Void Ratio of Clean, Fine, Uniform Cohesionless Soils. Clarkson College of Technology, Potsdam, NY, M.S. thesis, 1981, 146 pp.

Compressibility of Field-Compacted Clay

P.S. LIN AND C.W. LOVELL

This study investigates the compressibility of a plastic Indiana clay (St. Croix) compacted in the field. Correlation among compaction variables and compacted properties was a prime objective. The clay was compacted to three levels of effort and five levels of water content by two kinds of rollers. As-compacted compressibilities were assessed in the laboratory oedometer, and compaction prestress values were interpreted from the e-log p curves. These values were always less than the nominal roller pressures previously applied to the soil. A regression model was written in terms of the compaction pressure and an interaction between pressure and compaction water content. Other compacted samples were saturated under three levels of confinement, with the aid of vacuum and backpressure. The subsequent volume changes depended on the compaction variables as well as on the confinement during saturation. A correlation was developed among the volumetric strain, the initial void ratio, the compaction water content, and the confinement during saturation. Soaked compressibilities were also measured and compared with the as-compacted values. The variability of the field samples is large. Comparable studies with samples of laboratory-compacted clay had been previously made and reported. Coupling of the relations for field compaction with those previously established for laboratory compaction is also reported here.

Compacted soils are used in large quantities in the construction of roadway embankments and other fills. The stability of these structures against a slope failure is always of major concern, and in most cases it is the only criterion taken into consideration in the design. However, as the construction of higher embankments becomes more common, specification of compaction procedures so that embankment settlement can be predicted and controlled for both the short- and long-term conditions is increasingly more important.

During an embankment design, the geotechnical engineer quantitatively predicts and controls the overall performance of field-compacted soil. One method is to construct a special fill section by using a range of compaction processes and then testing samples from the soil mass after each process. Such a test pad with the associated costs of field sampling, laboratory testing, and analysis is not economically feasible for most projects. Therefore, the design engineer must infer the compressibility behavior of field-compacted soils from relations developed in the laboratory. Because this inference process may not be the most desirable, this paper presents a rational method of predicting the field-compaction response from laboratory tests.

This study investigates the compressibility behavior of a field-compacted soil in the as-compacted and soaked conditions. The soil used was plastic residual clay, and field compaction was achieved by using a Caterpillar model 825 tamping roller and a RayGo Rascal model 420C vibratory roller. Three energy levels and five molding water contents were used for each roller type to study their effects on compressibility behavior. To examine the as-compacted compressibility characteristics, the compacted samples were trimmed to appropriate size and loaded incrementally in the oedometer. Of particular interest was the value of compactive prestress. During the service life of an earthen embankment, environmental changes may affect an increase or decrease in the volume of the mass.

In order to simulate the changes in the mass that may occur in service, compacted samples were saturated by a back-pressure technique in the oedometer under an equivalent embankment load. Of major interest was the percentage of volume change on wetting under loading. Saturated compressibility was also measured.

A similar study of the compressibility characteristics of laboratory-compacted samples from the same area soil was made by DiBernardo (1). Combined, the results of both studies will allow the engineer to predict the field response from laboratory-compacted samples.

BACKGROUND

The concept of compactive prestress is generally defined as analogous to the preconsolidation pressure, where the pressure effect is caused by the compaction process (2). Lambe (3) agreed with this definition, but added that the value of the compactive prestress was sensitive to chemical and physical changes in the soil with time.

The process of compaction of a soil involves transmittal of the external compaction energy to the soil skeleton and pore fluids. On completion of the process, an induced prestress in the soil that may or may not be equal to the compaction pressure is produced. Abeyesekera (4) observed that this value of compactive prestress is important with respect to compacted shale behavior.

In order to determine the compactive prestress, Woodsum (2) statically compacted soil directly in oedometer rings, allowed the soil to come to equilibrium with water under an applied load, and performed the consolidation test. He found that, as the confining pressure remained constant and as the compaction pressure (P_{cp}) increased or void ratio decreased, the value of prestress (P_s) increased. Moreover, he found that, although the value of prestress increased with increasing compaction pressure, the prestress ratio (P_s/P_{cp}), which was similar to the overconsolidation ratio for saturated soils, varied but slightly. This prestress ratio reflects the effective transmittal of external compaction energy to the soil skeleton. On completion of the compaction process, the induced prestress in the soil may or may not be equal to the compaction

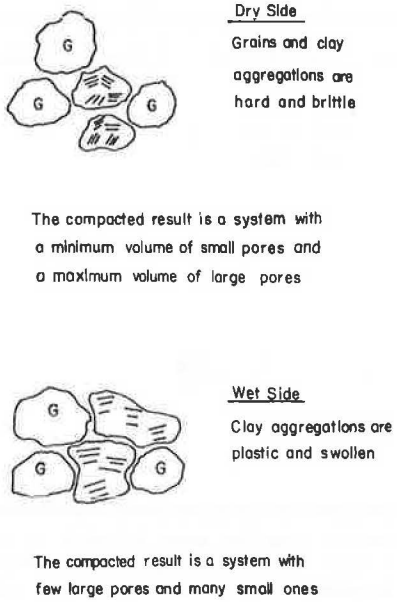

Figure 1. Effect of water content on compaction of a clayey soil.

pressure. In practical applications, this may suggest that, for a given compaction process and type of soil, the efficiency of the process does not increase with increasing effort.

The compressibility characteristics of compacted soils were reviewed by Wahls, Fisher, and Langfelder (5) in great detail. A compacted soil was considered to be a three-phase system composed of solids, air, and water. The volume decrease, which is caused by an applied load, is generally the result of (a) compression of the solids, (b) compression of the water, (c) compression of the air, and (d) escape of water or air from the pores. From a practical standpoint the change in volume is principally the result of c and d. They also concluded that the factors that primarily influence compacted compressibility were soil type, degree of saturation, molding water content, and method of compaction.

DiBernardo and Lovell (1) examined the effect of laboratory kneading compaction on the as-compacted and soaked compressibility behavior of St. Croix clay. They found that a large percentage of as-compacted compression occurred within the first minute of loading. The compression versus time relations indicated similar fluid continuity conditions (i.e., continuous air voids for dry and optimum conditions). They also summarized soaked compressibility behavior as follows:

1. For a given initial compaction condition, the soaked compressibility is greater than the as-compacted compressibility for the corresponding pressure ranges;
2. For a given compaction pressure and level of confinement on soaking, as the water content increases, the virgin compressibility (C_c) decreases; and
3. For a given degree of saturation and confinement level on soaking, as the compaction pressure increases, C_c decreases.

Hodek (6) explained the behavior of kaolinite compacted in the laboratory by static pressures under conditions of no lateral strain in terms of a deformable aggregate model. According to Garcia-Bengochea (7), pore-size distribution measurements for compacted clays have also provided strong evidence for a deformable aggregate model. Hodek and Lovell (8,9) developed a model or mechanism to explain the achievement of the compacted unit weight. The mechanism took into account the precompaction soil preparation and conditioning as well as the soil interactions that occur during compaction.

Figure 1 (8) illustrates the effect of moisture content on compaction of a clayey soil. The aggregation is a fabric unit within which individual clay particles of various sizes interact. On the dry side, the clay aggregates are shrunken, hard, and brittle. The compaction forces move these pieces around and perhaps even break some of them, but the result is a system that has a minimum volume of small pores and a maximum volume of large pores. In contrast, on the wet side, the clay aggregates are swollen and plastic. The compaction forces are able to not only move the pieces closer together but also to deform them to minimize the interaggregate space. The system now has few large pores and many small ones.

EXPERIMENTAL APPARATUS AND PROCEDURE

The soils used for both the field and laboratory compaction were obtained from the IN-37 realignment project in Perry County. The soil was St. Croix. The difference between the soils used for the field and laboratory compaction is given in the table below. It is apparently caused because the soil used for field compaction was taken from shallower depths (0-5.5 ft); the samples taken for laboratory compaction were from deeper depths (5.5-13.0 ft). Laboratory variability is low due to the soil being taken from several locations and thoroughly mixed before compaction and testing.

Item	Field			Laboratory
	Mean	Low	High	
Atterberg Limits				
Liquid limit, w_l (%)	40.0	30.0	53.2	53.0
Plastic limit, w_p (%)	18.4	16.7	21.3	21.0
Plasticity index, I_p (%)	21.9	16.4	29.0	32.0
Specific gravity (G_s)	2.78			2.80
Soil classification				
Unified	CL			CH
American Association of State Highway and Transportation Officials	A-6			A-7-6

Ten test pads were constructed of the test soils in the area of the relocation project of IN-37 in June 1978. The test pads were constructed in order to create field-compacted soil for subsequent investigation of mechanical properties and fabric descriptors. Each pad was 4.3-m (14-ft) wide and 35.4-m (116-ft) long.

Five test pads were rolled by a Caterpiller model 825 segmented pad tamping roller (C) and five pads were rolled with a RayGo Rascal model 420C segmented pad vibratory roller (R). Five different water contents were tested for each method of compaction. They had water contents on both the dry side and wet side of field optimum water contents. For identification these were designated 1-5, from the lowest to the highest moisture level. We hoped to maintain a uniform water content within each pad. Each test pad was sampled following the completion of 4, 8, and 16 passes of the compaction equipment over the pad. These samples were labeled A, B, and C, respectively, for identification of energy levels (10).

A Karol-Warner fixed ring consolidation cylinder was used in this investigation. The oedometer ring is 63.5 mm (2.50 in) in inside diameter, 101.6 mm (4.0 in) in outside diameter, and 25.4 mm (1.0 in) in height. The loading system used to compress the sample is a lever armweight type.

The first step in the trimming process for the field samples was to remove the wax and cheesecloth covering. This was accomplished by using a sharp knife to cut through the covering, and care was taken to prevent damage of the soil sample inside. The next step was to put the soil sample directly into the oedometer ring. The upper and lower faces of the sample were trimmed with a steel straightedge by using the top and bottom of the ring as guides.

Following the seating load adjustment period (typically 10 min), the applied pressure was increased, by using a load increment ratio (LIR) of 0.5 to 14.9, 22.3, 34.7, 49.5, and 76.8 kPa before the prestress value for the particular sample was reached. The applied pressure was decreased and then increased again until the prestress value for the particular sample could be well defined. The duration of each load and unload was 10 min, during which dial readings were typically recorded at 0, 0.1, 0.5, 1, 2, 4, 8, and 10 min.

During the service life of an earthen embankment, environmental changes may cause an increase or decrease in the volume of the mass. In order to simulate the changes in the mass that may occur in service, the field-compacted sample was compressed by using LIR = 0.5 and load duration of 10 min in the as-compacted condition until a vertical pressure of either 160, 320, or 480 kPa was applied. The samples were then saturated by a deairing and back-pressure procedure. The consolidating loads--either 160, 320, or 480 kPa--represent the pressure exerted by an equivalent embankment height of 7.8, 15.6, or 23.5 m (25, 50, or 75 ft), respectively.

DISCUSSION OF RESULTS

As-Compacted Compressibility

An as-compacted compressibility sample designated by R5B2 would indicate that the sample was compacted by the Rascal equipment (R) at the fifth water content level (5) and was the second sample (2) collected after the equipment made eight passes (B).

The relative compression (compression at time = t divided by the total compression at time = 10 min) versus time curves for dry, wet, and at optimum samples are shown in Figure 2. For the dry-side and optimum samples (C1A2, C2A3), the magnitudes of relative compression are virtually the same at each successive time plotted. The compression of both samples was dominated by the outflow of pore air; specifically, the air voids were interconnected (Yoshimi, 11). The magnitude of relative compression with time for an initially wet-of-optimum sample (C4A3) is also shown in Figure 2. In comparison the wet-side sample exhibits the least amount of relative compression within the 10-min period.

The effects of increasing water content and degree of saturation on compressibility behavior of samples compacted to energy level A (4 passes) are shown in Figure 3. This figure shows a marked difference in the compressibility behavior for dry- and wet-side samples, depending on the range of consolidation pressure considered. That is, in the low-pressure range (20-300 kPa), the wet-side sample is more compressible than the dry-side sample. However, in the high-pressure range (> 300 kPa), the dry-side sample is more compressible than the wet-side sample.

The effect of increasing the compactive effort on the compressibility behavior of initially dry of optimum samples is shown in Figure 4. This figure shows that the slope of the curves within the respective high-pressure ranges becomes steeper (i.e., increasingly more negative) with decreasing compactive effort.

The value of compactive prestress can be useful in design, because the compressibility behavior of the mass will be different at embankment-confining pressures above and below this value. Prestress ratio versus degree of saturation is plotted in Figure 5. This figure shows that the prestress ratio decreases with increasing saturation. For the partial range of saturation considered in this study, the prestress ratio is always less than one, which may indicate that not all of the energy delivered achieves densification. Figure 5 also shows that the prestress ratio of the Rascal vibratory roller is higher than that of the Caterpillar tamping roller at the same degree of saturation. The compactive efforts reported here are only nominal pressures [i.e., they are the pressures applied by the compactor during the compaction process (12)]. Therefore, the actual prestress ratios (i.e., compactive prestress-nominal compactive pressure) are more than likely greater than the values shown on Figure 5.

Soaked Compressibility

A soaked compressibility sample designated by C2A2a would indicate that the sample was compacted by the Caterpillar equipment (C) at the second water content level (2) was the second sample (2) collected after the equipment made four passes (A), and was incrementally loaded and soaked at an applied pressure that corresponds to an embankment height of 7.8 m (a).

DiBernardo and Lovell (1) showed typical soaked compression versus log time curves as in Figure 6. Each curve has a characteristics type 1 shape, as proposed by Leonards and Girault (13). The division of consolidation into primary and secondary components was illustrated by two techniques--the usual Casagrande approximation and pore water pressure measurements. As shown, the amount of compression at the end of primary consolidation (R_{100}), as determined by the two methods, is nearly identical. In addition, the time for full dissipation of pore pressure to occur (t_{100} value at $\Delta u = 0$) corresponds well with the Casagrande t_{100} value; however, typically the former time was 20 percent less. Because the Casagrande construction provides a very good approximation for the end of primary consolidation, doubly drained oedometer tests were performed without measuring pore water pressure for routine testing. Such a procedure will reduce the duration of each test considerably; however, a certain amount of time is still needed before each R_{100} can be determined by the Casagrande construction.

Testing of the compacted material in the as-compacted condition gives an indication of the expected compressibility behavior of that soil prior to modification by the environment. In order to get some measure of the effects of a change in the service environment, as-compacted samples were loaded to simulate different levels of embankment confining stresses and saturated by first soaking the samples and then applying back-pressure saturation. The one-dimensional percentage of volume changes ($\Delta V/V_o$) that occurred on incremental loading and wetting will be examined,

$$\Delta V/V_o = \Delta e/(1 + e_o) \quad (1)$$

where Δe is the change in void ratio on satura-

Figure 2. Comparison of relative compression for dry, wet, and at-optimum samples.

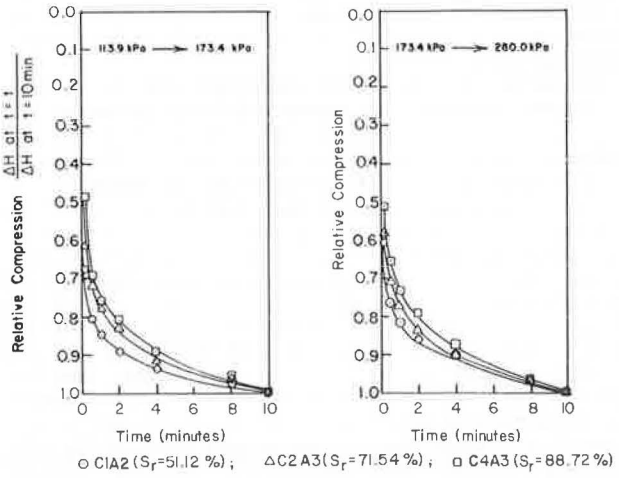

tion, and e_o is the initial void ratio.

The relation among percentage of volume change on wetting ($\Delta V/V_o$), initial void ratio (e_o), and the sustained load on saturation (P_o) is shown in Figure 7. This figure shows that, for a given sustained load, the percentage of increase in volume increases as initial void ratio decreases, and the percentage decrease in volume increases as the initial void ratio increases. Abeyesekera (4) and DiBernardo and Lovell (1) obtained similar results for a compacted shale and a compacted highly plastic clay, respectively.

The percentage of volume change on saturation versus confining stress is shown in Figure 8. This figure shows that most samples increase in volume when saturated under a confining stress of 161 kPa. This stress is approximately equivalent to a depth of cover of 7.6 m in a compacted earthen embankment. The higher confining stresses of 322 and 483 kPa corresponded to depths of cover 15.2 and 22.9 m, respectively. At these stresses most samples displayed a tendency for slight volume reduction, except for the near-optimum samples compacted with

Figure 3. Effect of moisture content on compressibility for four passes.

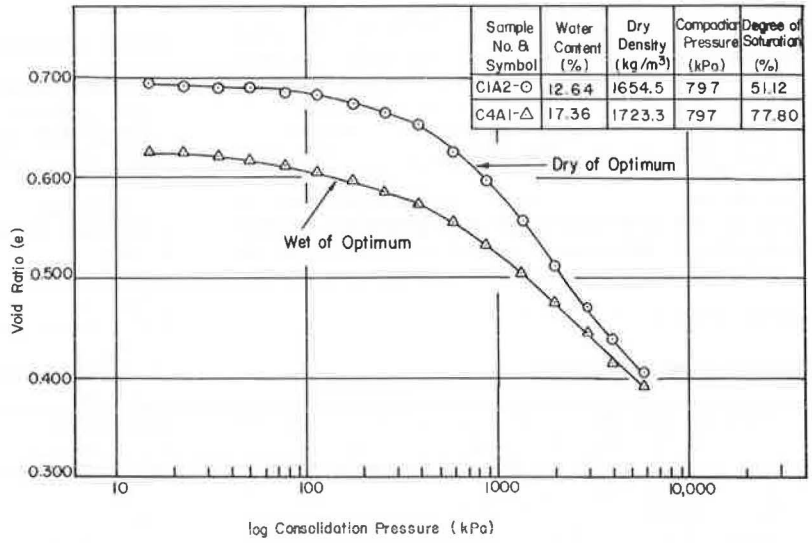

Figure 4. Effect of compactive effort on compressibility for dry of optimum.

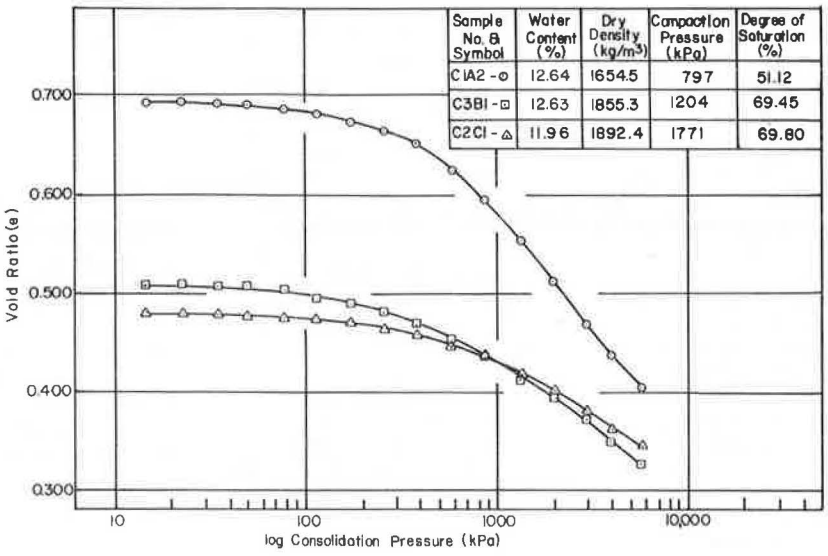

energy level C (16 passes). These showed a significant decrease in volume, which might be termed a collapse. Such large decreases occurred quickly on exposure to water. The volume changes for all the samples were essentially completed while the samples were soaking. There was little additional volume change (0.05 to 0.10 percent) during back-pressure saturation.

The introduction of water to an as-compacted sample affects the clay on both the microscale and macroscale. On the microscale, water that comes into contact with the clay minerals can result in significant swelling of the clay. The amount of swell depends on the degree of hydration of the clay minerals present and the initial moisture condition of the clay. At the macroscale, the expanding clay minerals result in a softening of the intact clay aggregates, which may result in greater deformations and consequently an increased compressibility under load. The addition of water to a partly saturated clay will decrease the negative pore water pressure, and the subsequent decrease in effective stress should permit swelling. The change in volume that results from any addition of water to a compacted clay can be seen to be the combination of several processes. Whether or not the net volume increases or decreases depends on the initial moisture content, the dry density, and the applied confining stresses.

At the low confining pressure of 161 kPa most samples compacted near optimum or dry of optimum swelled when saturated (Figure 8). Apparently, the swelling pressure from the hydrating clay minerals, in conjunction with the reduced effective stress due to saturation, exceeded the confining pressure and resulted in an increase in volume. The confining pressures of 322 and 482 kPa were sufficient to overcome the swelling tendency for all samples.

The sample compacted with energy level C (16 passes) to near-optimum condition collapsed when saturated under a confining stress of 483 kPa. As previously discussed, near the optimum the compacted structure is open, with large pores between the intact clay aggregates. The introduction of water to the compacted samples reduces the effective stress and softens the clay aggregates. The shear resistance at an aggregate contact will be reduced as the aggregate softens. If the confining stress is low, the samples may swell, as was observed for most dry-of-optimum samples that have a confining stress of 161 kPa. The tendency for swell is counteracted as the confining stress is increased. A critical confining stress, at which no volume change occurs during saturation, exists for each initial sample condition. At confining stresses greater than the critical stress, volume reduction occurred on saturation.

The collapse behavior may be related to the compactive prestress induced in a sample. The induced prestress is the level of stress below which a sample compresses little when loaded. The introduction of water will soften aggregate contacts and reduce resistance. Consequently, clay aggregates tend to rearrange, which results in a reduction in volume. When the confining stress is near the prestress, the soil skeleton will not have compressed much. However, any additional stress will exceed the prestress level and result in a large volume reduction.

Figure 5. Prestress ratio versus degree of saturation.

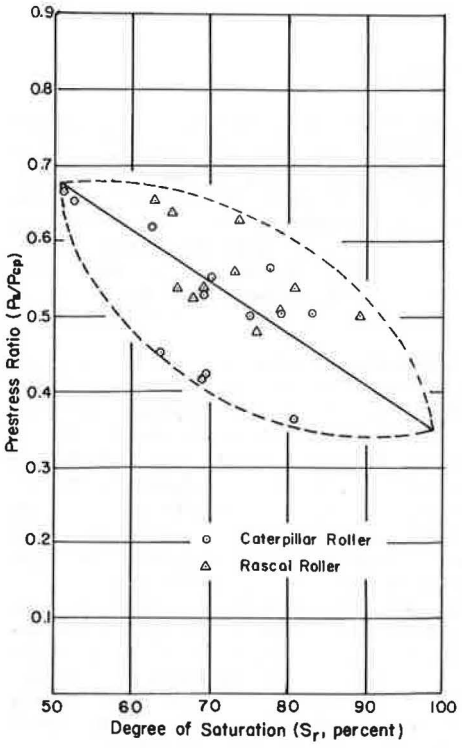

Figure 6. Comparison of methods for obtaining R_{100} and t_{100}.

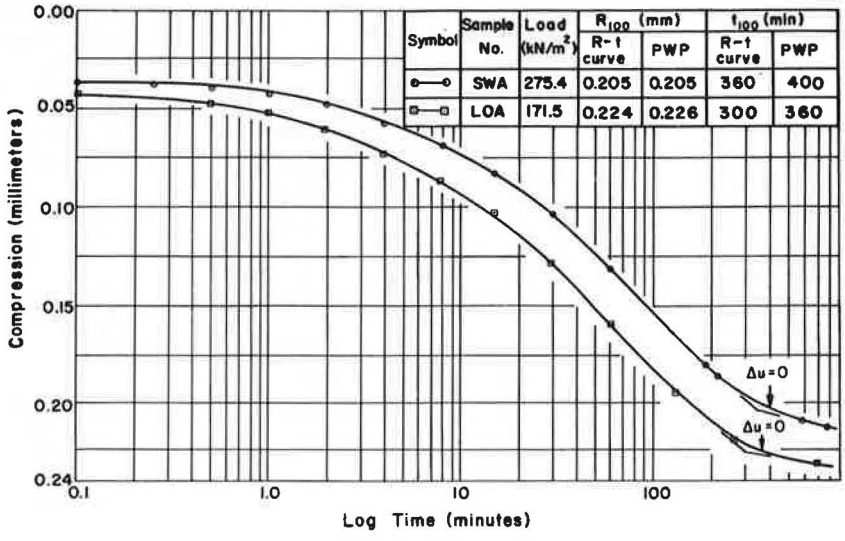

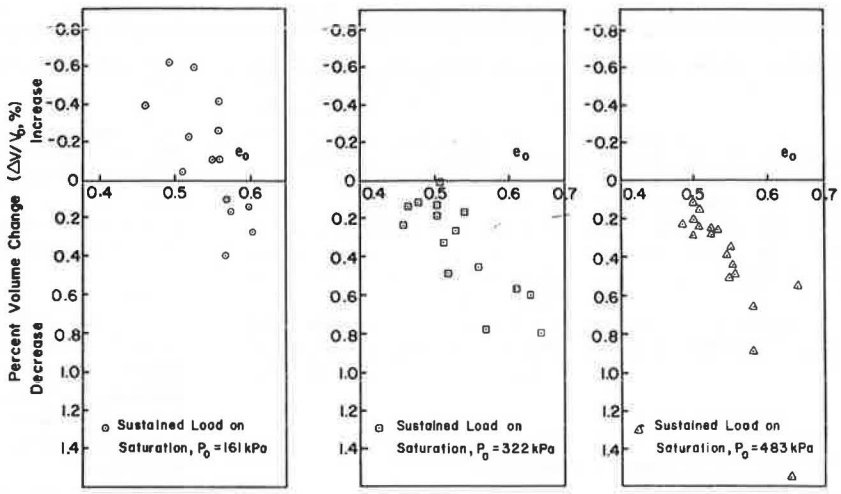

Figure 7. Percentage of volume change on saturation versus initial void ratio.

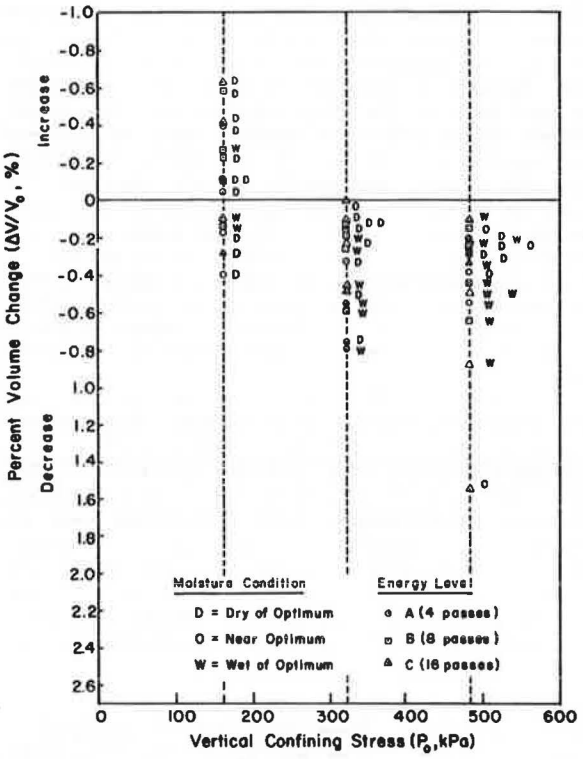

Figure 8. Percentage of volume change on saturation versus confining stress.

The effect of confinement on soaked compressibility behavior for dry-of-optimum samples is shown in Figure 9. At the low confining pressure of 161 kPa, sample R3C3a swelled on wetting. At the high confining pressures of 322 and 483, samples R4C3b and R2C6c compressed on wetting. This is consistent with the previous discussion (i.e., at low confinement the swell pressure from the hydrating clay minerals, in conjunction with the reduced effective stress due to saturation, exceeded the confinement and resulted in a volume increase). At high confinements the confining pressures were sufficient to overcome the swelling tendency and produced a volume decrease.

Statistical Correlations

Multiple regression is a useful technique for studying the relation between a dependent variable and a set of independent variables. It is used to develop a linear model of independent variables that can predict, control, or describe a dependent response. By using the data collected from the experimental tests, regression models were developed that could describe the response of either the as-compacted prestress or the percentage of volume change on saturation.

Each of the independent variables was first plotted against the appropriate dependent variable. This was done by using the Statistical Package for the Social Sciences (SPSS) procedure SCATTERGRAM. If the scatter plots showed a linear trend, the independent variable was considered to be correlated with the dependent variable and was selected for further investigation. Most of the computer procedures used for the regression analysis are included in SPSS procedural programs at Purdue University (14).

The next step was to isolate a subset of the independent variables that were found to be correlated with the dependent variable, so that an optimal expression that used as few variables as possible could be obtained. STEPWISE is an SPSS search procedure that progressively adds independent variables to the model and may delete variables already in the model after each step if they no longer add significantly to the model's descriptive capabilities. The program is also capable of testing for high correlation among the independent variables. Such correlated variables can then be prevented from entering the model. This option was suppressed during this analysis because the set of independent variables was derived from combinations of the initial sample conditions.

After the subset of variables had been isolated by the STEPWISE procedure a number of regression equations were obtained by using those variables singly and in combination. Criteria were set by which the models could be compared and the best model could be selected. Requirements for the overall multiple regression equation include the following:

1. A high coefficient of multiple determination (R^2), which indicates the amount of variation explained by the variables included in the model;
2. An increase in the adjusted coefficient of multiple determination (R_a^2) with each addi-

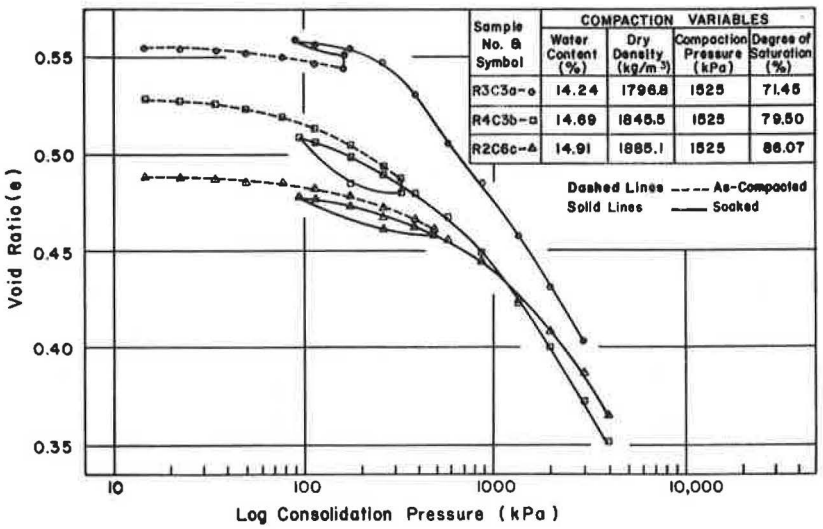

Figure 9. Effect of confinement on soaked compressibility behavior for dry of optimum.

tional independent variable entered into the model; and

3. The overall F-test at the $\alpha = 0.05$ significance level must be met.

If all of the above criteria were suitably met by more than one model, the final selection was based on the value of R_a^2 and the simplicity of the regression equation.

Two dependent variables were used in regression analysis--compactive prestress (P_s) and one-dimensional percent volume change on saturation ($\Delta V/V_o$). All independent variables based on the initial sample conditions were considered in the selection procedure. A number of regression equations met the criteria previously discussed for the compactive prestress. Before selecting one of these regression equations, the variables chosen by DiBernardo and Lovell (1) to predict the prestress for the laboratory-compacted St. Croix clay were forced into a regression equation for the field-compacted St. Croix clay. The adjusted coefficient of multiple determination (R_a^2) was 0.86.

The variables used by DiBernardo and Lovell (1) for predicting percentage of volume change on saturation (water content and compaction pressure) were forced into a regression equation for the field-compacted St. Croix clay, with very poor results. The equivalent embankment pressure on wetting had to be included in any regression relation in order to obtain an acceptable value of R_a^2. This is also rational for the laboratory-compacted data, and this prediction equation was rewritten to include the effect of confinement. The final regression models selected for the field-compacted soil, as well as prediction models for laboratory-compacted soil based on the DiBernardo (1) data, are given below.

For compactive prestress, ($\hat{P}_s$), in the laboratory,

$$\hat{P}_s = -343.52 - 0.002\,00\, w^2 P_{cp} + 48.91\, P_{cp}^{1/2} \quad (2)$$

In the field,

$$\hat{P}_s = -160.99 - 0.000\,63\, w^2 P_{cp} + 27.04\, P_{cp}^{1/2} \quad (3)$$

where

$\hat{P}_s$ = estimated value of compactive prestress (kPa),
w = water content (%),
P_{cp} = compaction pressure (kPa),
$w^2 P_{cp}$ = interaction term between water content (%) squared and compaction pressure (kPa), and
$P_{cp}1/2$ = square root of compaction pressure $(kPa)^{1/2}$.

For 1-D percentage of volume change on saturation ($\Delta\hat{V}/V_o$), in the laboratory,

$$\Delta\hat{V}/V_o = -6.50 + 1.102\, e_o P_o^{1/2} - 0.001\,02\, wP_o \quad (4)$$

In the field,

$$\Delta\hat{V}/V_o = -2.26 + 0.400\, e_o P_o^{1/2} - 0.000\,26\, wP_o \quad (5)$$

where

$\Delta\hat{V}/V_o$ = estimated value of 1-D percentage of volume change on wetting (%),
$e_o P_o^{1/2}$ = interaction term between initial void ratio and the square root of equivalent embankment pressure on wetting (kPa), and
wP_o = interaction term between initial water content (%) and equivalent embankment pressure on wetting (kPa).

The prediction model to estimate the compactive prestress ($\hat{P}_s$) induced by the compaction process is described in terms of compaction water content and compaction pressure. Figure 10 shows the compactive prestress regression models of the laboratory as-compacted soil and the field as-compacted soil, superimposed. This figure shows that, for a given water content, the estimated compactive prestress increases as the compaction pressure increases. Similar results had been obtained by Woodsum (2), Abeyesekera (4), and DiBernardo and Lovell (1). If the compaction pressure is held constant, an increase in the water content will result in a lower value of compactive prestress.

The percentage of volume change on the wetting model is described in terms of the initial void ratio (e_o) and the water content (w), each in combination with the equivalent embankment pressure (P_o). In these models a positive value of percentage of volume change indicates settlement and a negative value indicates swell when water is introduced under load. Because of the negative value of the constant term, any sample would swell if there

Figure 10. Compactive prestress models.

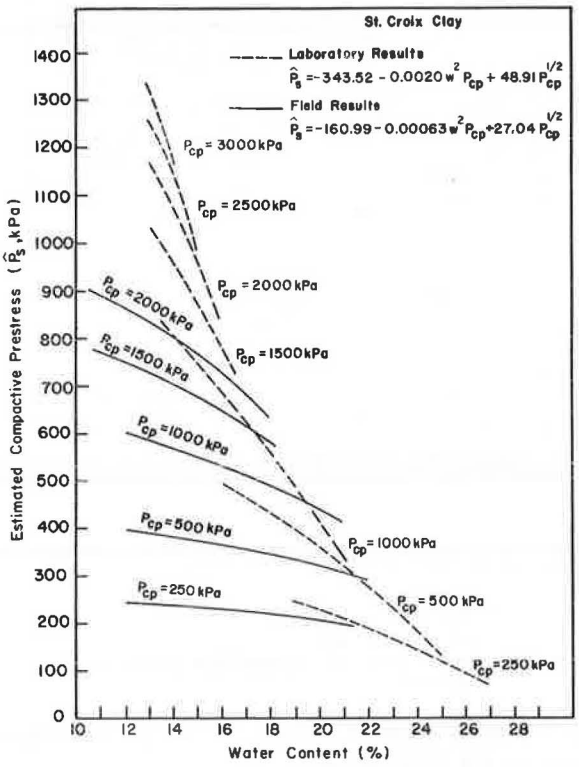

Figure 11. Effect of void ratio on percentage of volume change model for constant water content.

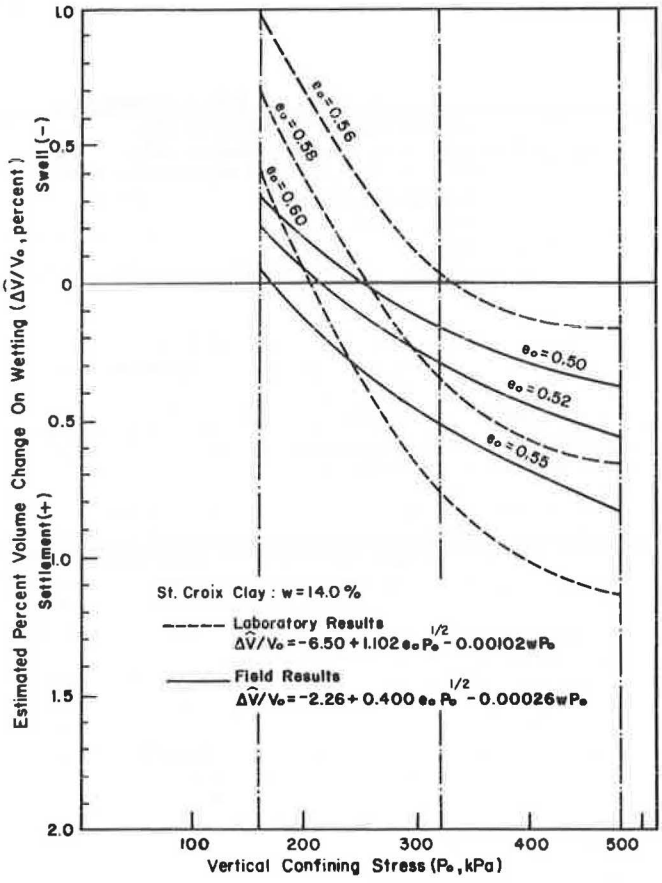

Figure 12. Effect of water content on percentage of volume change model for constant void ratio.

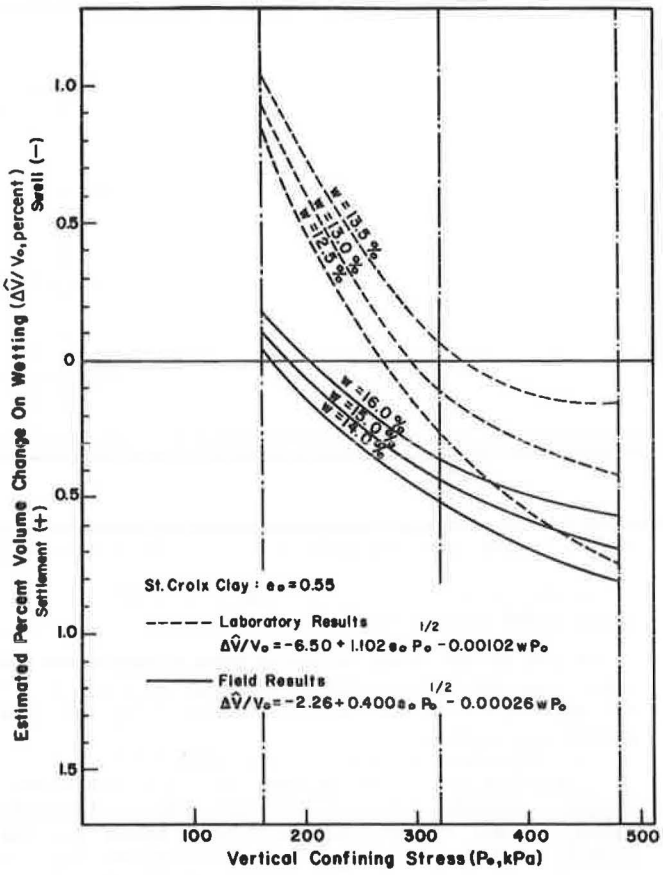

is no embankment pressure (P_o = 0). The reduction in effective stress on saturation and the volume increase of the clay minerals during hydration are the causes for the tendency to swell.

The effect of void ratio on the estimated percentage of volume change with constant water content is shown in Figure 11. The variable term in the model that involves the initial void ratio (e_o) and the square root of the equivalent embankment pressure ($P_o^{1/2}$) is preceded by a positive sign. This indicates that this term overcomes the tendency to swell. Figure 11 shows that an increase in the initial void ratio reduces the tendency to swell. As the equivalent embankment pressure increases, the percentage of volume change eventually becomes positive.

The variable term in the model that involves the water content (w) partly offsets the effect of the positive term. Figure 12 shows that an increase in water content reduces the expected volume decrease on saturation. The coefficients of the variables in the models are such that the negative term never exceeds the positive term within the range of values investigated. This ensures that under no conditions can sample swell exceed that of the free swell case.

Although the shapes of the field and laboratory compactive prestress and percentage volume change on wetting curves are similar, they are not identical. However, the simple procedure of superimposing equational models, as has been done in Figures 10-12, may prove to be a useful practical technique for predicting field response from laboratory tests.

An important objective of this study was to show how the laboratory-field correlation can be devel-

Figure 13. Prediction of field compactive prestress from laboratory-compacted samples.

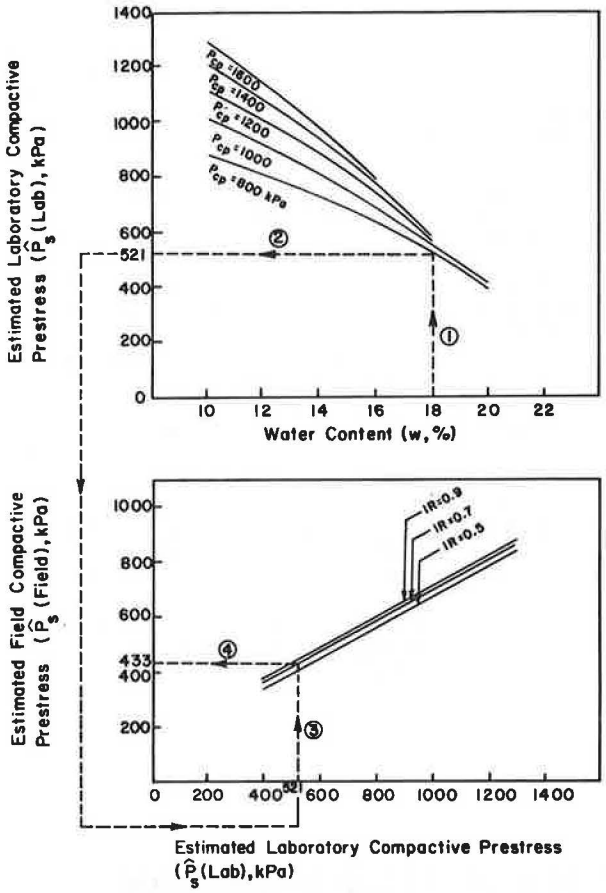

Figure 14. Prediction of field percentage of volume change on wetting from laboratory-compacted samples.

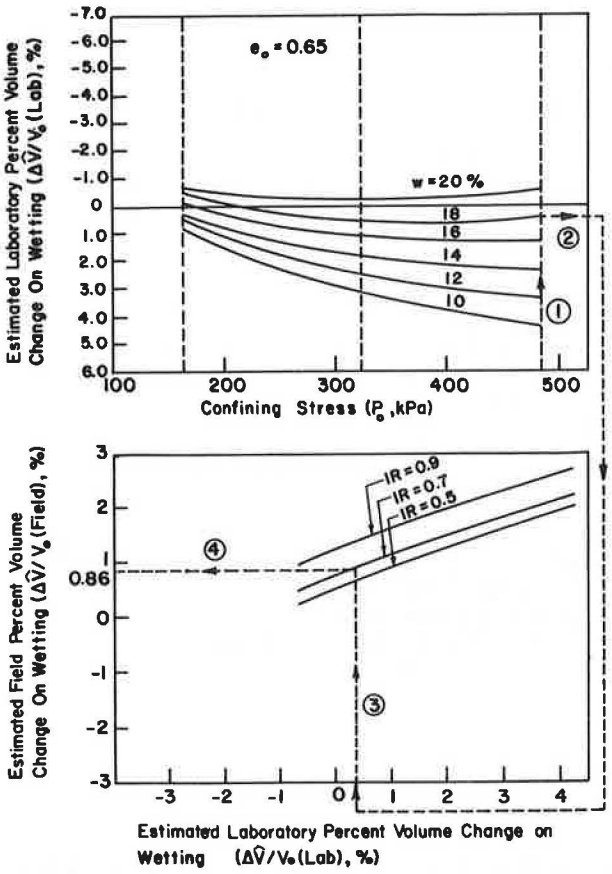

oped and used. These same procedures can be employed to cover additional typical soils and compaction rollers. Where the correlation between the laboratory- and field-compacted soils has been accomplished, the engineer can simply take bag samples from the excavation, run laboratory compaction and compressibility tests, and make good predictions of embankment compressibility. Thus, an alternate to the present procedures is (a) simply assume that the field-compacted values are the same as the laboratory-compacted ones or (b) generate the field-compacted parameters from test pad samples.

Behavior for soils similar to the St. Croix clay can be predicted by comparison of compaction curves and plasticity. A statistical prediction procedure was developed and is illustrated in Figures 13 and 14.

CONCLUSIONS

This paper has examined the effect of field compaction on the as-compacted compressibility, volume change on soaking, and soaked compressibility behavior of a plastic compacted clay (St. Croix).

The experimental and statistical results of the field-compaction study lead to the following conclusions:

1. The compression versus time relations show that a large percentage of the as-compacted compression occurs within the first minute of loading.
2. Samples compacted on the dry side of the line of moisture optimums for any compactive effort are less compressible than those compacted on the wet side of the line of optimums for loads less than the prestress level. However, the dry-side samples are more compressible than the wet-side samples when the applied load is greater than the prestress level.
3. The value of compactive prestress induced in a sample increases with increasing compaction pressure and decreases with increasing moisture content at a given compaction pressure.
4. For the saturated condition, at low confining stresses the swell pressure from the hydrating clay minerals, in conjunction with the reduced effective stress due to saturation, exceeded the effect of confinement and resulted in an increase in volume. At high confinements the confining pressures were sufficient to overcome the swelling tendency and resulted in a decrease in volume.
5. The field-compacted relations are similar to those developed by DiBernardo and Lovell (1), which involve the same variables, exponents, and signs. Regression constants are different.
6. The similarity of laboratoryand field-compacted relations allows the two predictions to be simply related in graphical form (Figures 10-12).
7. Predictions of field-compacted relations from laboratory tests can be accomplished for soils that are somewhat different by using IR = I_p (field)/I_p (laboratory). I_p is the Atterberg plasticity index.

ACKNOWLEDGMENT

We are grateful to the Joint Highway Project of

Purdue University, the Indiana Department of Highways, and the Federal Highway Administration for their financial support of the research reported here.

REFERENCES

1. A. DiBernardo and C.W. Lovell. The Effect of Laboratory Compaction on the Compressibility of a Compacted Highly Plastic Clay. Purdue Univ., West Lafayette, IN, Joint Highway Res. Project Rept. 79-3, May 1979.
2. H.C. Woodsum. The Compressibility of Two Compacted Clays. Purdue Univ., West Lafayette, IN, M.S.C.E. thesis, June 1951, 69 pp.
3. T.W. Lambe. The Engineering Behavior of Compacted Clay. Journal of the Soil Mechanics and Foundations Division, ASCE, Vol. 84, SM2, Paper No. 1655, pp. 1-35.
4. R.A. Abeyesekera. Stress Deformation and Strength Characteristics of a Compacted Shale. Purdue Univ., West Lafayette, IN, Joint Highway Res. Project Rept. 77-24, May 1978.
5. H.E. Wahls, C.P. Fisher, and L.J. Langfelder. The Compaction of Soil and Rock for Highway Purposes. Federal Highway Administration, Rept. FHWA-RD-78-8, 1966, 457 pp.
6. R.J. Hodek. Mechanism of the Compaction and Response of Kaolinite. Purdue Univ., West Lafayette, IN, Joint Highway Res. Project Rept. 72-36, Dec. 1972.
7. I. Garcia-Bengochea. The Relation Between Permeability and Pore Size Distribution of Compacted Clayey Silts. Purdue Univ., West Lafayette, IN, Joint Highway Res. Project Rept. 78-4, May 1978.
8. R.J. Hodek and C.W. Lovell. A New Look at Compaction Processes in Fills. Bull. of the Association of Engineering Geologists, Vol. 16, No. 4, Fall, pp. 487-499.
9. R.J. Hodek and C.W. Lovell. Soil Aggregates and Their Influence on Soil Compaction and Swelling. TRB, Transportation Research Record 733, 1979, pp. 94-99.
10. P.S. Lin and C.W. Lovell. Compressibility of Field Compacted Clay. Purdue Univ., West Lafayette, IN, Joint Highway Res. Project Rept. 81-8, Aug. 1981.
11. Y. Yoshimi. One-Dimensional Consolidation of Partially Saturated Soil. Northwestern Univ., Evanston, IL, Ph.D. thesis, Aug. 1958, 149 pp.
12. E.T. Selig. Unified System for Compactor Performance Specification. Paper 710727, SAE, Warrendale, PA, Sept. 1971, pp. 1-12.
13. G.A. Leonards and P. Girault. A Study of the One-Dimensional Consolidation Test. Proc., 5th International Conference on Soil Mechanics and Foundation Engineering, Paris, Vol. 1, 1961, pp. 213-218.
14. N.H. Nie and others. Statistical Package for the Social Sciences, 2nd ed. McGraw-Hill, New York, 1975, 675 pp.

Compaction Practice for Dam Cores at Hydro-Quebec

O. DASCAL

Glacial till is used mainly as an impervious material in earth and rockfill dams built in Quebec. It is, in general, a well-graded mixture of sand, silt, and gravel, with 25-80 percent passing the no. 200 sieve and a natural water content at or above optimum (Proctor standard). Its natural water content, together with its very high sensitivity to atmospheric humidity, strongly influence the choice of compaction equipment, compaction procedure, and time schedule. This paper presents Hydro-Quebec's experience with this type of material, including choice of the compaction equipment, establishment of the compaction procedure, pretreatment of the borrow pit material, as well as the results and performances obtained at various sites. In addition, the paper describes the particular compaction problems and results of a manufactured material (sand and sensitive clay mixture) used as core material in certain water-retaining dikes.

One of the main economical advantages of an earth or rockfill dam is the possibility of using relatively cheap local soil deposits as construction materials. In this context, glacial till deposits that cover large areas of the continental shelf of Canada are used extensively as material for the impervious zone of earth and rockfill dams. The use of natural clay deposits as impervious material is rather limited (a) because of its localized presence along the lowlands of the St. Lawrence valley and the eastern shore line of the James Bay, and (b) because its geotechnical characteristics (high sensitivity) require special placement and compaction procedures.

The till, an abrasion product of the glaciers, is frequently used in construction specifications as indicative of an unsorted unstratified heterogeneous mixture of clay, silt, sand, gravel, cobbles, and boulders. It also denotes a very dense and stiff material of low compressibility. These characteristics, when complimented with a proper amount of fine particles (<0.074 mm) and a well-graded grain size composition, represent those of an ideal material for dam cores.

However, the compaction characteristics of this material are substantially influenced by its water content. As a matter of fact, the soil is difficult to handle (compact) when the natural water content reaches 2 percent above optimum and becomes rapidly soupy when it reaches +3 percent or more. This is a severe limitation because it is often found in situ at a water content above optimum. The problem becomes more acute when one considers the adverse climatic conditions encountered in the northern regions of Quebec, where the construction season is short and rainy.

The importance of proper compaction should be emphasized in view of the close relation among density, shear strength, permeability, and compressibility. All these parameters are of particular importance in the safety and behavior of the dam.

This paper presents Hydro-Quebec's experience and practices in handling this type of material as illustrated by three case histories. The first project involved uses till that had a natural water content at or slightly above its optimum and hence presented no problem of placement or compaction. In the second project, the use of a till that had a natural water content substantially higher than

optimum created a set of difficult problems and necessitated the adoption of new solutions. A third example illustrates the use of a highly sensitive marine clay as core material, its placement, and compaction problems experienced during the construction of an earth-fill dike located in the St. Lawrence valley.

PROJECT A, DAMS 1 AND 2--OUTARDES 4

Project A includes two-zoned rock-fill dams with slightly inclined till cores 400 and 350 ft (122 and 106 m) high, respectively. Dam 1, with a crest length of 2100 ft (640 m), has a total volume of 9 900 000 yd^3 (7 569 097 m^3), the core volume being 885 000 yd^3 (676 631 m^3). Dam 2, with a total volume of 6 145 000 yd^3 (4 698 192 m^3), has a core of 601 500 yd^3 (459 880 m^3) of till and a crest length of 2380 ft (725 m).

The maximum horizontal width of the core at the base is about 120-130 ft (36-40 m). The crest width is reduced to about 20 ft (6 m). Thus, for both dams the working area at any elevation represents an average of about 40 000-45 000 ft^2 (3750-4000 m^2).

Geotechnical Characteristics of the Till

The borrow area situated a few miles upstream of dam 1 consists of a relatively well-graded till that has a maximum gravel content of 10 percent grain size larger than 6 in (150 mm). The percentage of fines (passing sieve no. 200) varies between 10 and 40 percent, with an average of 23 percent, and has a liquid limit between 11.5 and 14.2 percent. The plastic limit varies between 9 and 11 percent.

Laboratory compaction tests indicate a maximum dry density [standard Proctor (ASTM D698 method A)] of 126-136 $lb \cdot f/ft^3$ (2000-2175 kg/m^3), with an optimum water content that varies between 7 and 10 percent; the in situ natural water content ranges from 6 to 12 percent.

Laboratory permeability tests, carried out on the fraction that passes sieve no. 4 (U.S. Bureau of Public Roads standard E-12) indicate a coefficient $K = 10^{-6}$ to 10^{-7} cm/s.

Borrow Pit Operations

The borrow pit consists of two areas. The eastern part is more sandy with a relatively low fine content and in the western area the percentage that passes sieve no. 200 varies between 35 and 45 percent. Consequently, it is necessary to mix the material from both areas (in equal parts) at the pit. The excavation of the material is carried out by bulldozers, which push the till over a Koleman vibratory screen to eliminate cobbles larger than 6 in (150 mm). The material is loaded directly in trucks passing under the screen.

The quality of the mix is continuously checked by a rapid sieve analysis that establishes the percentage of fines (passing sieve no. 200).

Placement and Compaction Operations

The prevailing climatic conditions limit the placement of the till to a maximum of 70 days/year.

The till hauled to the dam's site by trucks is spread by bulldozers in lifts 10- to 12-in (250- to 300-mm) thick parallel to the dam's axis and subsequently compacted by six passes of 50-ton pneumatic tired rollers. To obtain a uniform moisture distribution before compaction, the spread material is mixed with 30-in (750-mm) diameter disc harrows. After the compaction and immediately before placement of the new lift the compacted material is scarified to a depth of about 3 in (75 mm) to avoid the formation of compaction joints. The scarifying also facilitates the water distribution, when the sun- or wind-dried material must be sprinkled. The compaction is carried out on strips parallel to the dam axis, as the equipment moves from one abutment toward the other.

The compacted till surface is always provided with a small slope toward its upstream and downstream edges (toward the filter zones) to facilitate the rainwater runoff. In areas where the access of heavy rollers is hindered or next to rock abutments, the till material is spread in lifts 4- to 6-in (100- to 150-mm) thick and compacted with a manual Vibro-Tamper 2-1, which has a weight of about 925 lb (420 kg), and which develops a dynamic force of 20 000 lb (9000 kg) at around 2100 cycles/min.

Placement and Compaction Control

The technical specifications call for a minimum degree of compaction (relative compaction) of 97 percent of the standard Proctor maximum density (ASTM D698 method A) at a water content ±2 percent of the optimum. A maximum of 15 percent of the results could be less than the specified minimum if they are not concentrated in the same section.

The same specifications ask for a grain size composition within the limits shown in Figure 1. To reach this goal, the technical specifications also demand a set of parameters to be respected during construction (e.g., lift thickness and number of passes of the compactor) and the type and frequency of the tests to be carried out. Thus, the control operations are carried out to cover the following two aspects:

1. Qualitative control of the construction procedures (i.e., lift thickness, scarification, sprinkling, and number of passes) and
2. Quantitative control of the materials characteristics by in situ and laboratory tests (i.e., water content, grain size composition, in situ density, Atterberg limits, and permeability).

Control Tests Results

The placement and compaction operations were performed during four summers. The number and the frequency of the tests carried out are given in Table 1. Statistical analysis of the control test results indicates that 80 percent of the results show a degree of compaction higher than 98 percent, and only 5 percent of the results were less than 97 percent. A degree of compaction higher than 100 percent was measured in more than 70 percent of the tests (Figure 2).

The average dry density of the compacted till is 141 lb/ft^3 (2250 kg/m^3). All of the results indicate a density higher than 125 lb/ft^3 (2000 kg/m^3) (Figure 3). Notice that the distribution of the results shows a larger deviation from a Gaussian distribution.

The average compaction water content of 8.9 percent is slightly higher than the optimum 8.0 percent. At the same time only 20 percent of the samples indicated a water content higher than 2 percent of the optimum. Less than 5 percent of the tests revealed a water content 2 percent below the optimum (Figure 4).

PROJECT B, MAIN DAM--MANICOUAGAN 3

The second project includes a 350-ft (106-m) high earth-fill dam resting on a 420-ft (128-m) deep sediment-filled canyon. The dam, which has a total

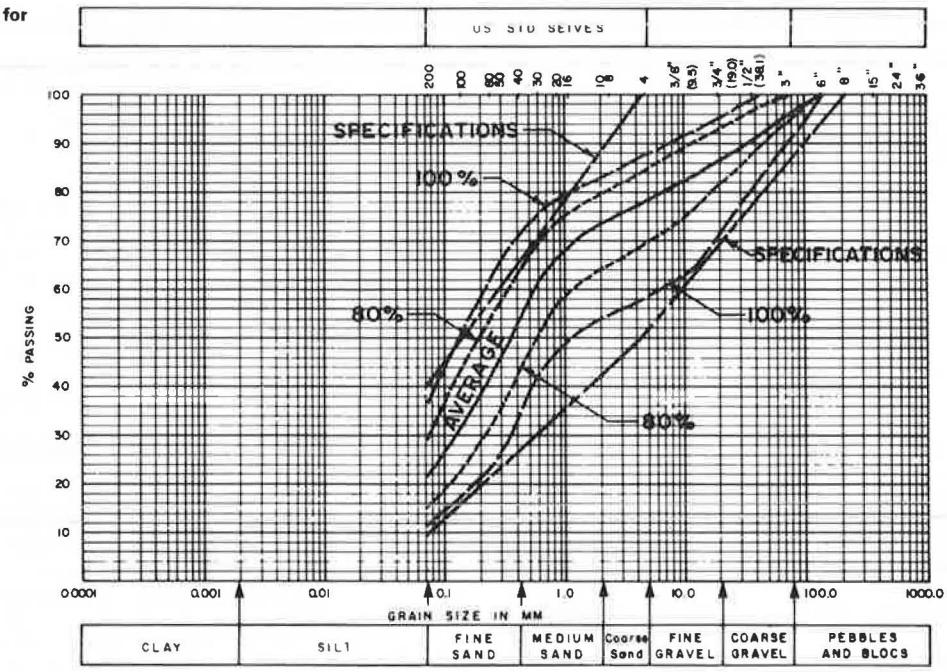

Figure 1. Grain size composition of till for project A.

Table 1. Frequency of control tests for project A.

Test	Site	Volume of Material (000s yd^3)	No. of Tests	Yards^3 Between Tests
In situ density water content	Dam 1	885.0	748	1 183
	Dam 2	601.5	833	722
Grain size analysis	Dams 1 and 2	1723.0	465	3 705
Standard Proctor		1723.0	382	4 510
Specific gravity		1723.0	25	68 918
Permeability		1723.0	32	53 843

volume of about 11 035 000 yd³ (8 436 867 m³), comprises a fairly thick symmetrical central core, that consists of till. An upstream blanket of about 30-ft (9-m) thickness links the central core with the upstream cofferdam and was provided to lengthen the seepage path under the embankment. It is constructed also from the till material. The total till volume for both the core and blanket is about 2 552 000 yd³ (1 951 144 m³).

The maximum width of the core at the dam's base is about 300 ft (90 m); at the same elevation the valley is about 500 ft (150 m). At the crest the core's width is reduced to about 20 ft (6 m), with a crest length of about 1280 ft (390 m). Thus, the working area for the till varies from about 150 000 ft² (13 500 m²) at base elevation to 25 500 ft² (2350 m²) at the crest. The working platform area for the blanket construction (at the base elevation) is about 350 000 ft² (31 500 m²).

Geotechnical Properties of Till

The borrow area is situated some 1.5 miles (2.5 km) downstream of the dam. It contains a till deposit that includes numerous thin layers or lenses of sand, which confer a somewhat stratified appearance.

The grain size analysis indicates a well-graded material that contains, on the average, 5 percent gravels and 50 percent silt-clay particles (Figure 5). The mineral composition of the particles between sieves no. 40 and no. 200 is mainly quartz (85-90 percent), feldspar, biotite, hornblende, garnet, and magnetite. The grains are in general equidimensional and angular. The same mineral composition prevails for the fraction that passes sieve no. 200, the presence of real clay minerals being very limited in spite of a clay size particle content (< 2μ) of 4-15 percent. In general, the material (fraction passing sieve no. 40) is nonplastic. However some samples indicated liquid limit around 17-18 percent and plastic limit of 12-13 percent.

The in situ material is relatively cold, even during the summer. Temperatures of 0°-5°C were recorded in the freshly stripped material. The material is dryed with difficulty by natural evaporation and it is rapidly covered by a film of condensed water when the air humidity rises. On the other hand, the in situ water content is substantially higher than its optimum (standard Proctor). The degree of saturation reaches 95 percent.

The laboratory compaction tests indicate high sensitivity of this material to the compaction water content. The dry density decreases rapidly with the increase of the moisture content (Figure 6). The end points of the compaction curves shown in Figure 6 indicate the water content at which the samples became too wet and too soft to be handled (compacted).

The maximum dry density (standard Proctor) varies between 125 and 137.5 lb•f/ft³ (2000-2200 kg/m³) with an optimum water content at 7.4-11.0 percent. The in situ water content of the till is 0.9-3.5 percent higher than the optimum. The permeability of the material measured in laboratory triaxial tests varies between 0.4 and 6×10^{-6} cm/s (material with fines passing sieve no. 200 around 45 percent).

Operation of the Borrow Area

The high natural water content of the material created numerous difficulties during placement and compaction operations. Consequently, special attention was given to the borrow pit operation to obtain some reduction of the moisture content. The excavation of the till was started by backhoes cutting 20- to

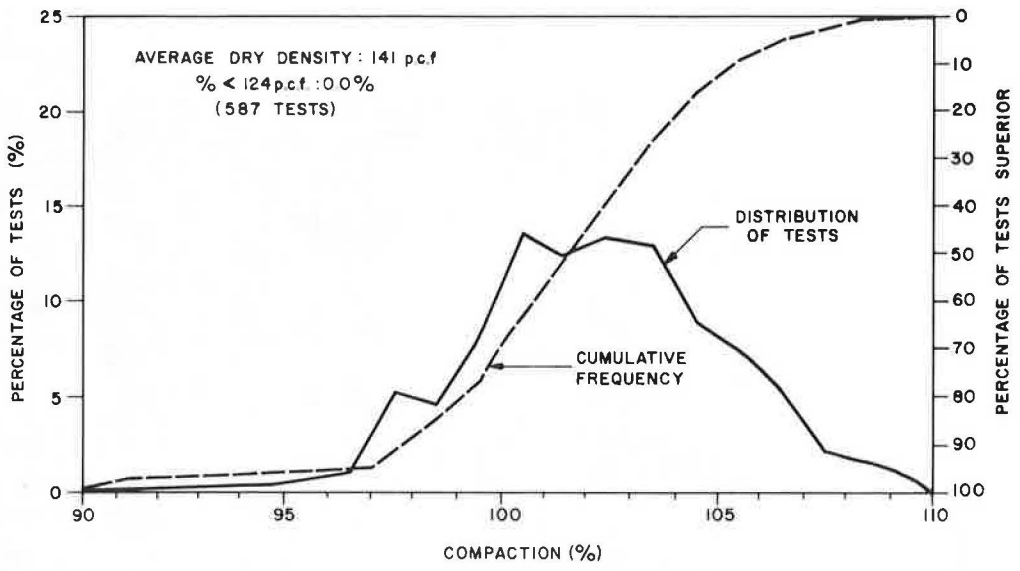

Figure 2. Compaction degree of till for project A.

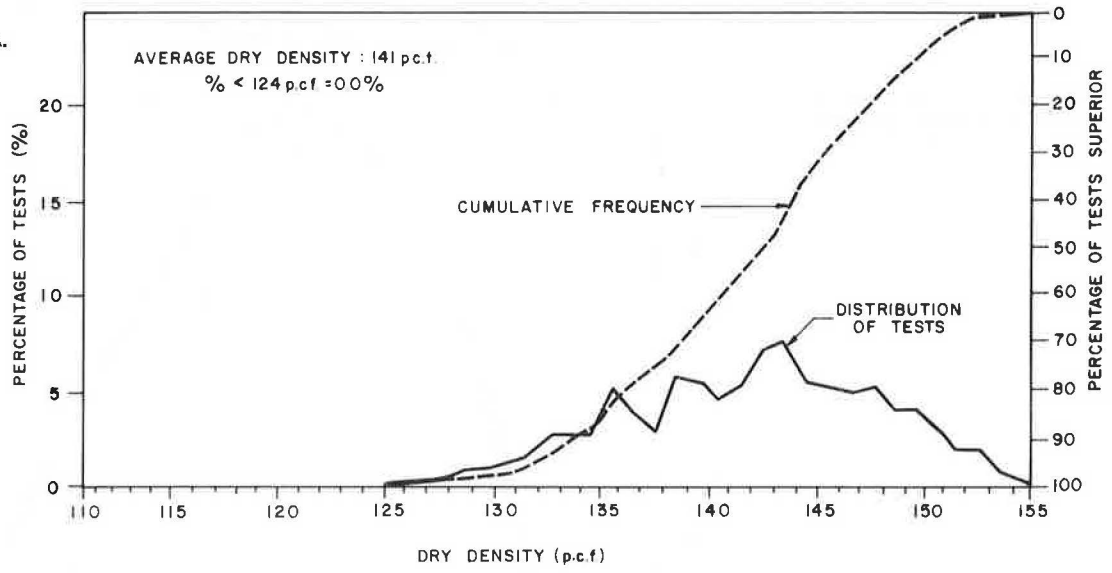

Figure 3. In situ dry density of till for project A.

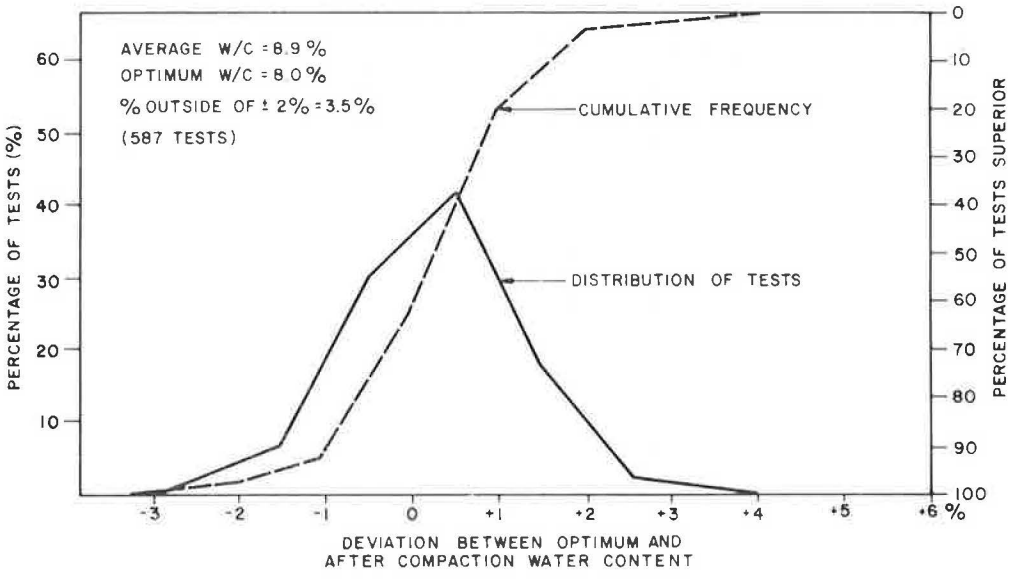

Figure 4. After compaction water content deviation from the optimum W/C for project A.

Figure 5. Grain size composition of the fill for project B.

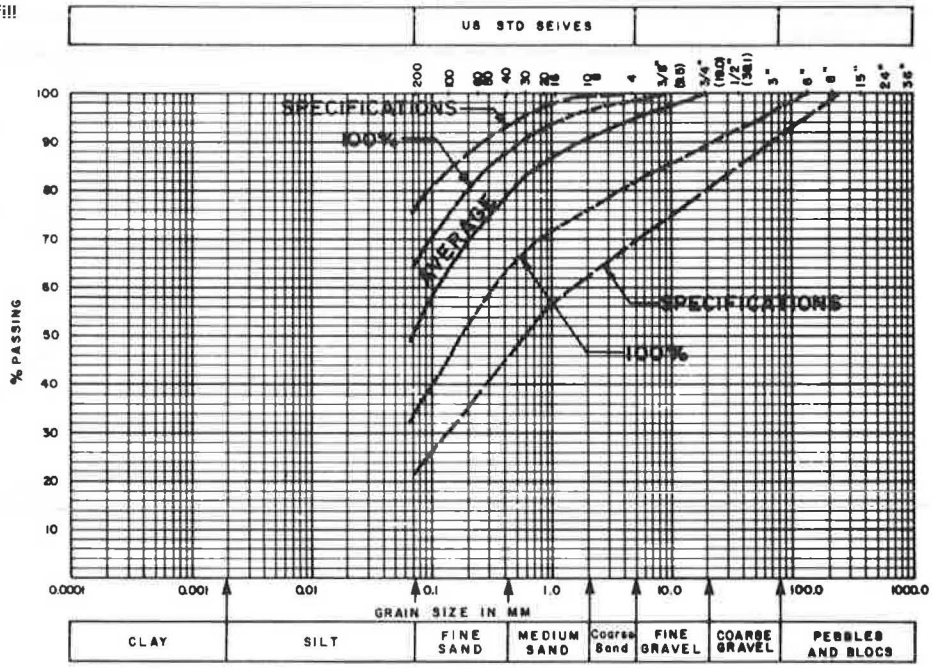

Figure 6. Dry density versus water content (standard Proctor) for various temperatures of the material for project B.

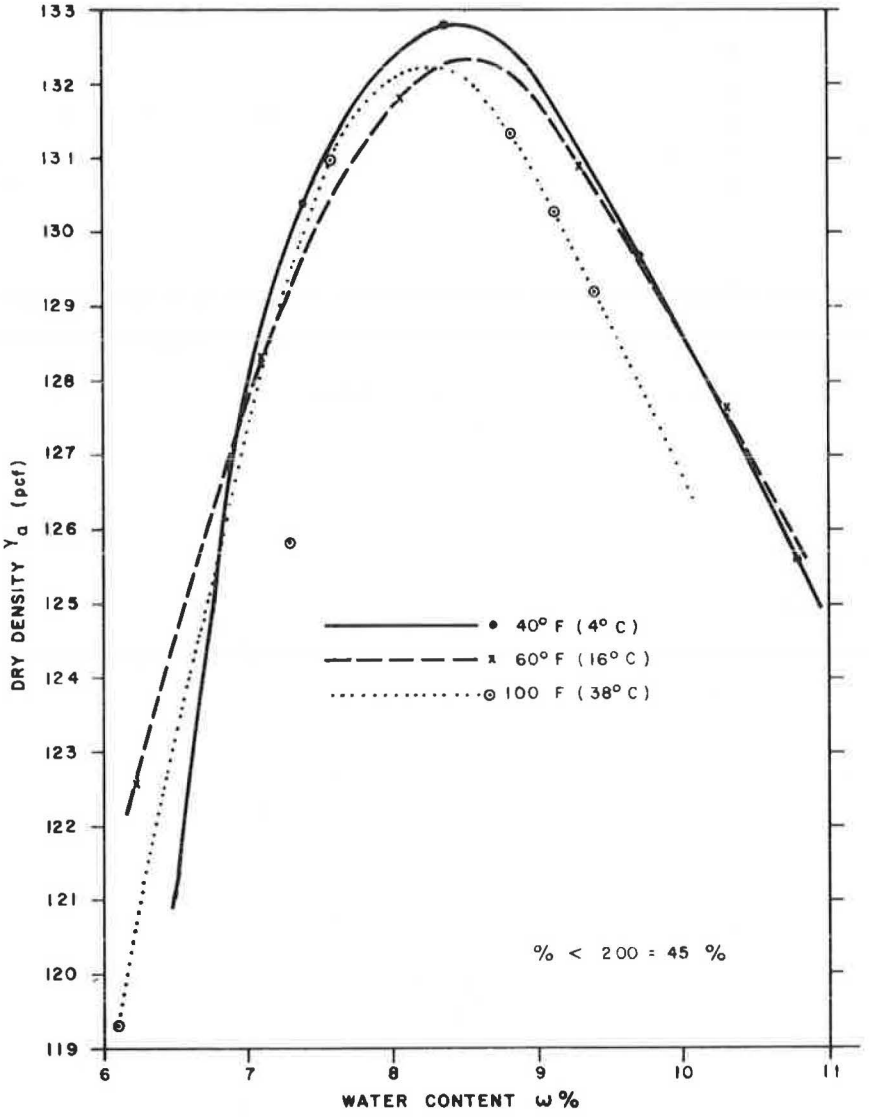

Figure 7. Compaction degree obtained with different compactors.

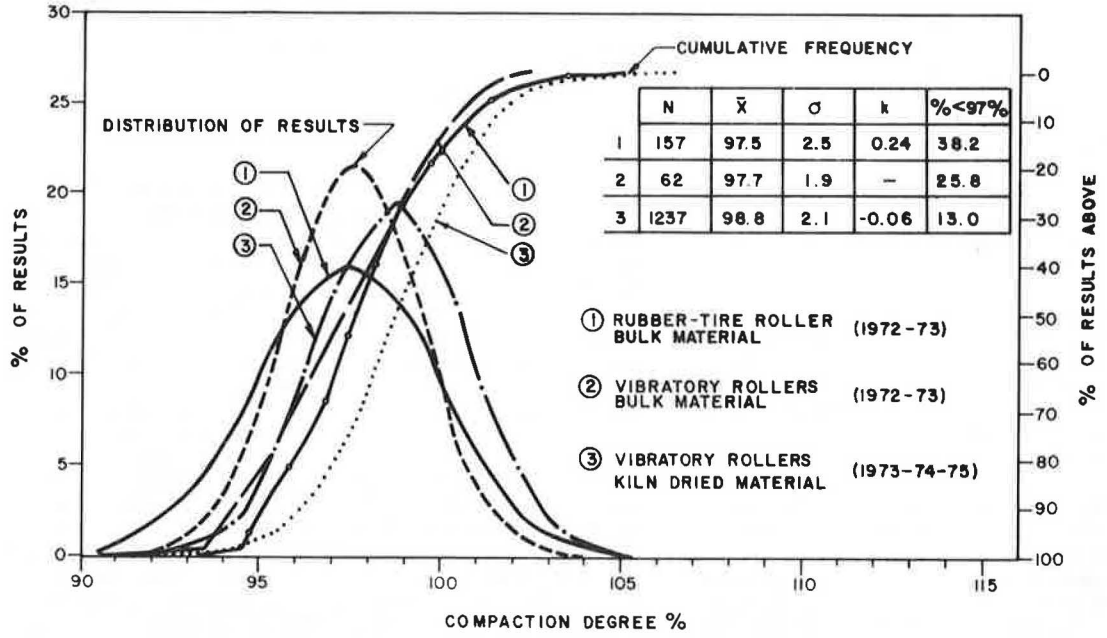

25-ft (6.1- to 7.6-m) high vertical faces. This method allows a good mixing of the material. However, the freshly cut face is too small to permit drying by sun or wind action. At the same time, this method does not permit a selective exploitation of the deposit (i.e., elimination of more wet or more sandy layers or lenses). Consequently, the method was abandoned and replaced by an excavation with bulldozer along subhorizontal surfaces. The working pad was at first scarified to a depth of 0.5-1.0 ft (0.15-0.30 m) and exposed to drying. Depending on the climatic conditions after a while (average 1 h), the material was sufficiently dry to be placed directly in the dam. The dried material is scarped in thin layers and pushed by bulldozers in piles and loaded in trucks with pneumatic loaders. This method produces a material that can be placed readily in the dam; however, the productivity is too low, which jeopardizes the construction schedule.

The installation of two Koleman vibrating screens to reject the oversize [>6 in (150 mm)] and belt conveyors increased the productivity somewhat. The material is pushed by bulldozers into a hopper, lifted by the conveyors on the screens, and the passing material falls directly in the trucks. The operation is frequently stopped, sometimes for a few days following rainy periods. Subsequently, to ensure that the construction schedule is respected, the artificial drying of the material, using an oil-heated rotary kiln, was adopted.

Placement and Compaction of the Till

First Stage Operations

Previous experiences with till and some preliminary compaction tests carried out before construction indicated that the pneumatic-tired roller would be adequate compaction equipment. Thus, the compaction of the till for the impervious blanket was started with 50-ton tired rollers pulled by bulldozers. Areas that have limited access to the tired rollers or were next to rock abutments were compacted with self-propelled 5.5-ton vibratory rollers and with manual vibration plates.

The high natural water content of the material, even at the beginning, created a lot of difficulties. The traffic of the loaded trucks and the heavy compaction equipment induced large deformation in the fill [ruts up to 8-in (200-mm) deep], which resulted in its decompaction and fissuration. A reduction in the layer thickness before compaction from 9 in (22.5 cm) to 6 in (15.0 cm) did not improve significantly the productivity and the quality of the operations. During the first year the majority of the in situ density tests indicated a degree of compaction below 97 percent. The large working area [350 000 ft² (31 500 m²)] exposed to weather inclemencies also contributed to low productivity. As a matter of fact, cleaning operation after a rainy period, which in many instances necessitated the removal and the rejection of the saturated (too wet) material, was very time consuming and expensive. Even when the removal of the wet material was not required, a deep scarifying was carried out to facilitate drying, which increased significantly the depth of the loose material to be compacted. Consequently, the efficiency of the compaction is reduced and that explains the low degree of compaction obtained during the first campaign.

Tests carried out with different types of compaction equipment, varying layer of thickness, and number of passes did not succeed in improving significantly the degree of compaction. Figure 7 presents, as an example, the degree of compaction obtained with 40-ton pneumatic tired rollers and 9-ton vibratory rollers on material at its natural water content (bulk material). As can be seen for both equipments, close to 50 percent of the results show a degree of compaction less than 97 percent (the technical specifications required a minimum degree of compaction of 97 percent standard Proctor, allowing a maximum of 15 percent below this limit).

To eliminate or at least to reduce some of the difficulties mentioned above, research was carried out

1. To reduce the water content of the till in the borrow pit,
2. To select an adequate protection system of the compacted material,

3. To select a compactor for the given soil conditions,
4. To reduce the water content of the till by artificial drying, and
5. To change the borrow area that contains a drier material.

The inefficiency of the drainage trenches installed in the borrow area and some negative results of laboratory tests on electro-osmosis, vacuum pumping led to abandonment of the first objective. At the same time, the idea to cover the compacted material with plastic sheets to avoid supplementary wetting by rain or condensation was also eliminated. The large surface involved and the high wind velocities that prevailed at the dam's site would have made the installation and the recovery of the sheets difficult. Another drawback of the system is that, during favorable climatic conditions, if the sheets are not removed the evaporation is hindered and condensation takes place at the fill's surface. A wrong decision concerning the time of installation or removal could damage the material or produce useless work stoppages. It was also concluded that this method would not change the high compaction water content of the till.

Concerning the compaction equipment, as mentioned above, tests carried out with various types of compactors did not improve the compaction of these wet materials.

Artificial drying of the material was contemplated by two means:

1. In situ drying in the borrow pit and
2. Drying the excavated material in special devices

In situ drying was experimented with by using propane-heated, infrared ray plates [4x9 ft (1.35x 2.70 m)] pulled by bulldozers. The plate produced an effective heat radiation of about 4000 cal/cm²/h (as compared with 65 cal/cm²/h radiated by the sun at the dam's site) and dried only the upper 2-4 in (5-10 cm) of the material, which necessitated a subsequent harrowing and a second pass of drying. The application of this procedure would have implied the use of a large number of plates and bulldozers, consequently its economy would have been questionable.

Tests with infrared heaters installed above a belt conveyor were abandoned because too much time was needed to build and put in operation such a device. The second option, the drying of the excavated material by using a rotary kiln, was finally accepted.

Consequently, a readily built rotary kiln, which had a diameter of 14 ft (4.25 m), a length of 80 ft (24.4 m), and delivering about 28×10^9 cal/h, was installed. The kiln capacity is about 455 ton/h (200 yd³/h), the temperature of the material leaving the oven varies between 60° and 70°C. Fuel consumption is 7.4 l/m³ and reaches 11.3 l/m³ for the most humid material.

The material leaving the kiln is stored in cone-shaped stockpiles. The slopes of the pile, the accumulated heat (the temperature in the pile is maintained at about 32°-50°C), and the compactness of the material constitute an adequate protection against water penetration (rain), without necessity for any protective shelter (Figure 8).

The efficiency of the kiln is illustrated in Figure 9; the average water content of the material before drying of 11.9 percent is reduced to about 10.3 percent or by about 1.6 percent. At the same time, the deviation between the optimum water content and the water of the material before and after drying is also narrowed. As can be seen, more than 85 percent of the dried material has a water content lower than optimum +2 percent, which allows much easier handling (compaction).

Also note that, due to the accumulated heat in the stockpile, the material obtains a more homogeneous water content while an additional reduction takes place in the stockpile.

Second Stage Operation

The 8- to 9-ton vibration roller was adopted following the positive results obtained with it. This equipment gives a satisfactory compaction by 3-4 passes in lifts of 4-in (100-mm) material, even when the water content is as much as 2 percent over the optimum. A light scarifying of the compacted surface before spreading the new layer allows an intimate connection between the two lifts. Control trenches excavated in the material did not reveal the presence of any compaction joints. However, the till compacted at a water content over its optimum continued to deform under the truck loads.

These deformations are associated with the opening of fissures in the compacted material, which cannot be tolerated in the dam's core. Consequently, a major modification of the placement and compaction procedure was introduced. The traffic of the trucks hauling the till was limited to the transition zones only. The material dumped on the upstream and downstream edges of the core was spread by bulldozers in layers of 4-6 in (100-150 mm) along the upstream-downstream axis and followed by the compaction along the same direction (Figure 10). This direction of compaction is a major deviation from the general practice adopted by the profession. Performance to date indicates that homogeneous material obtained did not have any weakness zones along compaction joints in the direction of flow through the core.

During midsummer periods the compacted surface can became too dry, in which case the scarified material is sprinkled to get a water content slightly above the optimum. However, when the drying of the material is deeper [3-6 in (75-150 mm)], following an extended work stoppage (1-3 days), removal of the entire dried material is more economical. Some rewetting tests carried out indicated that the results are acceptable; however, the wetting operation needs many hours without getting assurance that a homogeneous material will be obtained. The removal of the same materials following a rain also seems more economical than its in situ drying. This allows a much more rapid resumption of the compaction operations.

Placement and Compaction Inspection

The qualitative inspection involving operation procedures (number of passes, lift thickness, compaction overlapping, movement speed of a compactors, scarification, and harrowing) is carried out by field inspectors. Technician crews attached to the field laboratory execute quantitative analyses (in situ dry density, laboratory grain size analysis, water content, and standard Proctor).

The inspection also is extended to the borrow pit and the kiln operation. At the borrow pit, the inspector supervises the excavation operation and, following a visual inspection and a rapid test of material passing sieve no. 200 and water content (speedy moisture), approves the material to be shipped to the dam. Once the kiln operation has started, the inspection in the borrow pit is reduced, but at the kiln it is extended. The material is tested at the feeder and at the outlet of the kiln to allow the adjustment of the burner and the feeder's discharge, which controls the temperature and the water content of the dried material. The

Figure 8. Rotary kiln drying plant.

Figure 9. Water content of the till before and after kiln drying for project B.

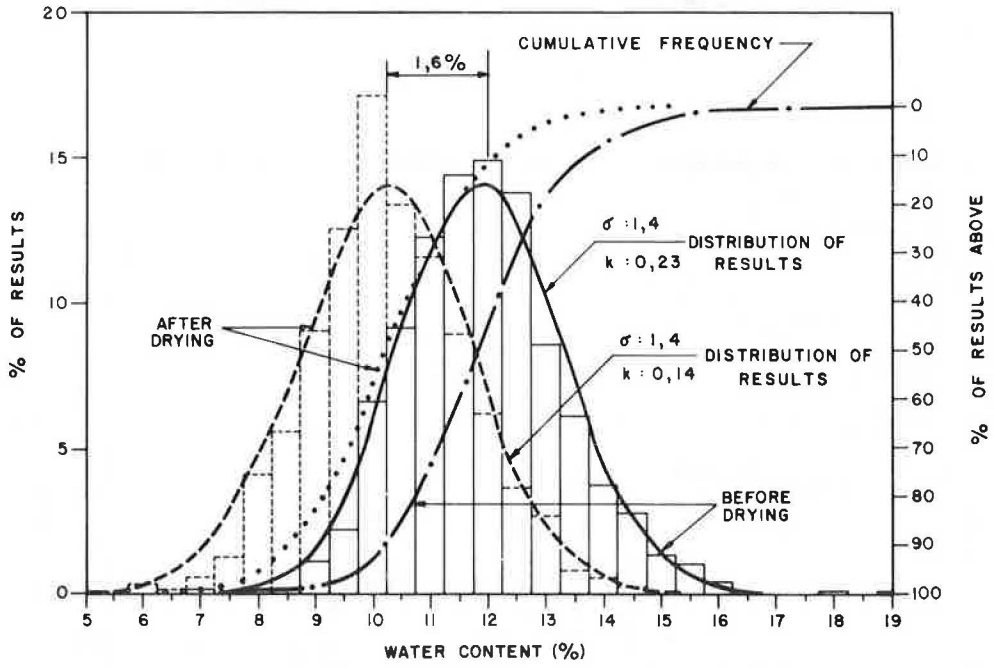

Figure 10. Placing operations of the impervious core.

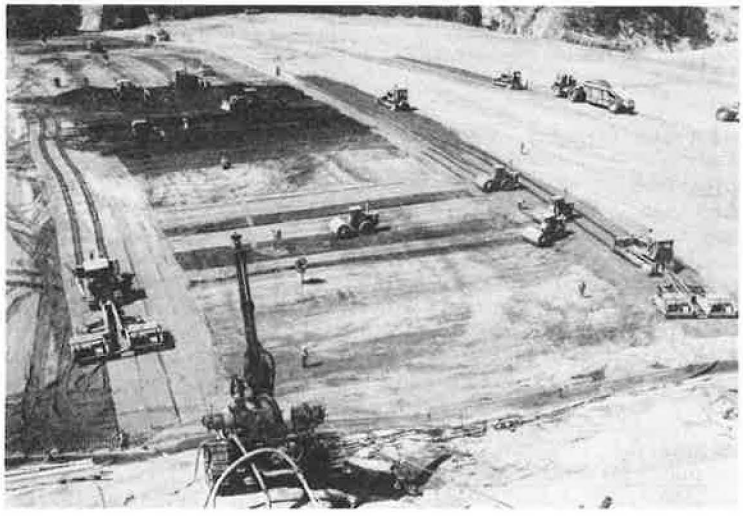

Figure 11. Compaction degree for the total till volume placed in the core and blanket for project B.

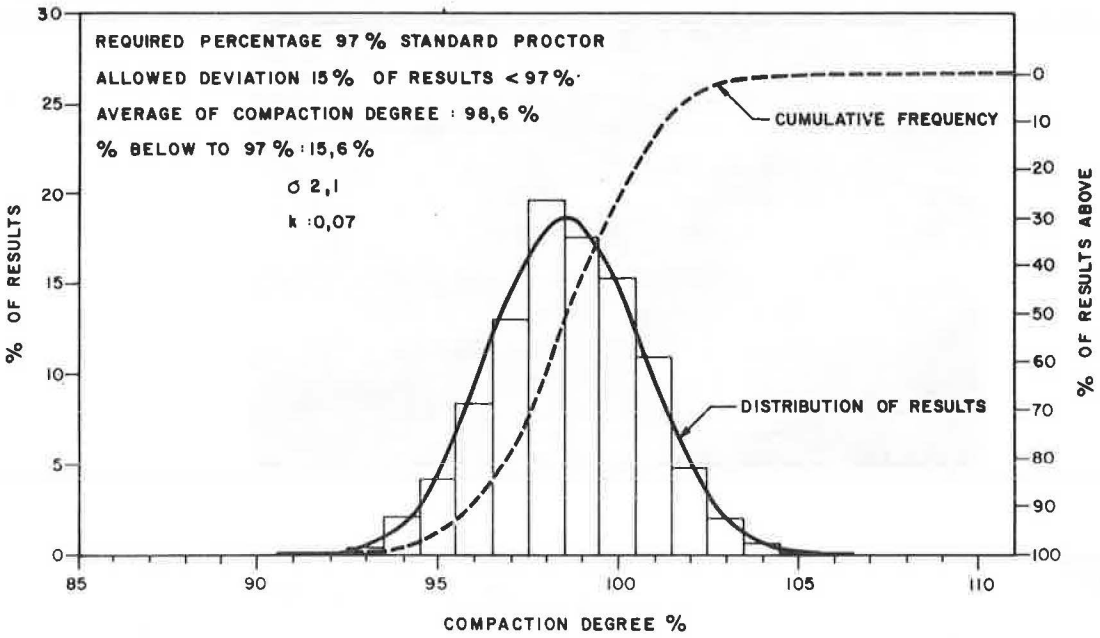

Figure 12. In situ dry density obtained with different compactors before and after drying the till for project B.

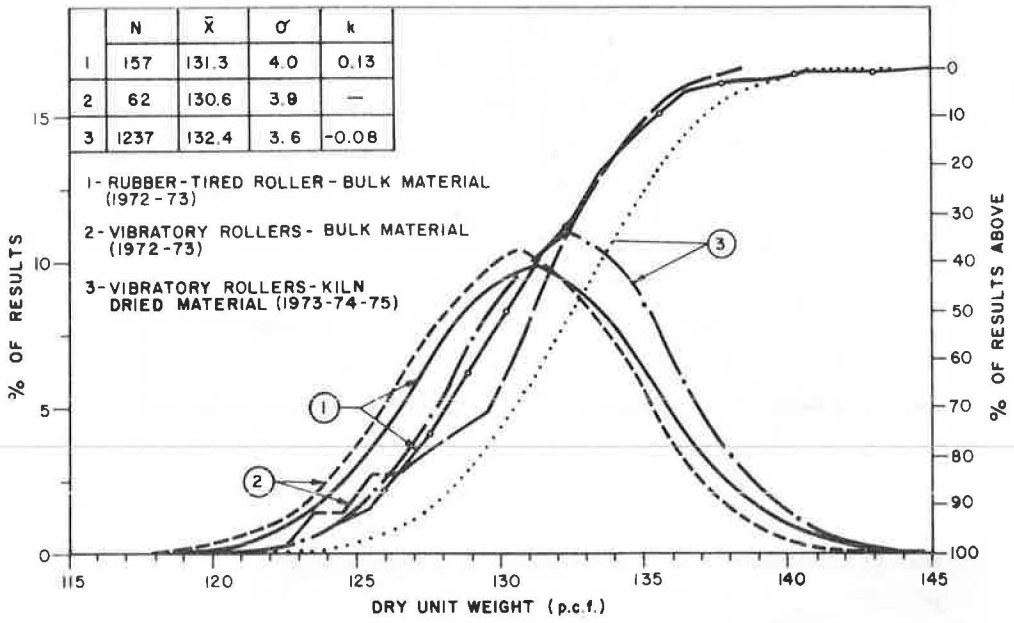

frequency of the rapid tests (passing sieve no. 200 and water content) is about 5-8/10-h shift.

One of the main objectives of the quality inspection was the lift thickness. This parameter has a particular influence on the compaction results. The lift thickness was checked by topographical survey, along a quadrilateral mesh covering the working area. The survey was carried out before and after compaction covering the working area.

The frequency of the principal routine tests is shown in the table below (note 1 yd^3 = 0.765 m^3):

Test	Volume of Material (000 yd^3)	Yards³ Between Tests
Grain size	2550	5000
In situ density and water content	2550	1350
Standard Proctor	2550	5000

Summary of Quantitative Test Results

The average degree of compaction is 98.6 percent with a standard deviation of 2.1 and with 15.6 percent of the results below 97 percent (Figure 11). Note that, after the kiln started to function, the average degree of compaction was maintained around 100 percent. The average dry density reached a value of 132 lb/ft^3 (2110 kg/m^3). Figure 12

shows the dry density obtained by the tired rollers after drying.

The water content after compaction is an average of 0.9 percent over the optimum with a standard deviation of about 0.9 percent. The degree of saturation of the compacted material varies between 70 and 100 percent.

Economy of Drying Operation

Based on 1974 prices, the drying operations increased the material cost by about 72 percent (1), considering that the drying installation is entirely depreciated. However, considering that only about 700 000 yd^3 (510 595 m^3) of material is dried, the increase is 51 percent of the total cost of the till, and only 10.5 percent of the total cost of the dam's fill.

The increase costs can be distributed as follows:

Item	Percent
Investment--purchase and installation of the kiln and conveyor	32
Operation--fuel, parts, and main power	53
Supplementary cost for transportation and loading	15

Notice that the main costs are those of operations, particularly maintenance and repairs costs. In 1974-1975, the fuel cost represented only about 13 percent. In spite of the increase of the till cost, the drying operation on the whole was more than economical, considering the implied expenses if the completion of the project would have needed an extra year.

Project C, East-West Dikes--Outardes 2

The water-retaining structures of project C include a concrete-faced rock-fill dam and two earth-fill dikes. The sand and gravel dikes are provided with a relatively large impervious central core consisting of a mix of sand-gravel and clay. Dike 1 (east), with a maximum height of 110 ft (33.5 m), has a crest length of 8700 ft (2650 m), and dike 2 (west) has a maximum height of 95 ft (29 m) and a crest length of 3800 ft (1160 m). The total volume of material involved is 1 822 700 yd^3 (1 393 555 m^3) for dike 2; the core material represents 262 000 and 185 000 yd^3 (200 314 and 141 443 m^3), respectively. The dikes, being founded on a relatively soft clay and silt foundation, were built with gentle slopes (up to 1V:6H) and this explains the relatively low ratio between the core volume and the total volume of the structure (2).

Geological and geotechnical investigations carried out for the project area [within an economical radius of about 20-25 miles (30-40 km)] did not disclose the presence of any deposit of natural impervious material that could have been used for core construction. However, the same investigation localized large deposits of sand and gravel and extended clay formations. Because of the high sensitivity of the clay (in its remolded stage the clay became fluid), it does not lend itself to being used as construction material. Thus, following the results obtained at Mirobo Dam in Japan (3), where the core was built from a mix of clay and weathered granite, a similar solution was adapted for these dikes. The mix was obtained at Mirobo by excavating a vertical face in a pile consisting of alternative layers of clay and weathered granite. In our case the sensitive clay liquifies by remolding and so it cannot be spread in layers. Subsequently, different mixing procedures were developed. Initially, the clay placed inside a U-shaped enclosure consisting of dumped sand-gravel piles is liquefied by moving bulldozers that also push the surrounding sand-gravel and mix together the two materials. When the mix became sufficiently homogeneous it is spread in thin layers on a stockpile. In a later stage, the mixing operation was realized in a mixing drum provided with rotary blades.

Geotechnical Characteristics of Core Material

Clay Material

The clay deposit contains about 37 percent clay and 58 percent silt particles and is of low plasticity (plasticity index about 7) due to the lack of real clay minerals. Even the particles smaller than 2 μ consist of inert minerals like quartz or feldspars and only about 4 percent represent clay minerals (e.g., illite or clorite). The average natural water content is 33 percent compared with an average of 25 percent liquid limit and 18 percent plastic limit. The high liquidity index (L_L = 2) is a good indicator of its high sensitivity, which is situated around S = 1000 (measured by Swedish cone tests). The laboratory permeability of the clay measured following Bowles method is around 10^{-8} cm/s.

Sand and Gravel

The grain size composition of the material used in the mix varies from a medium-fine sand to a sand and gravel. The average that passes sieve no. 4 is 75 percent and about 1.4 percent passes sieve no. 200. The average natural water content of the sand is 7 percent.

Manufacturing of the Sand-Gravel and Clay Mix

The excavation of the clay in the borrow pit is carried out with a backhoe of 1.5 yd^3 (1.15 m^3) capacity that cuts vertical faces of 16 ft (5 m) in height. The sand-gravel is also excavated along vertical faces with pneumatic loaders. Trucks of 22-ton and 35-ton capacities transport the material to the mixing area.

At the initial stage, two bulldozers carried out the mixing. One mix (batch) contains about 250 yd^3 (190 m^3), with a ratio of 30 percent clay to 70 percent sand (in volume). The mixing operation of a batch takes about 2 h. The mixed material is spread in a stockpile in layers of about 12-in (30-cm) thick.

In the second stage the mixing was realized in a 2-yd^3 (4.6-m^3) rotary drum fed by a belt conveyor. Two hoppers, one for the sand and one for the clay, proportion the materials on the conveyor. The proportioning of the sand is controlled by a timing mechanism. An endless screw, which also partly liquefies the clay, controls the clay content. The average production of the plant is about 150 yd^3/h (115 m^3/h).

The water content of the mix in both procedures is too high to be placed directly in the dike and requires a drainage period in the stockpile. To eliminate this drawback, a rotary kiln of 150 yd^3/h (115 m^3/h) capacity was installed to dry the sand. It provided a mix at a water content close to its optimum.

Placement and Compaction of Material

The compaction operations were carried out by 6-ton vibratory rollers with four passes. The materials were brought to the site in trucks of 22-ton to 30-ton capacities and were spread by bulldozers in

Figure 13. Grain size composition of the sand-gravel and clay mixture for project C.

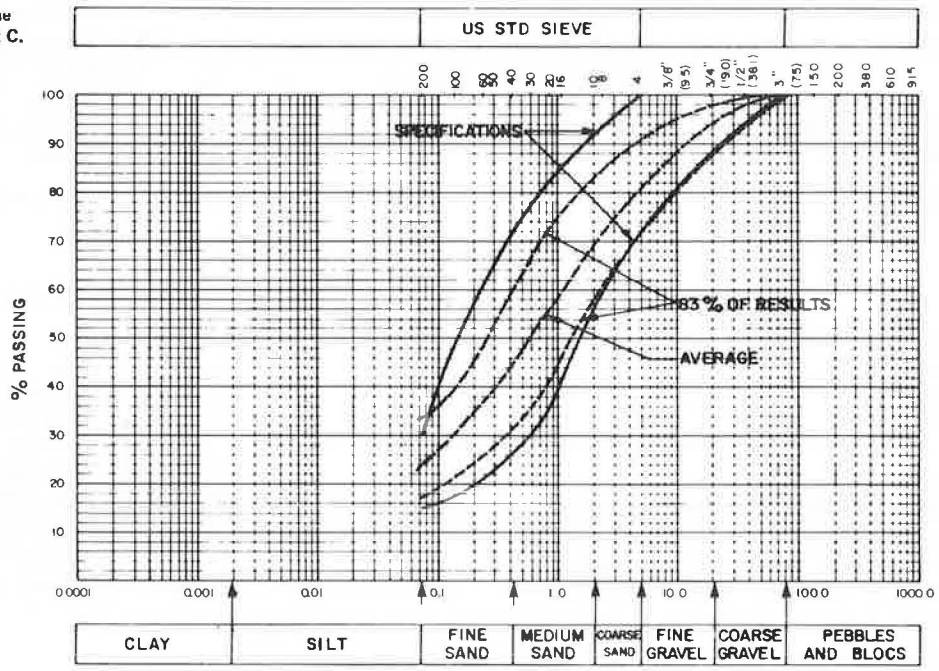

Figure 14. In situ dry density of the sand-gravel and clay mixture for project C.

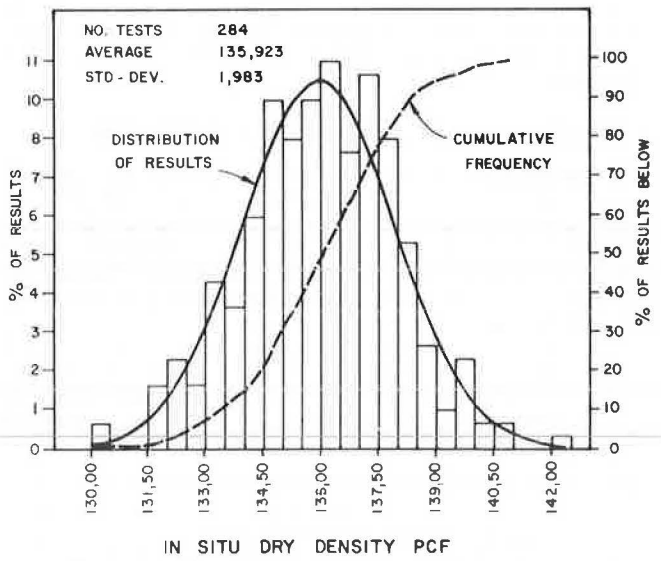

Figure 15. Compaction degree of the sand-gravel and clay mixture for project C.

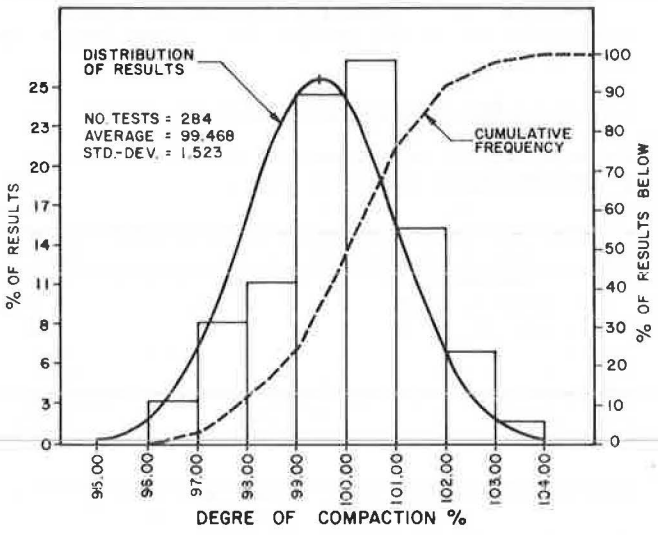

lifts 12-in (30-cm) thick. The compactors moved along the longitudinal axis of the dike with a maximum speed of 3 miles/h (5 km/h). Before placing the next lift the material is scarified to a depth of 3 in (8 cm) with a disc harrow.

The grain size composition of the mix placed in the dikes is illustrated in Figure 13. This shows that more than 83 percent of the results are within the limits laid down by the technical specifications. The average fine content (<0.074 mm) is 23.5 percent with a standard deviation of 3.7 percent.

The average water content after compaction is 7.4 percent (standard deviation of 0.8 percent) as compared with the average optimum water content (standard Proctor) of 7.7 percent (standard deviation of 0.4 percent).

The in situ dry density, measured with a Troxler nuclear apparatus gave an average value of 135.9 lb/ft³ (2175 kg/m³) with a standard deviation of 2 lb/ft³ (32 kg/m³) (Figure 14). The degree of compaction reached an average of 99.5 percent (standard deviation of 1.5 percent) (Figure 15). Less than 5 percent of the results indicate a degree of compaction less than 97 percent.

Placement and Compaction Inspection

The inspection operations were simulated to that of the other structures presented previously. The qualitative inspection was realized by inspectors in the field (i.e., lift thickness, number of passes, and traveling speed of the compactors). The quantitative inspection at the mixing plant, field, and laboratory was executed by technicians, all under the supervision of the resident soil engineer.

ACKNOWLEDGMENT

I am grateful to Hydro-Quebec for authorizing the publication of this article.

REFERENCES

1. C.A. Bouliane and P.H. Reid. Problems Due to the Use of a Special Impervious Material Used at the Manicouagan-3 Dam. Proc., 12th International Conference on Large Dams, Vol. 44, Mexico, 1976.
2. Y. Hammamji, Y. Pigeon, P.M. Gremeaux, and R. Anderson. Sand-Clay Core for the Dykes of the Outardes-2 Hydro-Electric Development. Proc., 14th International Conference on Large Dams, Vol. 55, Rio de Janiero, 1982.
3. J. Asao. The Miboro Dam. Proc., 8th International Conference on Large Dams, Vol. 31, Edimburg, 1964.

Lateral Pressure Developed During Compaction

ZVI OFER

The relation between the horizontal and vertical components of stress at a point within a soil mass depends on the physical and mechanical properties of the soil and its stress and strain histories. A series of compression tests and repeated loading tests were performed on sand and clay by using the lateral soil pressure ring MkII. This newly developed apparatus allows the laboratory determination of the lateral soil pressure response to vertical loading at rest condition or, alternatively, when limited controlled lateral strain develops. Correlations between the horizontal to vertical stress ratio (K) and the vertical load are presented. After placement of a cohesionless sample, when the material is loose, K is high and it decreases to an ultimate value. Unsaturated clay specimens exhibit somewhat different behavior—K decreases to a minimum value and then it increases with an increase in the load. During the unloading process K increases with an increase in the overconsolidation ratio, and a general relation between K and the overconsolidation ratio is suggested. However, repeated loading results in a decrease in K with an increase in the vertical load. It was also found that the grain size and distribution of grain size affect K. The present testing system does not have facilities for pore water pressure and dynamic loading measurements, which would enable more comprehensive testing and determination of soil parameters in terms of effective stress.

The relation between the horizontal and vertical components of stress at a point within a soil mass depends to a great extent on the stress and strain histories of the soil mass and the degree to which it is remembered. Other basic soil properties such as grain size and shape, grain size distribution, moisture conditions, and Atterberg's limits also affect the stress ratio. The elastic parameters of the soil [e.g., Poisson's ratio (μ)] and the modulus of elasticity (E) depend on the stress-strain characteristic of the soil as well. These parameters are major engineering considerations in many facets of road design and are used extensively in the design of layer thickness, earth-retaining structures, culverts, and slope-stability analysis.

The horizontal-to-vertical stress ratio at a point within a soil mass is defined as the coefficient of lateral earth pressure. This coefficient varies between a lower limit, when a soil element is allowed to expand laterally subsequent to vertical loading, and an upper limit, when a soil element mobilizes as a result of lateral thrust. These two extremes are defined as the coefficient of active lateral pressure (K_a) and the coefficient of passive lateral pressure (K_p), respectively. When lateral yielding is prevented, the ratio of the horizontal to vertical stress is known as the coefficient of lateral pressure at rest (K_o). These coefficients are correlated to the angle of internal friction of the soil (ϕ). However, this correlation is invalid in the case of highly overconsolidated materials. During a process of compaction or while clay soil swells as a result of an increase in its moisture content, the coefficient of lateral pressure at rest (K_o) may exceed unity value that results from combined effect of soil dilation and locked-in stress and, therefore, it cannot be correlated to ϕ.

The objective of this study was to examine the development of lateral stress in a remoulded soil mass during the compression process and to correlate it to several basic elastic and mechanical soil parameters that are of interest to the road engineer. This paper describes an instrument that allows laboratory determination of the lateral soil pressure response to vertical loading without lateral yielding and with limited controlled lateral yielding. A series of repetitive loading tests performed on river sand and remoulded norite clay is described and test results are presented and discussed.

LABORATORY K_o COMPRESSION TESTING

A laboratory K_o compression testing method must satisfy two requirements:

1. The soil must deform freely in the vertical direction and
2. The lateral yielding must be either zero or of negligible magnitude.

If either of these requirements is not satisfied (e.g., either the vertical yielding is restrained or lateral yielding occurs) the tested specimen is mobilized toward an active or passive failure condition. At rest condition is simulated in the laboratory by using either a modified triaxial testing or a modified oedometer compression testing technique.

A simple sensing device that consists of a metal band clamping a triaxial soil specimen was developed by Murdock (1). The metal band has an adjustable screw and a lamp connected to a power source. Before a vertical load increment is applied, the electrical circuit is closed by adjusting the screw until the lamp lights up. The radial deformation that results from an increase in the vertical load cuts the electrical circuit. A subsequent increase in the cell pressure recovers the radial deformation until the electrical circuit is closed and the lamp lights up again. At this stage no lateral strain occurred and the horizontal-to-vertical stress ratio at rest (K_o) is determined.

A visual lateral strain indicator was introduced

by Bishop and Henkel (2). It consists of two curved metal strips joined together by a low friction hinge on one end and a mercury reservoir with a diaphragm and a capillary tube outlet on the other end. The indicator clamps a soil sample placed in a triaxial test apparatus. The lateral deformation of the specimen is indicated by the level of the mercury in the outlet tube and it is possible to maintain the soil sample at rest condition by changing the vertical load and the cell pressure simultaneously. A similar concept of monitoring the radial yielding of a triaxial soil specimen has been used by many researchers and various visual and electrical indicators were developed and used (3-8). The radial deflection of a diameter is measured and at rest condition is reinstated by means of adjusting the triaxial cell pressure until the lateral yielding is zero.

The horizontal-to-vertical stress ratio during a loading test can also be determined by means of a modified oedometer test. The concept behind this testing method is that the lateral stress developed in a soil specimen placed in the modified oedometer ring during a loading test results in a small but measurable yielding of the oedometer ring wall. The resultant strain is recorded by means of strain gauges cemented to the oedometer ring wall and connected to a strain recorder, or alternatively, by means of a pressure transducer attached to the oedometer or test chamber wall (9-11). A section of the oedometer ring wall is trimmed to a thickness of less than 1 mm and the sensor is attached to this section. Note that some strain develops during the test that, in return, may affect the recorded lateral stress (12-14). True K_o conditions can be achieved only when the oedometer thin wall section is a part of an annular chamber filled with fluid. The strain of the thin section is registered electrically and it is maintained constantly at zero by continuous adjustment of the annular chamber pressure to compensate for the change that results from the variation in the vertical load (15,16). This concept is implemented in the instrument used for this study. The instrument is a null-type apparatus that allows the laboratory determination of the lateral soil pressure response to vertical loading during either at rest conditions or when lateral strain develops.

LATERAL SOIL PRESSURE RING MkII

A section through the lateral soil pressure ring MkII (LSP MkII) is shown in Figure 1. The apparatus is a modified oedometer ring that consists of a main ring (A) and a tightly fitted casing (b). The main ring has an inside diameter of 70 mm, outside diameter of 103.4 mm, and height of 42 mm. The middle section of the ring is trimmed to a wall thickness of 0.8 mm and a long strain gauge (C) is cemented to the thin section along its center line. Electric wires (D) connect the strain gauge to a digital strain indicator, and air pressure is supplied through a vent (E) drilled in the main ring. When the casing is placed on the main ring, an air-tight annular chamber is formed. A photograph of the components of the calibration and testing system is shown in Figure 2. The LSP MkII (A) and a temperature compensator (B) are connected to a digital strain indicator (C). The ring and a piston (D), which simulates a soil specimen, are connected independently to an air pressure supply system that consists of a main air pressure supply line (E), pressure regulators (F), and pressure gauges (G).

For the calibration of the ring the piston is placed inside the ring. Two calibration tests are performed. First, air pressure is introduced into the piston and the resultant hoop strain of the ring wall that corresponds to each pressure increment is recorded. The relation between the air pressure in the piston and the corresponding hoop strain gives a calibration chart that represents the relation between the lateral soil pressure developed during an actual test and the ring wall hoop strain that results from the soil pressure when a small lateral strain is allowed to develop. Another calibration test is performed by using a null method--air pressure is introduced into the piston in small increments. Simultaneously, the pressure in the annular chamber is increased so that the ring wall hoop strain maintains a null condition. This test correlates the lateral pressure developed in a soil specimen with the annular pressure for an actual test.

Both calibration tests render consistent results and linear pressure-strain and pressure-annular pressure relations. The coefficient of linear correlation for any of the test recordings of 500 random readings within a simulated soil sample lateral pressure range of 0-600 kPa was better than 0.999.

MATERIALS

Two materials were used in this study:

1. Honeydew sand and
2. Rustenburg black clay.

Honeydew sand is river sand of weathered granite origin obtained from a sand quarry located about 25 km northwest of Johannesburg. The dominant minerals are quartz and felspar with some mica. The specific gravity of the particles is G_s = 2.65 and the particles' shape is angular and subangular. Nine different gradings were tested. Their physical properties are listed in Table 1.

Rustenburg black clay is a highly expansive clay obtained from the Rustenburg platinum mine about 100 km west of Pretoria. X-ray diffraction analysis of the clay shows that the dominant mineral is smectite with some traces of kaolinite. The clay is residual of norite origin, and it is listed among the most highly expansive soils in South Africa (17). The particle size distribution of the clay is shown in Figure 3 and its physical properties are listed in the table below.

Item	Amount
Liquid limit	80 percent
Plastic limit	28 percent
Plasticity index	52 percent
Linear shrinkage	18 percent
Clay fraction, D <0.002 mm	52 percent
Activity	1.00
Potential expansiveness (18)	Very high
Unified soil classification	CH
Specific gravity of particles (G_s)	2.71
Maximum standard AASHO dry unit weight (γ_d)	14.22 kN/m³
Optimum standard AASHO moisture content	26 percent

TEST PROCEDURES

All sand specimens were molded and tested in an air-dried condition (moisture content, w = ±2 percent). The sand was placed in the LSP MkII ring in a very loose condition (D_r < 15 percent) and the desired density was achieved by vibrating the specimen lightly under a vertical load of 12.7 kPa. The specimen was then statically loaded up to a vertical pressure of 634.5 kPa and unloaded back to

12.7 kPa. During the loading and unloading cycles, the vertical deflection and the lateral pressure that correspond to each vertical load increment were recorded. Each specimen was subjected to four loading and unloading cycles. Some specimens were tested when lateral deflection was allowed, and some comparative triaxial compression tests were carried out by using Bishop and Henkel's K_o belt (2).

The clay was air dried before the test to a moisture content of 6 percent. Samples at four different moisture contents (20, 24, 27, and 30 percent) were prepared and stored at a constant temperature of 26°C for two weeks. Each specimen was placed in the LSP MkII ring in three layers, 10.8-mm thick (0.425 in), and the desired initial density was achieved by means of static vertical load. Samples at initial dry unit weight of 10.8 kN/m³, 12.3 kN/m³, and 13.7 kN/m³ were prepared. At the end of the initial compression process the vertical load was removed and the ring was placed in a consolidation loading frame under a vertical load of 12.7 kPa. The clay specimen was allowed to relax for 15 min and then the vertical deflection and lateral pressure were recorded. The specimen was then loaded in increments of 126.9 kPa up to a load of 761.4 kPa and then unloaded in double increments back to a vertical load of 12.7 kPa. The load increments were applied at a frequency of one increment per minute and at the end of each period the vertical deflection and the lateral pressure were recorded. Four loading and unloading cycles were performed and the clay specimen was allowed to relax for 15 min between the loading cycles. Some samples

Figure 1. Section through LSP MkII.

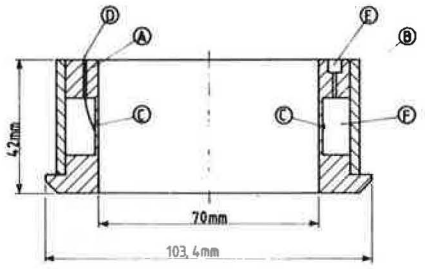

A = Main ring
B = Casing
C = Strain gauge
D = Electric wires
E = Air pressure vent
F = Air-tight chamber

Figure 2. LSP MkII calibration and testing system.

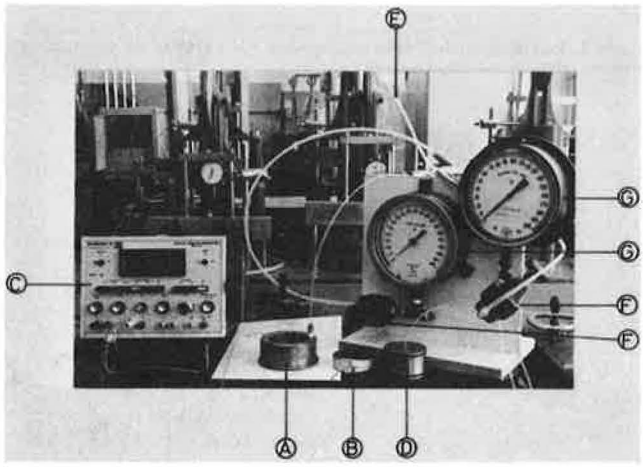

A = Lateral soil pressure ring
B = Temperature compensator
C = Digital strain indicator
D = Calibration piston
E = Air pressure pipe
F = Air pressure regulator
G = Pressure gauge

Table 1. Physical properties of Rustenburg black clay.

Item	Uniform Sand				Poorly Graded Sand				
	1	2	3	4	5	6	7	8	9
Maximum grain diameter (mm)	2.360	1.200	0.600	0.300	2.360	2.360	2.360	2.360	2.360
Minimum grain diameter (mm)	1.200	0.600	0.300	0.075	0.075	0.075	0.075	0.075	0.075
Effective size (D_{10})	1.420	0.750	0.360	0.108	0.260	0.200	0.160	0.128	0.095
30 percent fractile diameter (D_{30})	1.570	0.085	0.390	0.147	0.720	0.540	0.350	0.275	0.172
60 percent fractile diameter (D_{60})	1.720	0.885	0.440	0.182	1.450	1.050	0.790	0.525	0.392
Coefficient of uniformity (C_u)	1.21	1.18	1.22	1.69	5.58	5.25	4.94	4.10	4.13
Coefficient of curvature (C_c)	1.01	0.98	0.96	1.10	1.38	1.39	0.97	1.13	0.79
Unified soil classification	SP	SP	SP	SP	SP	SP	SP	SP	SP

Figure 3. Particle size distribution of Rustenburg black clay.

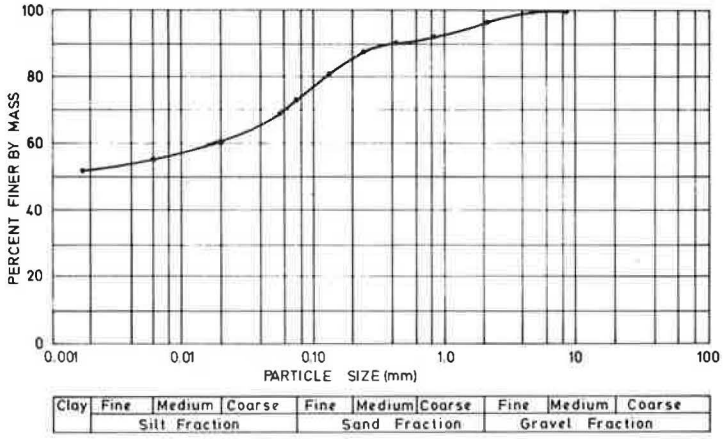

were tested when the period between the loading cycles was longer, and two specimens were subjected to normal consolidation tests to study the effect of time on the development of lateral pressure.

TEST RESULTS AND DISCUSSION

Tests on Sand

Some results of sand compression tests are presented in Figures 4-7. Typical relations between the lateral-to-vertical stress ratio and the vertical pressure are shown in Figure 4. At a very loose condition and under a low vertical pressure the lateral-to-vertical stress ratio is high and it decreases to an ultimate value with an increase in the vertical pressure and the subsequent densification of the sand. The stress ratio is also affected by grain size--grading 1 is a uniform coarse sand and grading 4 is a uniform fine sand. The stress ratio of the uniform coarse sand is considerably lower than that of the fine sand. Grading 9 is poorly graded sand, 50 percent of its mass is fine sand (grading 4) and 12.5 percent of its mass is coarse sand (grading 1). The stress ratios during a compression test of grading 9 are somewhat lower than those of grading 4.

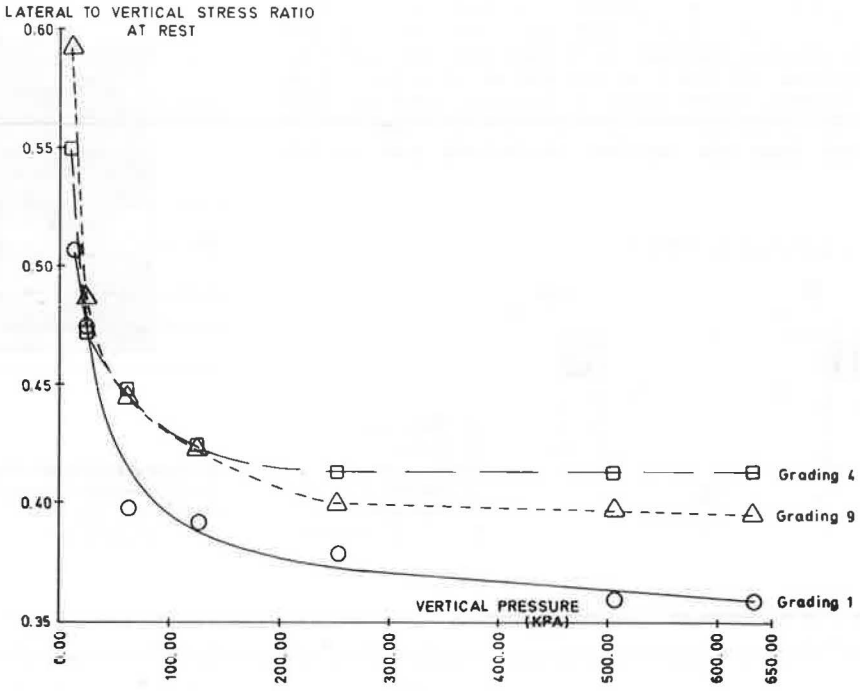

Figure 4. Lateral-to-vertical stress ratio-vertical pressure relations for tests on sand.

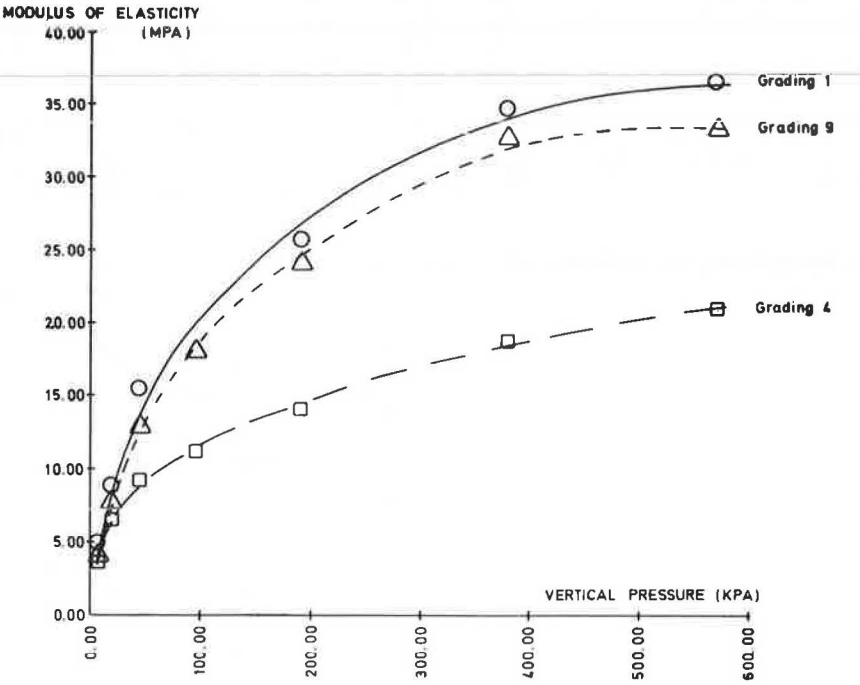

Figure 5. Modulus of elasticity-vertical pressure relations for tests on sand.

The elastic properties of the sand were determined by using the stress-strain characteristic of the sand, and the following relations. For isotropic elastic materials, the value of Poisson's ratio (μ) may be expressed as

$$\mu = K_o/(1 + K_o) \quad (1)$$

The constrained tangent modulus of deformation (D), which is the ratio of vertical stress difference ($d\sigma_v$) with respect to vertical strain difference ($d\epsilon_v$) under zero radial strain may be expressed by definition as

$$D = d\sigma_v/d\epsilon_v \quad (2)$$

The modulus of elasticity of an elastic material (E) may be expressed in terms of Poisson's ratio and the constrained modulus as

$$E = D(1 + \mu)(1 - 2\mu)/(1 - \mu) \quad (3)$$

or, alternatively, in terms of the constrained modulus and the lateral-to-vertical stress ratio at rest, as follows,

$$E = D(1 + 2K_o)(1 - K_o)/(1 + K_o) \quad (4)$$

Equations 3 and 4 do not apply for overconsolidated materials where K_o is equal to or greater than 1.

The relation between the modulus of elasticity (E) and the vertical pressure (σ_v) during compression tests of gradings 1, 4, and 9 are shown in Figure 5. E increases with an increase in the ver-

Figure 6. At test stress ratio-overconsolidation ratio relation for tests on sand.

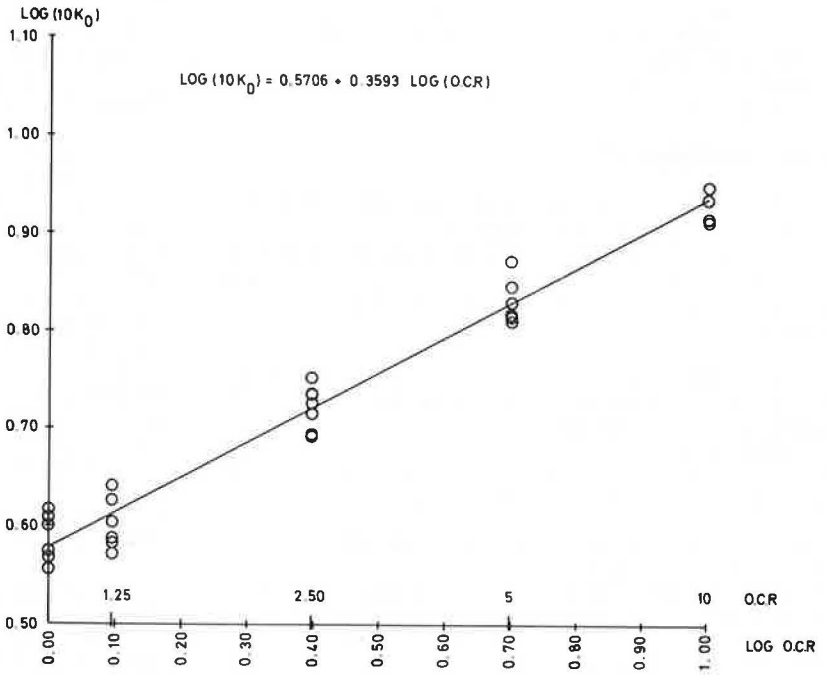

Figure 7. Vertical pressure-at rest stress ratio relations for repeated loading tests on sand.

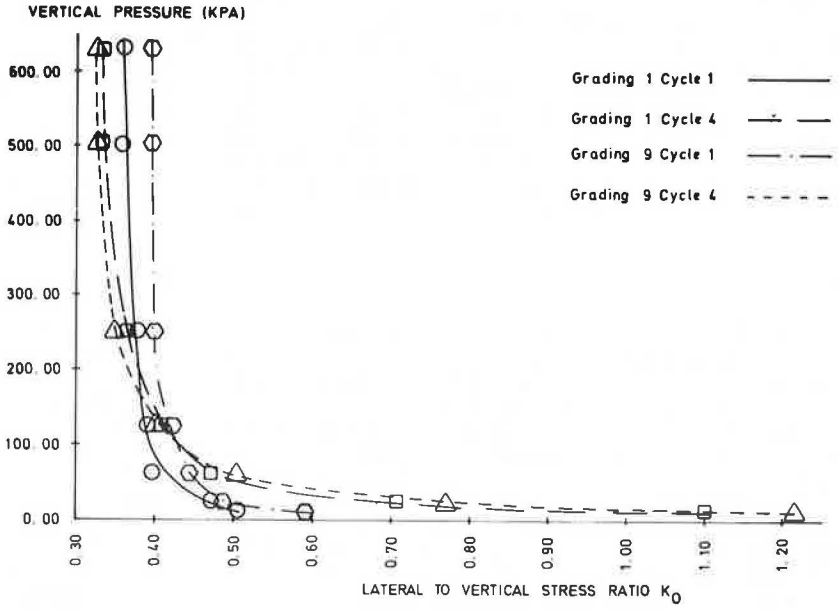

tical pressure and the subsequent densification of the sand. However, note that the mass of coarse sand developed a much higher modulus of elasticity than the mass of fine sand, although the initial test conditions were similar. The characteristic of the modulus of elasticity of the poorly graded sand (grading 9) was similar to that of the uniform coarse sand, although only 12.5 percent of its mass was coarse sand (2.360 mm > particle size > 1.200 mm).

The correlation between the lateral-to-vertical stress ratio at rest and the overconsolidation ratio during the unloading stage of a compression test is shown in Figure 6. The correlation is linear if presented in double logarithmic scale. During the unloading stage the Honeydew sand may be characterized by the expression

$$\text{Log}(10K_o) = 0.5786 + 0.3593 \log (\text{OCR}) \quad (5)$$

where K_o is the lateral-to-vertical stress ratio at rest and OCR is the overconsolidation ratio.

Different linear double log correlations were obtained for other materials, and it may be expressed generally as

$$\text{Log}(10K_o) = R_1 + R_2 \log (\text{OCR}) \quad (6)$$

where R_1 and R_2 are the load release parameters that characterize the soil behavior.

The effect of repeated loading is shown in Figure 7. Only the first and fourth loading cycles are shown for gradings 1 and 9. Two distinct features are noticed:

1. The stress ratio decreases with an increase in the number of loading cycles and the subsequent compaction of the soil and
2. When the overconsolidation ratio is greater than five, the stress ratio decreases sharply with an increase in the vertical pressure.

These phenomena were common to the uniform and poorly graded sand specimens.

Some comparative triaxial K_o loading tests were carried out by using Bishop and Henkel's K_o belt (2) and the results were similar. However, this technique yielded somewhat higher lateral-to-vertical K_o values. Another series of comparative tests was carried out to evaluate the effect of radial strain on the stress ratio. We found that, for uniform sand, irrespective of grain size, the stress ratio decreased by about 5 percent when the radial strain was 0.000 06. In poorly graded sand radial strain of 0.000 06 resulted in an 11 percent decrease in the stress ratio, and a radial strain of 0.000 13 resulted in a 17 percent decrease in the stress ratio. This decrease is attributed to the dissipation of vertical stress in the sand specimen due to the development of shear stress within the soil mass.

Tests on Clay

Results of compression tests on clay samples are shown in Figures 8-11. During the compaction operation, which was simulated in the laboratory by rapid loading, pore fluid pressure developed during the compression process only dissipates partly. Since the LSP MkII is not equipped with facilities for measuring pore pressure, only an analysis in total stress terms could be carried out. However, total stress analysis represents the actual condition in a clay mass during, and shortly after, a compaction operation, because the dissipation of excess pore pressure is a time-consuming process.

A typical relation between the lateral-to-vertical pressure ratio and the vertical pressure during a loading and unloading cycle is shown in Figures 8 and 9. After the initial placement operation is completed and under a small vertical load, the clay specimen is in an overconsolidated condition and the stress ratio is high. The stress ratio decreases with an increase in the vertical pressure and the subsequent decrease in the overconsolidation ratio. A further increase in the vertical load results in an increase in the stress ratio. During the unloading operation the stress ratio increases with a decrease in the vertical load and the subsequent increase in the overconsolidation ratio. On reinstatement of the vertical load to its initial magnitude, the stress ratio is higher than the stress ratio recorded at the beginning of the loading cycle. However, under a small vertical load in a partly saturated condition, the lateral pressure developed in the clay specimen decreases with time. If evaporation takes place, the clay sample shrinks and full dissipation of the lateral stress may occur.

Results of statistical regression analysis of all the loading tests performed on clay are shown in Figure 10. Test results were analysed irrespective of the placement density, and it is apparent that the moisture content affects the stress path during the loading test. During placement of a dry clay specimen, a high vertical pressure is required to achieve the desired initial dry density. However, the initial vertical pressure required in order to achieve identical placement dry density decreases if the moisture content of the clay is increased in the dry of optimum range. The lateral-to-vertical pressure ratio at the beginning of a loading cycle is high for a dry clay specimen, and it decreases with an increase in the moisture content (Figure 9). An increase in the vertical pressure results in a decrease in the stress ratio, and this characteristic is similar to that found in sand.

Bear in mind that all the observations were made on clay samples that have an initial dry density lower than maximum standard American Association of State Highway Officials (AASHO) dry density and moisture contents in the range of 0.20-0.30. The samples are partly saturated and consequently the pore pressure response to loading is only partial. This condition is shown in Figure 10, which demonstrates the lateral pressure response to an increase in the vertical pressure. When a clay sample is fully saturated, an increase in the vertical pressure is reflected by an identical increase in the lateral pressure. This condition has never been encountered in this series of tests (the maximum degree of saturation achieved in any of the tests was 0.92).

The relation between the lateral-to-vertical pressure ratio and overconsolidation ratio when the clay specimens were unloaded is shown in Figure 11. The general relation suggested in Equation 6 is valid for the clay; e.g.,

$$\text{Log}(10K) = R_1 + R_2 \log (\text{OCR}) \quad (7)$$

However, note that in terms of total stress R_1 decreases and R_2 increases simultaneously with a decrease in the moisture content, and this relation is valid for the range of clay properties tested.

Two more important observations were made during this series of tests. First, repeated loading up to five cycles did not affect the lateral pressure response to loading, which was almost identical during any loading and unloading cycle. The other observation relates to the effect of time on the lateral pressure developed during compression. The time interval between the application of load incre-

ments was 1 min, which is insufficient for full dissipation of pore pressure in the clay tested. In another series of slow consolidation tests performed on the same clay, during loading the immediate lateral pressure developed in the clay specimens was high and it decreased if a period of 24 h was allowed between loading increments. This trend is reversed during the unloading process. When a load was removed, the lateral pressure decreased instantly and subsequently increased with time. If the clay sample is not kept under constant controlled moisture condition, evaporation takes place, which results in shrinkage and a subsequent decrease in the lateral pressure.

A comparison between the test results for sand and clay demonstrates the similarities and differences in the characteristics of the lateral pressure developed in the soil samples during compaction. The general stress-strain and vertical pressure-lateral pressure relations are similar in nature. However, in sand these relations are independent of time, whereas in clay time and moisture content affect the behavior of the tested specimen and its physical parameters. Quantitatively, the values of vertical deflection and lateral pressure response to

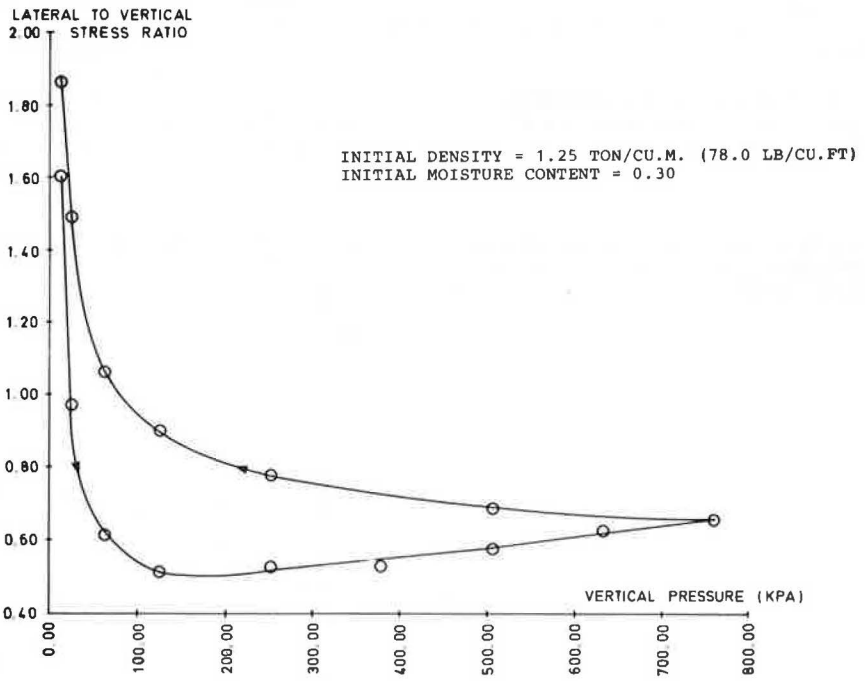

Figure 8. Typical total stress ratio-vertical pressure relation for test on clay specimen.

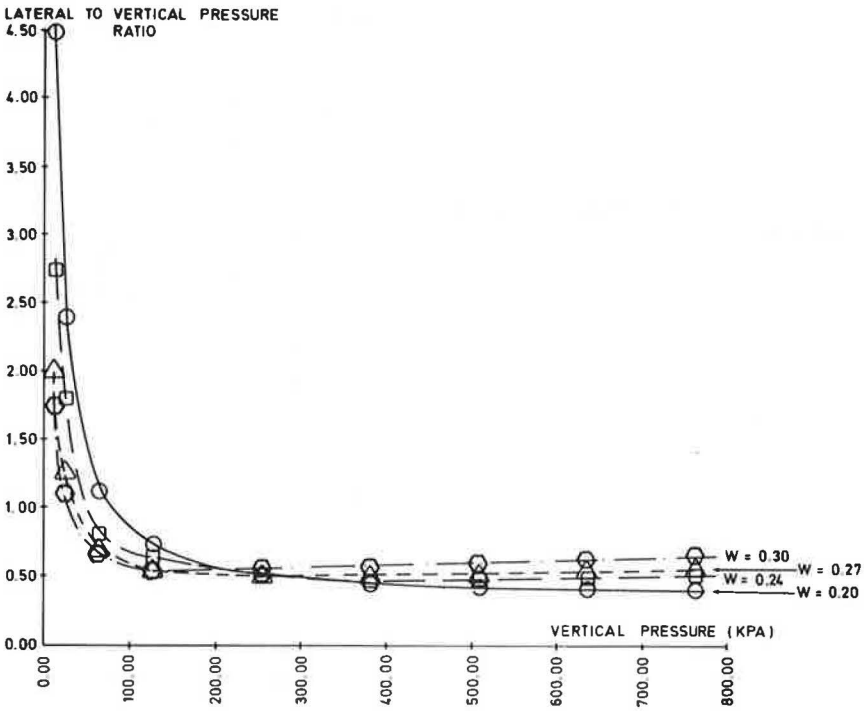

Figure 9. Effect of moisture content on the pressure ratio-vertical pressure relation for tests on clay samples.

axial loading increase with a decrease in the effective grain size. Therefore, we expected that the magnitude of the parameters determined from test results of clay specimens would follow this trend. Determination of the effect of pore pressure and swelling characteristics on the measured parameters was beyond the scope of this study.

SUMMARY, CONCLUSIONS, AND RECOMMENDATIONS

A series of static compaction tests on sand and clay was performed by using LSP MkII. The apparatus is a modified oedometer ring that measures the lateral pressure developed in a soil specimen during compression in a null method (at rest condition), or alternatively, when some lateral strain is allowed to develop. The following characteristics were found.

1. After placement and under a low vertical pressure, the lateral-to-vertical pressure ratio (K_o) of the soil specimen is high, and it decreases with an increase in the vertical pressure. In sand the pressure ratio decreases to an ultimate value. In clay, the pressure ratio decreases to a minimum value and then it may increase again to a value less than unity for unsaturated clay.

2. When a sand or clay specimen is unloaded, the lateral-to-vertical pressure ratio increases with an increase in the overconsolidation ratio, and a general relation between the pressure ratio (K) and the overconsolidation ratio (OCR) is suggested

$$\text{Log}_{10}(10K) = R_1 + R_2 \log_{10}(OCR) \quad (8)$$

This relation is insensitive to moisture, particle size, particle size distribution, moisture content, and time for the sand tested. However, it is sensitive to moisture content and time for clay. Hence, the stress ratio is a function of the stress history of the soil.

3. Small lateral strain results in a decrease in the lateral-to-axial pressure ratio in sand, but it does not affect the total stress ratio during quick

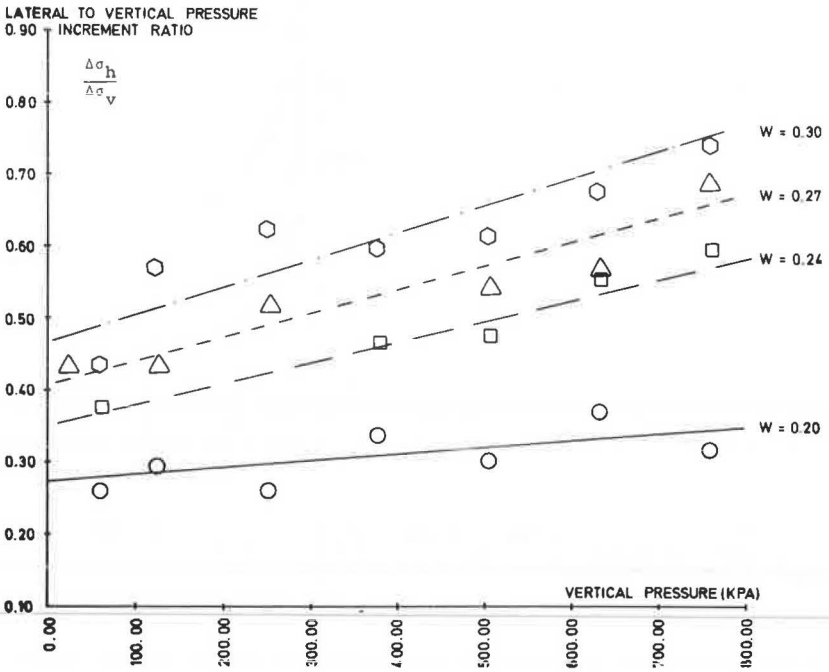

Figure 10. Pressure increment ratio-vertical pressure relations and loading of clay samples for initial dry unit weight = 13.7 kN/m³.

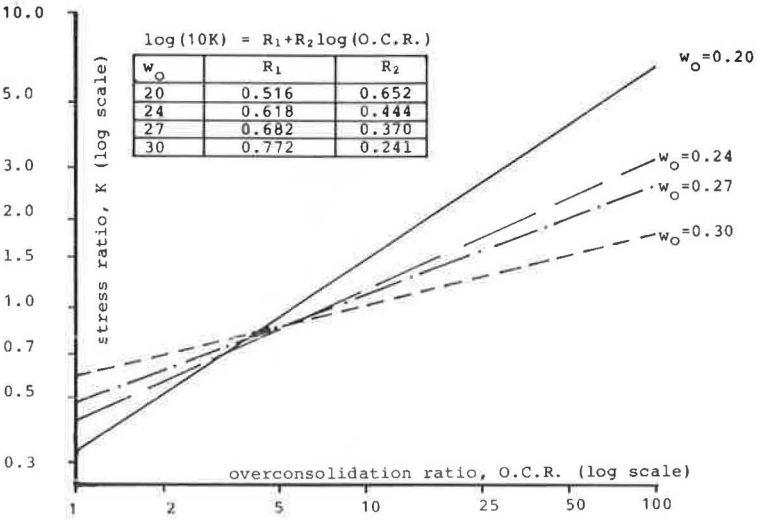

Figure 11. Stress ratio (K)-OCR relations for unloading of clay samples.

loading and unloading of clay samples.

4. Repeated loading results in a decrease of the pressure ratio in sand. The pressure ratio followed a similar path during repeated loading of the clay specimen.

5. Tests that use the LSP MkII provide reliable and consistent results. It was convenient and easy to use for compression tests of at rest condition. Bishop and Henkel's K_o belt (2) tended to give slightly higher K values in sand; however, its use for clay testing is inconvenient.

The results of this research should be developed further by means of incorporating pore pressure measuring facilities to the LSP MkII. The recording facilities of the LSP MkII should be improved for quicker and dynamic loading tests. Finally, a study should be conducted that will investigate the time and pore pressure parameters on several nonfree draining soils.

REFERENCE

1. L.J. Murdock. Consolidation Tests on Soils Containing Stones. Proc., 2nd International Conference on Soil Mechanics and Foundations Engineering, Rotterdam, Holland, Vol. 1, 1948, pp. 169-173.
2. A.W. Bishop and D.J. Henkel. The Measurement of Soil Properties in the Triaxial Test. E. Arnold, London, 1962, pp. 70-74.
3. K. Akai and T. Adachi. Study on the One Dimensional Consolidation and the Shear Strength Characteristics of Fully Saturated Clay, in Terms of Effective Stress. Proc., 6th International Conference on Soil Mechanics and Foundations Engineering, Montreal, Canada, Vol. 1, 1965, pp. 146-150.
4. C.A. Moore. Effect of Mica on K_o Compressibility of Two Soils. Journal of the Soil Mechanics and Foundation Division, ASCE, Vol. 97, No. SM9, 1971, pp. 1275-1289.
5. J.R. Boyce and S.F. Brown. Measurement of Elastic Strain in Granular Material. Geotechnique, Vol. 26, No. 4, 1976, pp. 637-640.
6. S.F. Brown and M.S. Snaith. The Measurement of Recoverable and Irrecoverable Deformation: the Repeated Load Triaxiam Test. Geotechnique, Vol. 24, No. 2, 1974, pp. 255-259.
7. A.A. El Ruwayih. Design Manufacture and Performance of a Lateral Strain Device. Geotechnique, Vol. 26, No. 2, pp. 215-216.
8. B.K. Menzies. Discussion, Design Manufacture and Performance of a Lateral Strain Device. Geotechnique, Vol. 26, No. 3, 1976, pp. 542-544.
9. A. Komornik and J.G. Zeitlen. An Apparatus for Measuring Lateral Soil Swelling Pressure in the Laboratory. Proc., 6th International Conference on Soil Mechanics and Foundation Engineering, Montreal, Canada, 1965, pp. 278-281.
10. Z. Ofer. Instruments for Laboratory and In-situ Measurement of the Lateral Swelling Pressure of Expansive Clays. Proc., 4th International Conference on Expansive Soils, Denver, CO, 1980, pp. 45-53.
11. M.S. Abdelhamid and R.J. Krizek. At Rest Lateral Earth Pressure of a Consolidating Clay. Journal of the Geotechnical Engineering Division, ASCE, Vol. 102, No. GT7, 1976, pp. 721-738.
12. R.E. Fulton and A.J. Hendron. Discussion of Impact Waves in Sand: Theory Compared with Experiments on Sand Columns. Journal of the Soil Mechanics and Foundations Division, ASCE, Vol. 87, No. SM6, 1961, pp. 69-73.
13. K.Z. Andrawes and M.A. El-Sohby. Factors Affecting Coefficient of Earth Pressure K_o. Journal of the Soil Mechanics and Foundations Division, ASCE, Vol. 99, No. SM7, 1973, pp. 527-538.
14. M.M. Al-Hussaini and F.C. Townsend. Investigation of K_o Testing in Cohesionless Soil. U.S. Army Engineer, Waterways Experiment Station, Vicksburg, MS, Tech. Rept. S-75-16, 1975.
15. E.W. Brooker and H.O. Ireland. Earth Pressure at Rest Related to Stress History. Canadian Geotechnical Journal, Vol. 2, No. 1, 1965, pp. 1-15.
16. Z. Ofer. Laboratory Instrument for Measuring the Lateral Soil Pressure and Swelling Pressure. Geotechnical Testing Journal, ASTM, 1981.
17. A.B.A. Brink. Engineering Geology of Southern Africa. Building Publications, Pretoria, Republic of South Africa, Vol. 1, 1979, pp. 284-301.
18. D.H. Van Der Merwe. The Prediction of Heave from the Plasticity Index and the Percentage Clay Fraction. Transaction, South African Institution of Civil Engineers, Vol. 6, No. 6, 1964, pp. 103-107.